1

COMPLEX RESISTIVITY OF THE EARTH

J. R. Wait

1.1 Preliminary Theory

a. D.C. Current Flow

As a starting point we consider a point source of direct current I in a homogeneous medium of conductivity σ. The radial current density J_r, in amps/m, is given by the expression

$$J_r = I/(4\pi r^2) \tag{1}$$

where r is the radial distance to the point of observation from the source point. The corresponding radial electric field E_r is obtained simply from Ohm's law:

$$E_r = J_r/\sigma = I/(4\pi\sigma r^2) \tag{2}$$

By symmetry there is no other components of the electric field. Thus, in vector notation, the electric field is written

$$\overline{E} = \hat{r}E_r = \hat{r}I/(4\pi\sigma r^2) \tag{3}$$

where $\hat{r}$ is a unit vector in the r direction.

We now introduce the concept of potential by postulating that $\overline{E}$ can be derived from the gradient of a scalar function V. Thus we write

$$\overline{E} = -\text{grad}\, V \tag{4}$$

or, in the present example,

$$E_r = -\partial V/\partial r \tag{5}$$

If we stipulate the V vanishes as $r \to \infty$, it is clear that

$$V = I/(4\pi\sigma r) \tag{6}$$

We are now in the position to derive the field expressions for a pair of current point sources of equal and opposite signs. The situation is indicated in Fig. 1.1.1 where, for convenience, we have chosen a cylindrical coordinate system (ρ, ϕ, z). The positive current source $+I$ is located at $z = +L/2$ while the negative current source $-I$ (i.e. a

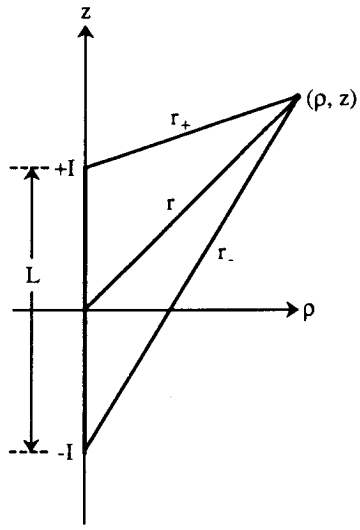

Figure 1.1.1 A current point source and a current point sink.

point sink) is located at $z = -L/z$. Both are located on the z axis. The observer at (ρ, z) is independent of the azimuthal angle ϕ.

Making use of (6), it is a simple matter to show that the resultant potential V at (ρ, z) is given by

$$V = (I/4\pi\sigma)(r_+^{-1} - r_-^{-1}) \tag{7}$$

where

$$r_+ = \left[\rho^2 + (z - L/2)^2\right]^{\frac{1}{2}} \tag{8}$$

and

$$r_- = \left[\rho^2 + (z + L/2)^2\right]^{\frac{1}{2}} \tag{9}$$

The corresponding electric field components are obtained from (4). Thus we easily deduce that

$$E_\rho = -\frac{\partial V}{\partial \rho} = \frac{I\rho}{4\pi\sigma}\left[\frac{1}{r_+^3} - \frac{1}{r_-^3}\right] \tag{10}$$

and

$$E_z = -\frac{\partial V}{\partial z} = \frac{I}{4\pi\sigma}\left[\frac{z - L/2}{r_+^3} - \frac{z + L/2}{r_-^3}\right] \tag{11}$$

Exercise. Show that in rectangular coordinates

$$E_x = \frac{Ix}{4\pi\sigma}\left[\frac{1}{r_+{}^3} - \frac{1}{r_-{}^3}\right] \tag{12}$$

and

$$E_y = \frac{Iy}{4\pi\sigma}\left[\frac{1}{r_+{}^3} - \frac{1}{r_-{}^3}\right] \tag{13}$$

where now

$$r_+ = \left[x^2 + y^2 + (z - L/2)^2\right]^{\frac{1}{2}} \tag{14}$$

and

$$r_- = \left[x^2 + y^2 + (z + L/2)^2\right]^{\frac{1}{2}} \tag{15}$$

Then verify that V, E_x, E_y and E_z satisfy Laplace's equation, i.e.

$$\nabla^2 V \quad \text{or} \quad \frac{\partial^2 V}{\partial x^2} + \frac{\partial^2 V}{\partial y^2} + \frac{\partial^2 v}{\partial z^2} = 0 \tag{16}$$

b. D.C. Magnetic Fields Simply Obtained

To obtain expressions for the magnetic field $\overline{H}$ of the two current point sources, we need to be a bit more specific about the configuration of the circuit connections from the generator (e.g. battery) to the electrodes. For simplicity we will consider a linear thin wire carrying a constant current I as depicted in Fig. 1.1.2. For this situation we can assert that the magnetic field has only an azimuthal component H_ϕ which itself is independent of ϕ.

A simple statement of Ampere's law for the present configuration is

$$\int_0^{2\pi} H_\phi \rho d\phi = \int_{\phi'=0}^{2\pi}\int_{\rho'=0}^{\rho} J_z(\rho', \phi', z)\rho' d\phi' d\rho' \tag{17}$$

which is a statement that the integral of the tangential magnetic field around a closed circuit of radius ρ is equal to the *total* enclosed current in the vertical (i.e. z) direction. Because of symmetry

$$2\pi\rho H_\phi = 2\pi \int_0^{\rho} J_z(\rho', z)\rho' d\rho' \tag{18}$$

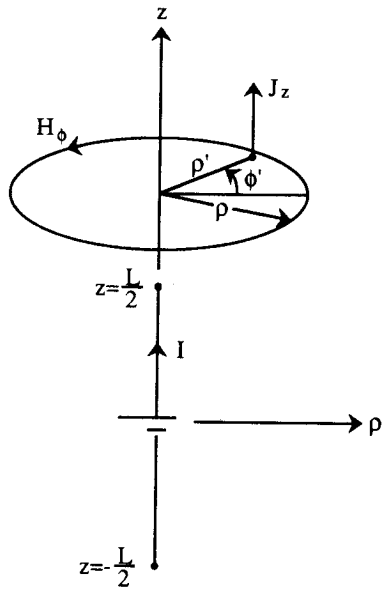

Figure 1.1.2 Concentric circular path to deduce magnetic field.

where, for the case $|z| > L/2$,

$$J_z(\rho', z) = \frac{I}{4\pi}\left[\frac{z - L/2}{(r_+')^3} + \frac{z + L/2}{(r_-')^3}\right] \tag{19}$$

and

$$r_+' = \left[(\rho')^2 + (z - (L/2))^2\right]^{\frac{1}{2}} \tag{20}$$

$$r_-' = \left[(\rho')^2 + (z + (L/2))^2\right]^{\frac{1}{2}} \tag{21}$$

The integration over ρ' can be carried out to give

$$H_\phi = \frac{1}{4\pi\rho}\left(\frac{z - (L/2)}{\left\{\rho^2 + [z + (L/2)]^2\right\}^{\frac{1}{2}}} - \frac{z - (L/2)}{\left\{\rho^2 + [z - (L/2)]\right\}^{\frac{1}{2}}}\right) \tag{22}$$

which is the resultant magnetic field at (ρ, z) for the linear current I grounded at $z = \pm L/2$.

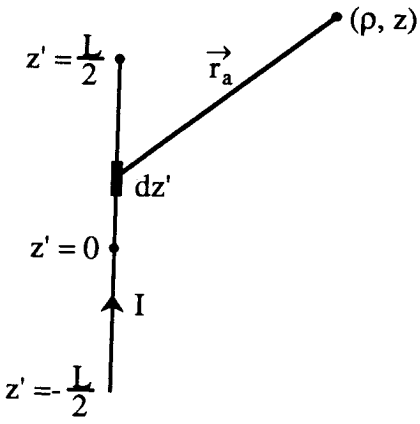

Figure 1.1.3 Geometry for applying the Biot-Savart law.

We can deal with the case $|z| < L/2$ by noting that (18) is modified to read

$$2\pi\rho H_\phi = I + 2\pi \int_0^\rho J_z(\rho', z)\rho' d\rho' \tag{23}$$

because the current on the wire now intersects the plane of the loop. Then, for example, if $z > L/2$ we can see that in the limit $\rho' \to 0$

$$\frac{I}{2}\left(z - \frac{L}{2}\right)\left(-\frac{1}{r_+'}\right) = \frac{I}{2}\left(z - \frac{L}{2}\right)\left(-\frac{1}{\left[(\rho')^2 + \left(z - \frac{L}{2}\right)^2\right]^{\frac{1}{2}}}\right) \to \frac{I}{2} \tag{24}$$

bearing in mind that $r_+' > 0$ always. The up shot is that the same expression for the magnetic field H_ϕ is obtained as before. Thus it is valid for all values of z.

Exercise Show that (22) may also be derived by an application of the Biot-Savart law

Solution The relevant form is

$$\overline{H} = \frac{I}{4\pi} \int_{-L/2}^{L/2} \frac{d\overline{z}' \times \overline{r}_a}{{r_a}^3} \tag{25}$$

where

$$r_a = \left[\rho^2 + (z - z')^2\right]^{\frac{1}{2}} \tag{26}$$

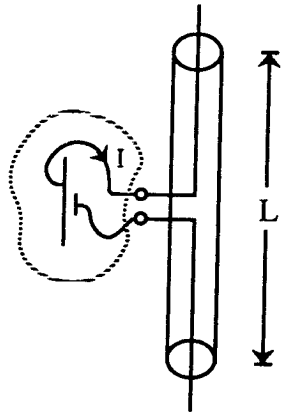

Figure 1.1.4 Idealization of an insulated current carrying wire with bare ends.

and where $\overline{r}_a$ is the vector of magnitude r_a from the element $d\vec{z}'$ to the observer at (ρ, z). See Fig. 1.1.3 . The details of the solution are given elsewhere. [Wait 1985, p. 36]

Exercise Show that yet still another method to obtain (22) is to use the vector potential $\overline{A}$ for the problem.

Solution Noting that $\overline{H} = \text{curl } \overline{A}$ it follows quite easily from the symmetry of the problem that

$$H_\phi = -\frac{\partial A_z}{\partial \rho} \tag{27}$$

where

$$A_z = \frac{I}{4\pi} \int_{-L/2}^{L/2} \frac{1}{r_a} dz' \tag{28}$$

is the only component of A. This solution is also detailed in the referenced text book [Wait 1985, p. 37].

c. *Current Injection and Voltage Pick Up*

Perhaps it is desirable if we indicate that a linear current-carrying wire in a conducting medium can be realized by a physical structure

such as illustrated in Fig. 1.1.4. The filamental wire of length L is fed by the battery or zero-frequency generator at two terminals. The structure is covered by a concentric insulated cover throughout its length but the ends are exposed. Thus the current I is conveyed to the medium at the bare end points. As we have indicated, the structure is represented analytically as a point source and point sink of current separated by a distance L. The electric fields so produced are deduced on this basis. However, the magnetic field is dependent on the assumption of symmetry about the axis of the structure. Here we make no attempt to say that the magnetic field is produced by the current along the wire or whether it is a manifestation of the current flow within the external medium. But as we have indicated in the preceding exercises, consistent results for H_ϕ are obtained by either supposition.

Another point of interest is that we ignore the presence of the insulating cover in deducing the magnetic field using the Biot-Savart law or the vector potential method. A possible justification for this idealization is to note that the derived field expression for H_ϕ given by (22) reduces to $I/(2\pi\rho)$ as ρ becomes vanishingly small provided $|z| < L/2$. Thus $2\pi\rho H_\phi$ can be associated with the total current I whether we choose $\rho =$ wire radius or $\rho =$ insulation radius.

Other physical approximations involve the precise method that we feed the structure and how it is terminated in the medium. In some applications, both of these questions are important but in geophysical prospecting schemes the voltage drop at the electrodes is not crucial because the injected current I into the medium is monitored. Also, the connecting leads from the battery or generator to the structure are configured such that the resulting fields are minimized (e.g. by using twisted pair lead wire of minimum length).

A few words might also be said about how the fields are to be measured within the conductor. The ideal probe for the electric field is again an insulated linear wire of say length ℓ with open ends. The induced voltage v is then observed at the terminal pairs as suggested by the sketch in Fig. 1.1.5. Now it is clear, under the assumption that the linear wire is perfectly conducting, the full induced voltage will appear at the terminals. Thus

$$v = -\int_{-\ell/2}^{\ell/2} E_z(z')dz' \tag{29}$$

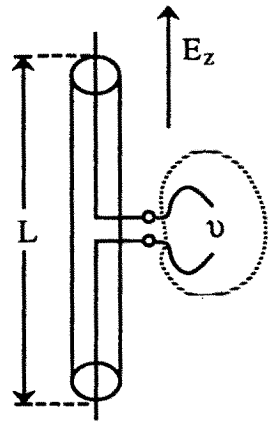

Figure 1.1.5 Idealization of an insulated linear wire with bare ends for use as an electric field probe.

which is the open circuit voltage for the case when the linear wire probe is aligned in the z direction. If E_z was substantially constant over the length ℓ we could write $v \simeq -E_z \cdot \ell$ indicating that the electric field is directly proportional to the voltage v at the detector. It is clear that the probe system requires the ends of the linear wire have electrical contact with the medium but the precise nature of the interface is not crucial provided negligible current is drawn by the voltage detector.

When E_z is not a constant along the linear wire (i.e. probe is "near" the source) it is desirable to express v in terms of the potentials at the ends of the structure. Thus in the context of Fig. 1.1.5, we note that

$$E_z = -\frac{\partial V}{\partial z}$$

so that

$$v = V(z' = \frac{\ell}{2}) - V(z' = -\frac{\ell}{2}) \tag{30}$$

is the expression for the induced potential.

A specific four electrode measuring scheme is illustrated in Fig. 1.1.6 where again the surrounding medium is assumed to be homogeneous of conductivity σ. The "current electrodes" A and B are fed by the battery or DC source so that essentially A is a point source of current I and B is a point sink. The voltage v or difference of potential between the electrodes M and N is then measured by the

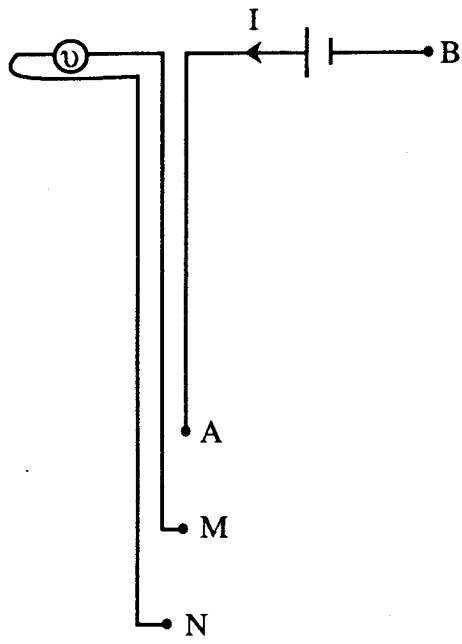

Figure 1.1.6 Four electrode array showing voltage and current circuits.

detector.

From what we have said above, it is clear that the so called transfer resistance R of the four electrode array is given by

$$R = \frac{v}{I} = \frac{1}{4\pi\sigma}\left[\frac{1}{AM} + \frac{1}{BN} - \frac{1}{AN} - \frac{1}{BM}\right] \tag{31}$$

where AM, BN, AN and BM are linear distances. This particular configuration is relevant to boreholes or well logging. Here, for example, A, M and N are located on the axis of the hole and they make contact with the adjacent medium. Obviously, we have ignored the influence of the hole, itself including the effect of any conductive fluids therein. More about this type of measurement scheme will be brought up later when more realistic conditions are considered.

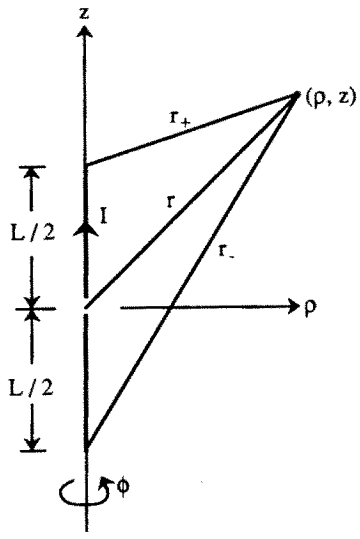

Figure 1.1.7 Linear wire of length L.

d. The Dipole Concept

In many instances the fields of the linear wire of length L, carrying a current I, are observed at distances r large compared with L. The situation is illustrated in Fig. 1.1.7 where $r = (\rho^2 + z^2)^{\frac{1}{2}}$ is measured from the center point to the observer at (ρ, z) again using cylindrical coordinates. Now if $r \gg L$ it is clear that

$$\begin{aligned} r_+^{-1} &= \left[\rho^2 + (z - L/2)^2\right]^{-\frac{1}{2}} \\ &= \left[\rho^2 + z^2 - zL + L^2/4\right]^{-\frac{1}{2}} \\ &\simeq (r^2 - zL)^{-\frac{1}{2}} = r^{-1}(1 - zL/r^2)^{-\frac{1}{2}} \\ &\simeq r^{-1}(1 + zL/2r^2) = r^{-1} + zL/2r^3 \end{aligned} \tag{32}$$

Similarly

$$r_-^{-1} \simeq r^{-1} - zL/2r^3 \tag{33}$$

The potential as given by (7) is now approximated as follows:

$$V = \frac{I}{4\pi\sigma}\left[\frac{1}{r_+} - \frac{1}{r_-}\right] \simeq \frac{ILz}{4\pi\sigma r^3} \tag{34}$$

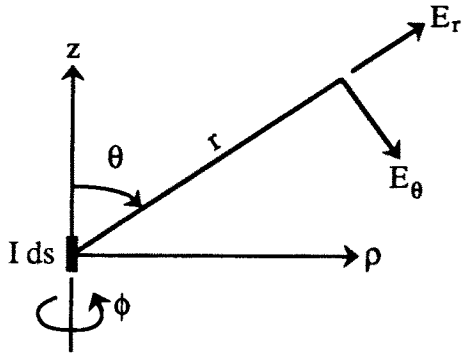

Figure 1.1.8 Electric dipole or short current element.

which is proportional to the product IL called the current moment of the resulting electric dipole. Clearly an alternative form of (34) is

$$V \simeq \frac{IL}{4\pi\sigma r^2}\cos\theta \tag{35}$$

in terms of spherical coordinates (r, θ, ϕ) as indicated in Fig. 1.1.8. In both (34) and (35) above we now replace IL by Ids to signify that the current element has an infinitesimal length ds. Thus, we write (35) as an equality

$$V = \frac{Ids}{4\pi\sigma r^2}\cos\theta \tag{36}$$

The corresponding electric fields for the dipole source are obtained from (4) so that we arrive at the explicit expressions:

$$E_r = -\frac{\partial V}{\partial r} = \frac{Ids}{2\pi\sigma r^3}\cos\theta \tag{37}$$

and

$$E_\theta = -\frac{1}{r}\frac{\partial V}{\partial \theta} = \frac{Ids}{4\pi\sigma r^3}\sin\theta \tag{38}$$

The inverse distance dependence, to the inverse third power, is characteristic of the static fields of an elementary dipole.

Exercise Obtain the electric field components of the electric dipole Ids expressed in cylindrical coordinates.

Solution We proceed directly by working with (4) and (34). Thus

$$E_\rho = -\frac{\partial V}{\partial \rho} = \frac{3Ids\rho z}{4\pi\sigma r^5} = \frac{Ids}{4\pi\sigma}\cdot\frac{3\rho z}{(\rho^2+z^2)^{5/2}} \tag{39}$$

and

$$E_z = -\frac{\partial V}{\partial z} = \frac{Ids}{4\pi\sigma}\left(\frac{-1}{r^3}+\frac{3z^2}{r^5}\right) = \frac{Ids}{4\pi\sigma}\frac{2z^2-\rho^2}{(\rho^2+z^2)^{5/2}} \tag{40}$$

where we have noted that $\partial r/\partial z = z/r$ and $\partial r/\partial \rho = \rho/r$.

The static magnetic field of the electric dipole Ids can be obtained directly from (22) in the limiting case where $\rho^2+z^2 \gg L^2$ and IL is replaced by Ids. Then

$$H_\phi = \frac{Ids\rho}{4\pi r^3} = \frac{Ids}{4\pi r^2}\sin\theta \tag{41}$$

which, of course, is valid for either cylindrical or spherical coordinates.

Our next observation is to note that the fields of the dipole can be conveniently derived from a vector potential with only a z component A_z. Thus, we readily confirm that if

$$A_z = Ids/4\pi r \tag{42}$$

then

$$\sigma E_\rho = \partial^2 A_z/\partial\rho\partial z \tag{43}$$

$$\sigma E_z = \partial^2 A_z/\partial z^2 \tag{44}$$

and

$$H_\phi = -\partial A_z/\partial\rho \tag{45}$$

lead back to (39), (40) and (41), respectively.

These relations are consistent with the general forms

$$\overline{E} = -\text{grad}\, V \tag{46}$$

and

$$\overline{H} = \text{curl}\,\overline{A} \tag{47}$$

where $\overline{A}$ and V are related by $\sigma V = -\text{div}\,\overline{A}$.

e. Dynamic Fields

Up to this point we have been dealing with purely static fields in a homogeneous conductor of infinite extent. We now wish to generalize the results to time varying fields. For convenience we specify that the fields vary harmonically with an *angular frequency* ω. Thus, for example, the component E_x is a phasor or complex quantity with an *amplitude* $|E_x|$ and phase ϕ_x. The actual physical quantity is then

$$e_x(t) = \text{Re}\,\{E_x e^{j\omega t}\} = |E_x| \cos(\omega t + \phi_x) \tag{48}$$

Correspondingly, the complex vector $\overline{E}$ is written explicitly in the form

$$\overline{E} = \hat{x}E_x + \hat{y}E_y + \hat{z}E_z \tag{49}$$

when E_x, E_y and E_z are phasors. The physical time-varying vector is then

$$\overline{e}(t) = \hat{x}e_x(t) + \hat{y}e_y(t) + \hat{z}e_z(t) \tag{50}$$

where

$$e_y(t) = \text{Re}\,\{E_y e^{j\omega t}\} \quad \text{and} \quad e_z(t) = \text{Re}\,\{E_z e^{j\omega t}\} \tag{51}$$

It is important that the reader not confuse the meanings of vectors and phasors. In what follows we will deal almost exclusively with complex phasors corresponding to a single *angular frequency* ω. There is no loss of generality here because general time varying quantities can be handled by Fourier synthesis involving spectra over all values of ω.

At this juncture we write down Maxwell's equations for *a source-free* region characterized by a conductivity σ, (electric) permittivity ϵ, and (magnetic) permeability μ. For the implied time factor $\exp(j\omega t)$:

$$-j\mu\omega\overline{H} = \text{curl}\,\overline{E} \tag{52}$$

$$(\sigma + j\epsilon\omega) = \text{curl}\,\overline{H} \tag{53}$$

where $\overline{E}$ and $\overline{H}$ are the vector complex electric and magnetic fields, respectively. If the region is homogeneous, we readily deduce that

$$\text{curl curl}\,\overline{E} + \gamma^2\overline{E} = 0 \tag{54}$$

and

$$\text{curl curl}\,\overline{H} + \gamma^2\overline{H} = 0 \tag{55}$$

where

$$\gamma^2 = j\mu\omega(\sigma + j\epsilon\omega)$$

In the case of rectangular coordinates, these two equations reduce to the well known scalar wave equation such that each field component (e.g. E_x) satisfies

$$\left(\frac{\partial^2}{\partial x^2} + \frac{\partial^2}{\partial y^2} + \frac{\partial^2}{\partial z^2} - \gamma^2\right) E_x = 0 \tag{56}$$

However, the situation can be more complicated in cylindrical and spherical coordinates. Thus, it is more convenient to utilize the vector potential $\overline{A}$ defined such that

$$\overline{H} = \text{curl}\, \overline{A} \tag{57}$$

Then from (53) we see that

$$\overline{E} = \frac{1}{\sigma + j\epsilon\omega} \text{curl curl}\, \overline{A} \tag{58}$$

In particular if we choose $\overline{A} = \hat{z}A_z$ (i.e. z directed vector potential) it follows that

$$H_\phi = -\partial A_z/\partial\rho \tag{59}$$

and

$$E_\rho = \frac{1}{\sigma + j\epsilon\omega} \frac{\partial^2}{\partial\rho\partial z} A_z \tag{60}$$

$$E_z = \frac{1}{\sigma + j\epsilon\omega} \left(-\gamma^2 + \frac{\partial^2}{\partial z^2}\right) A_z \tag{61}$$

where we have made use of elementary results from vector calculus (Wait 1986). We have also assumed azimuthal symmetry (i.e. $\partial/\partial\phi = 0$). Then we can show that

$$(\nabla^2 - \gamma^2)A_z = 0 \tag{62}$$

where in cylindrical coordinates

$$\nabla^2 = \frac{1}{\rho}\frac{\partial}{\partial\rho}\left(\rho\frac{\partial}{\partial\rho}\right) + \frac{\partial^2}{\partial z^2} \tag{63}$$

is the Laplacian operator.

Now in the case of zero frequency, it is clear that $\gamma^2 = 0$ and $\nabla^2 A_z = 0$ which is Laplace's equation. For the elementary source dipole of current moment Ids we showed that the static (i.e. $\omega = 0$) solution for the problem was given by

$$A_z = \frac{Ids}{4\pi r} \tag{64}$$

where

$$r = (\rho^2 + z^2)^{\frac{1}{2}}$$

The appropriate solution of (62) that reduces to (64) is clearly given by

$$A_z = \frac{Ids}{4\pi r} e^{-\gamma r} \tag{65}$$

where $\gamma = [j\mu\omega(\sigma + j\epsilon\omega)]^{\frac{1}{2}}$ is defined such that Re $\gamma > 0$. Using (59) we readily deduce that

$$\begin{aligned} H_\phi &= \frac{Ids}{4\pi r^3}(1 + \gamma r)e^{-\gamma r}\rho \\ &= \frac{Ids}{4\pi r^2}(1 + \gamma r)e^{-\gamma r}\sin\theta \end{aligned} \tag{66}$$

which reduces to (41) as it should when $\gamma r \to 0$. The corresponding electric field components are most easily obtained from (53). In spherical coordinates

$$E_r = \frac{Ids}{2\pi(\sigma + j\epsilon\omega)r^3}(1 + \gamma r)e^{-\gamma r}\cos\theta \tag{67}$$

and

$$E_\theta = \frac{Ids}{4\pi(\sigma + j\epsilon\omega)r^3}(1 + \gamma r + \gamma^2 r^2)e^{-\gamma r}\sin\theta \tag{68}$$

We can observe that (67) and (68) reduce to the corresponding static forms (37) and (38), respectively, in the limit $\gamma r \to 0$ and $\omega \to 0$.

It is useful to note here that, if $|\gamma r| \ll 1$, (without requiring that $\omega \to 0$), (67) and (68) are approximated by the "so-called" quasi-static forms

$$E_r = \frac{Ids}{2\pi(\sigma + j\epsilon\omega)r^3}\cos\theta \tag{69}$$

and

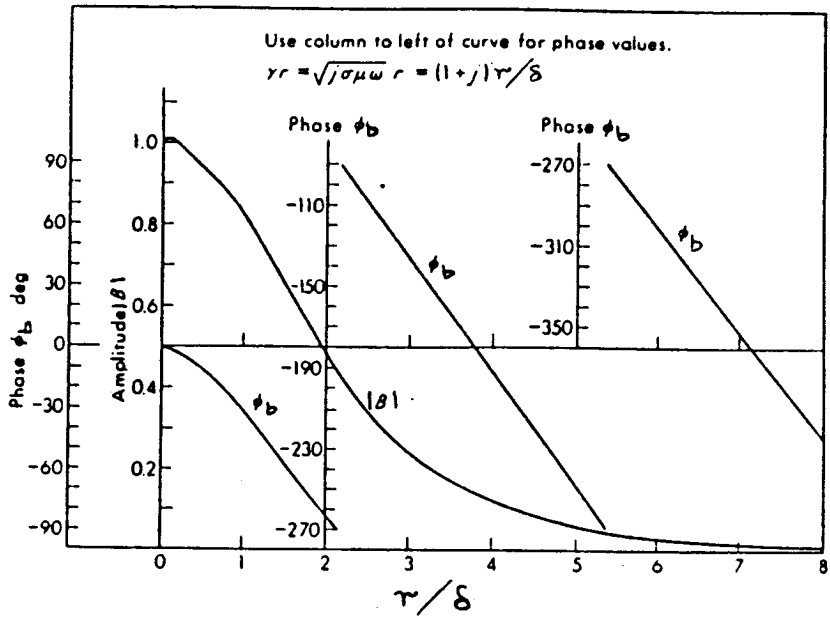

Figure 1.1.9 Amplitude and phase of the generic field function B as a function of normalized distance to source.

$$E_\theta = \frac{Ids}{4\pi(\sigma + j\epsilon\omega)r^3}\sin\theta \tag{70}$$

Now, if we let $\omega \to 0$, the static forms given by (37) and (38) are recovered.

f. Generic Field Structure

To give some insight to the nature of the field structure of the dipole we will assume that $\sigma \gg \epsilon\omega$. In this case the conduction currents dominate the displacement currents. Then we may approximate the propagation constant as follows

$$\gamma = [j\mu\omega(\sigma + j\epsilon\omega)]^{\frac{1}{2}} \simeq (j\mu\omega\sigma)^{\frac{1}{2}} = (1+j)/\delta \tag{71}$$

where

$$\delta = [2/(\sigma\mu\omega)]^{\frac{1}{2}}$$

is the classical skin depth. Now we may write (66), (67) and (68) in the forms

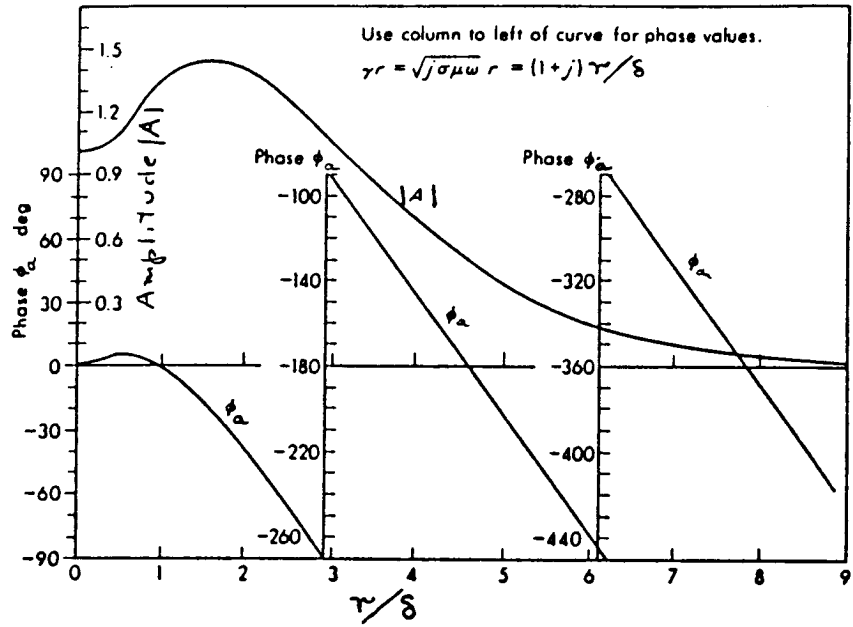

Figure 1.1.10 Amplitude and phase of the generic field function A as a function of normalized distance to source.

$$H_\phi = \frac{Ids}{4\pi r^2} B(r/\delta) \sin\theta \tag{72}$$

$$E_r = \frac{Ids}{2\pi\sigma r^3} B(r/\delta) \cos\theta \tag{73}$$

$$E_\theta = \frac{Ids}{4\pi\sigma r^3} A(r/\delta) \sin\theta \tag{74}$$

where

$$B(r/\delta) = [1 + (1+j)r/\delta] \exp[-(1+j)r/\delta] \tag{75}$$

and

$$A(r/\delta) = [1 + (1+j)r/\delta + 2jr^2/\delta^2] \exp[-(1+j)r/\delta] \tag{76}$$

The dimensionless complex functions $B = |B|e^{j\phi_b}$ and $A = |A|e^{j\phi_a}$ represent the normalized actual fields at a normalized distance r/δ from the source dipole. The amplitude and phase values of B and A

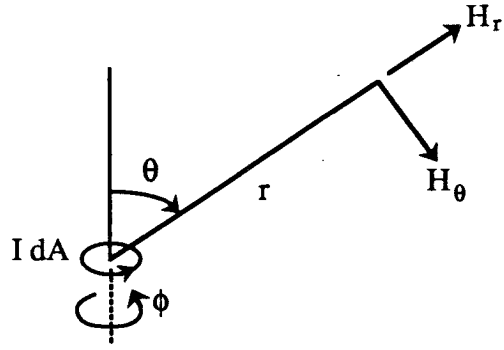

Figure 1.1.11 Magnetic dipole or small current carrying loop.

are plotted in Figs. 1.1.9 and 1.1.10, respectively. As indicated both A and B approach 1 as $r/\delta \to 0$ which, of course, is the static limit. On the other hand, if $r/\delta \gg 1$, the functions are exceptionally damped and the phase lag behaves as r/δ radians.

An interesting property of the A function is that its magnitude is actually 1.4 for $r/\delta \simeq 1.8$. Thus, contrary to simple intuition, the field $|E_\theta|$ is much greater than that predicted on the basis of simple plane wave theory.

g. The Magnetic Dipole

While we have been dealing exclusively with an electric dipole source, the generic functions A and B are actually relevant to a magnetic dipole source. We call attention to this fact for future reference.

A magnetic dipole is here regarded as a small loop of area dA carrying a current I as indicated in Fig. 1.1.11. Again, the surrounding medium is considered to be homogeneous with conductivity σ, permittivity ϵ, and magnetic permeability, μ. We refer the reader to standard texts for the derivations of the field expressions. For example, the principle of duality may be exploited which shows that the oscillating magnetic dipole source is analogous to the electric dipole source if the role of $\vec{E}$ and $\vec{H}$ are suitably interchanged [Wait 1985, p. 39].

Using spherical coordinates (r, θ, ϕ) with the magnetic dipole (i.e. small loop with vertical axis) located at the origin we can express the non-zero field components as follows

$$E_\phi = -\frac{j\mu\omega I dA}{4\pi r^2}(1+\gamma r)e^{-\gamma r}\sin\theta \qquad (77)$$

$$H_r = \frac{IdA}{2\pi r^3}(1+\gamma r)e^{-\gamma r}\cos\theta \tag{78}$$

and

$$H_\theta = \frac{IdA}{4\pi r^3}(1+\gamma r+\gamma^2 r^2)e^{-\gamma r}\sin\theta \tag{79}$$

These expressions are analogous to the electric dipole forms given by (66), (67) and (68). In particular, we note that in the static limit $\omega \to 0$

$$H_r = \frac{IdA}{2\pi r^3}\cos\theta \tag{80}$$

$$H_\theta = \frac{IdA}{4\pi r^3}\sin\theta \tag{81}$$

which are the classical forms for the DC magnetic field of the static magnetic dipole source. Of course, in this limit $E_\phi \to 0$. But, in the quasi-static sense where $\omega \neq 0$ and $|\gamma r| \ll 1$, we may approximate (77) by

$$E_\phi \simeq -\frac{j\mu\omega IdA}{4\pi r^2}\sin\theta \tag{82}$$

When the surrounding medium is a good conductor (i.e. $\sigma \gg \epsilon\omega$) we can express (77), (78) and (79) in the useful forms

$$E_\phi = -\frac{j\mu\omega IdA}{4\pi r^2}B(r/\delta)\sin\theta \tag{83}$$

$$H_r = \frac{IdA}{2\pi r^3}B(r/\delta)\cos\theta \tag{84}$$

$$H_\theta = \frac{IdA}{4\pi r^3}A(r/\delta)\sin\theta \tag{85}$$

where the complex functions B and A are given by (75) and (76), respectively. Thus, the plots in Figs. (1.1.9) and (1.1.10) are still applicable.

h. Dispersion of σ and ϵ

At this stage, one could extend the calculation of the fields to include displacement currents. Thus, one could utilize the forms given by (66), (67) and (68) for the field components with γ defined by

$$\gamma = [j\mu\omega(\sigma + j\epsilon\omega)]^{\frac{1}{2}}$$

Typically such calculations assign a fixed value for σ and ϵ. Unfortunately, such results are very artificial because in actual geological media, both σ and (particularly) ϵ vary significantly with frequency. We prefer to deal with the complex resistivity function $\rho(j\omega)$ which is defined as

$$\rho(j\omega) = [\sigma(\omega) + j\omega\epsilon(\omega)]^{-1}$$

in terms of the frequency dependent real conductivity $\sigma(\omega)$ and real permittivity $\epsilon(\omega)$.

We defer further discussion of the influence of dispersion (i.e. frequency dependence) of the conductivity and permittivity. Obviously, it is an important topic.

References

[1] Wait, J. R., *Electromagnetic Wave Theory*, Harper and Row, 1985.

[2] Wait, J. R., *Introduction to Antennas and Propagation*, Peter Peregrinus Ltd., Stevenage, UK, 1986.

1.2 Complex Resistivity Concept

a. Ohm's Law

The essential property we exploit in the induced polarization method of geophysical is the frequency dispersion of the medium. From a macroscopic point of view, we are saying that the real conductivity $\sigma(\omega)$ and the real permittivity $\epsilon(\omega)$ are functions of the angular frequency ω. Thus, for a particular point in the medium, we may assert that electric field $\overline{E}(j\omega)$ and the associated current density $\overline{J}(j\omega)$ are connected by Ohm's law

$$\overline{E}(j\omega) = \rho(j\omega)\overline{J}(j\omega) \tag{1}$$

where

$$\rho(j\omega) = [\sigma(\omega) + j\epsilon(\omega) \cdot \omega]^{-1} \tag{2}$$

is the complex resistivity*. It is assumed here and in most of what follows that $\rho(j\omega)$ does not depend on the magnitude of the current density $\overline{J}$. That is, we are dealing with linear phenomena. The implied time factor is $\exp(j\omega t)$.

b. Basic Dipole Model

While (1) is valid for an inhomogeneous region, we find it convenient to deal with piecewise homogeneous regions. In fact, in order to deal with basic concepts at the most elementary level, it is desirable to imagine that the source of the excitation is an electric dipole with current moment $I(j\omega)ds$. The surrounding medium is homogeneous with complex resistivity $\rho(j\omega)$. We may now write down expressions for the field components with reference to spherical coordinates [Wait 1986a]:

$$E_r(j\omega) = \frac{I(j\omega)ds\,\rho(j\omega)}{2\pi r^3} B(j\omega)\cos\theta \tag{3}$$

$$E_\theta(j\omega) = \frac{I(j\omega)ds\,\rho(j\omega)}{4\pi r^3} A(j\omega)\sin\theta \tag{4}$$

and

* The use of the lower case rho to represent complex resistivity should not cause confusion with the radial cylindrical coordinate.

$$H_\phi(j\omega) = \frac{1}{4\pi r^2} I(j\omega) ds\, B(j\omega) \sin\theta \tag{5}$$

where

$$B(j\omega) = [1 + \gamma(j\omega)r] \exp[-\gamma(j\omega)r] \tag{6}$$

and

$$A(j\omega) = [1 + \gamma(j\omega)r + \gamma^2(j\omega)r^2] \exp[-\gamma(j\omega)r] \tag{7}$$

The complex propagation constant is here written in terms of the complex resistivity as follows

$$\gamma(j\omega) = \{j\omega\mu[\sigma(\omega) + j\omega\epsilon(\omega)]\}^{\frac{1}{2}} = [j\omega\mu/\rho(j\omega)]^{\frac{1}{2}}$$

Here we can see the complexity of the problem resulting from the dispersion in the medium. For example, if we were to measure the ratio $E_\theta(j\omega)/I(j\omega)$ for some fixed point (r, θ), the resulting frequency dependence would be related to the frequency dependence of $\rho(j\omega)$ in a rather complicated manner. This fact means that any inverse procedure to deduce the complex resistivity of the medium from the measured field is not simple. We shall consider various aspects of this problem below and in the following chapters.

c. Quasi-Static Limit

There is a great simplification when the angular frequency ω is low and/or the radial distance r is sufficiently small such that

$$|\gamma(j\omega)r| \ll 1$$

Then $B(j\omega)$ and $A(j\omega)$ can both be replaced by 1. This restriction is equivalent to the quasi-static assumption discussed earlier. We can now say that an electric field component $\Psi(j\omega)$ is linearly related to the complex resistivity in the manner

$$\Psi(j\omega) = I(j\omega) F \rho(j\omega) \tag{8}$$

when F depends only on the geometry. More explicitly, we would write

$$E_r(j\omega) \simeq I(j\omega) \left[\frac{ds}{2\pi r^3} \cos\theta\right] \rho(j\omega) \tag{9}$$

and

$$E_\theta(j\omega) \simeq I(j\omega)\left[\frac{ds}{4\pi r^3}\sin\theta\right]\rho(j\omega) \tag{10}$$

On the other hand, $H_\phi(j\omega)$ is independent of $\rho(j\omega)$ at least within the quasi-static idealization. Thus

$$H_\phi(j\omega) \simeq I(j\omega)\left[\frac{ds}{4\pi r^2}\sin\theta\right] \tag{11}$$

Linear system theory [Wait 1984] can be employed to discuss the time domain or transient response of the electric field response $\Psi(t)$ (i.e. $e_r(t)$ or $e_\theta(t)$) for a suddenly applied current $i(t)$ at $t = 0$. Using Laplace transform notation, we can pose the problem as follows: Given the source current, deduce the response; thus, begin by taking the Laplace transform

$$I(s) = \int_0^\infty i(t)e^{-st}dt = \mathcal{L}i(t) \tag{12}$$

where formally we identify s with $j\omega$ — but we can allow $\mathrm{Re}\{s\} > 0$ to guarantee convergence of (12). Then clearly

$$\Psi(t) = \mathcal{L}^{-1}\Psi(s) = \frac{1}{2\pi j}\int_{\delta-j\infty}^{\delta+j\infty} e^{st}\psi(s)ds \qquad (\text{where } \delta > 0) \tag{13}$$

or, to be explicit,

$$\Psi(t) = F\mathcal{L}^{-1}I(s)\rho(s) \tag{14}$$

In the interests of conciseness, we have used the symbols $\mathcal{L}$ and $\mathcal{L}^{-1}$ to denote the direct and inverse Laplace transform operations, respectively.

While the Laplace transformation really involves all frequencies here, we argue that the procedure is valid in an approximate sense even though we have invoked the limitation that $|\gamma(s)r| \ll 1$. The early part of the transient response would be modified if propagation effects were allowed for. This question is related to "electromagnetic coupling" which we discuss later.

d. Apparent Resistivity

When the medium is inhomogeneous, we need to revise our approach. To illustrate the problem, consider the situation shown in Fig.

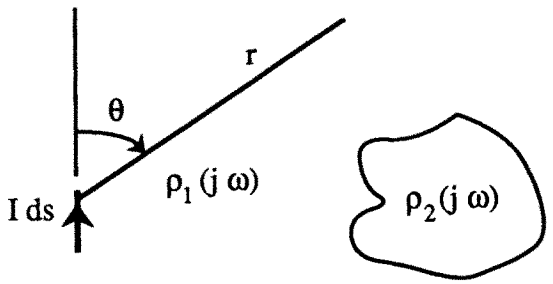

Figure 1.2.1 Current element source in homogeneous region (1) in presence of target region (2).

1.2.1. An electric dipole of current moment $I(j\omega)ds$ is located in a homogeneous region of resistivity $\rho_1(j\omega)$ which is unbounded except for an adjacent region of resistivity $\rho_2(j\omega)$. The symmetry of the problem has been destroyed but it is useful to introduce the concept of apparent (complex) resistivity $\rho_a(j\omega)$ with reference to the homogeneous model [i.e. where $\rho_2(j\omega) = \rho_1(j\omega)$]. For example, in the homogeneous case, we might deal with the radial field $E_r(j\omega)$ at $\theta = 0$. Thus

$$E_r(j\omega) = I(j\omega)ds\rho_1(j\omega)/2\pi r^3 \quad \text{for } \rho_2 = \rho_1 \text{ and } \theta = 0 \quad (15)$$

Now, in the presence of the inhomogeneity, we can write

$$E_r(j\omega) = I(j\omega)ds\rho_a(j\omega)/2\pi r^3 \quad \text{for } \rho_2 \neq \rho_1 \text{ and } \theta = 0 \quad (16)$$

In other words, the apparent complex resistivity for the configuration indicated is an effective parameter that is normalized by the homogeneous medium parameter.

In a functional sense, we can write

$$\rho_a(j\omega) = \rho_a[\rho_1(j\omega), \rho_2(j\omega)] \quad (17)$$

for a specific configuration of the source dipole and receiving circuit. However, such a statement is only valid in the quasi-static sense where all propagation effects are ignored. Some interesting properties can be discussed using this model. In fact, as pointed out by Seigel (1985), it is generally true that for any dimensionless factor λ

$$\rho_a(\lambda\rho_1, \lambda\rho_2) = \lambda\rho_a(\rho_1, \rho_2) \quad (18)$$

In other words, if the resistivities are increased by a factor λ, then the electric field components will also be increased by λ. Clearly now, if we differentiate both sides of (18) with respect to λ we get

$$\frac{\partial \rho_a(\lambda\rho_1, \lambda\rho_2)}{\partial(\lambda\rho_1)}\rho_1 + \frac{\partial \rho_a(\lambda\rho_1, \lambda\rho_2)}{\partial(\lambda\rho_2)}\rho_2 = \rho_a(\rho_1, \rho_2) \tag{19}$$

Now, we set $\lambda = 1$ to give

$$\rho_1\frac{\partial \rho_a}{\partial \rho_1} + \rho_2\frac{\partial \rho_a}{\partial \rho_2} = \rho_a \tag{20}$$

Clearly, this equation is equivalent to

$$\frac{\partial \ln \rho_a}{\partial \ln \rho_1} + \frac{\partial \ln \rho_a}{\partial \ln \rho_2} = 1 \tag{21}$$

which is true for any frequency — again within the limits of the quasi-static approximation. An alternative statement of (20) or (21) is

$$\rho_a = K{\rho_1}^{B_1}{\rho_2}^{B_2} \tag{22}$$

where

$$B_1 = \frac{\rho_1}{\rho_a}\frac{\partial \rho_a}{\partial \rho_1} \quad \text{and} \quad B_2 = \frac{\rho_2}{\rho_a}\frac{\partial \rho_a}{\partial \rho_2} \tag{23}$$

and K is a constant. The functional frequency dependence of ρ_a, K, ρ_1 and ρ_2 is understood. In fact, we can write

$$\frac{\rho_a(j\omega)}{\rho_a(0)} = \frac{K(j\omega)}{K(0)}\left(\frac{\rho_1(j\omega)}{\rho_1(0)}\right)^{B_1(j\omega)}\left(\frac{\rho_2(j\omega)}{\rho_2(0)}\right)^{B_2(j\omega)} X(j\omega) \tag{24}$$

where we have normalized all factors by the zero-frequency values and where

$$X(j\omega) = \rho_1(0)^{B_1(j\omega)-B_1(0)}\rho_2(0)^{B_2(j\omega)-B_2(0)} \tag{25}$$

By making use of the identity

$$B_1(j\omega) + B_2(j\omega) = 1 \tag{26}$$

it is possible to write the above expression in the form

$$X(j\omega) = [\rho_2(0)/\rho_1(0)]^{B_2(j\omega)-B_2(0)} \tag{27}$$

which agrees with Song and Vozoff [1985]. They argue that a useful approximation to (24) is to set $[K(j\omega)/K(0)]X(j\omega) = 1$ whence

$$\frac{\rho_a(j\omega)}{\rho_a(0)} \simeq \left[\frac{\rho_1(j\omega)}{\rho_1(0)}\right]^{B_1(j\omega)} \left[\frac{\rho_2(j\omega)}{\rho_2(0)}\right]^{B_2(j\omega)} \tag{28}$$

The applicability of this type of approximation has been confirmed by Song and Vozoff [1985] who carried out extensive numerical experiments using relevant geophysical parameters for both a layered earth model and a buried spherical target. They show extensive plots of the frequency dependent dilution factors B_1 and B_2 using a Cole-Cole model for the complex resistivity functions $\rho_1(j\omega)$ and $\rho_2(j\omega)$. Presumably, they use the real parts of B_1 and B_2 although this point is not made clear.

A closely related approach is to return to (22) and take logarithms of both slices. Thus,

$$\ln \rho_a = \ln K + B_1 \ln \rho_1 + B_2 \ln \rho_2 \tag{29}$$

If we write

$$\rho_a = |\rho_a| e^{j\phi_a}, \qquad \rho_1 = |\rho_1| e^{j\phi_1}, \quad \text{and} \quad \rho_2 = |\rho_2| e^{j\phi_2}$$

it follows that

$$\begin{aligned} \ln|\rho_a| = \ln|K| + \mathrm{Re}\{B_1\} \ln|\rho_1| - \mathrm{Im}\{B_1\}\phi_1 \\ + \mathrm{Re}\{B_2\} \ln|\rho_2| - \mathrm{Im}\{B_2\}\phi_2 \end{aligned} \tag{30}$$

and

$$\begin{aligned} \phi_a = \phi_k + \mathrm{Re}\{B_1\}\phi_1 + \mathrm{Im}\{B_1\} \ln|\rho_1| \\ + \mathrm{Re}\{B_2\}\phi_2 + \mathrm{Im}\{B_2\} \ln|\rho_2| \end{aligned} \tag{31}$$

If we now focus our attention on the frequency dependence of $\ln|\rho_a|$ and ϕ_d and neglect higher order terms, we obtain Guptasarma's (1984) approximations. They read

$$\frac{d \ln|\rho_a|}{d \ln \omega} \simeq \mathrm{Re}\{B_1\} \frac{d \ln|\rho_1|}{d \ln \omega} + \mathrm{Re}\{B_2\} \frac{d \ln|\rho_2|}{d \ln \omega} \tag{32}$$

and

$$\phi_a \simeq \mathrm{Re}\{B_1\}\phi_1 + \mathrm{Re}\{B_2\}\phi_2 \tag{33}$$

where we note that $\mathrm{Re}\{B_1\} = 1 - \mathrm{Re}\{B_2\}$.

In order for (32) and (33) be valid approximations to (30) and (31), it is evident that $B_2(j\omega)$ should not vary too rapidly with ω and also the imaginary part of $B_2(j\omega)$ should be small compared with the real part. The neglect of ϕ_k would be justified because $\phi_a \to 0$ when both ϕ_1 and $\phi_2 \to 0$. It is also evident that (32) and (33) also follow from (28) if the imaginary parts of B_1 and B_2 are ignored. Thus, in spite of widely differing derivations, Song and Vozoff's [1985] final working formulas are very similar to those presented by Guptasarma [1984]. In both cases, frequency dependent dilution factors are needed. While the authors present convincing evidence that their methods work for specific situations, it is not clear if such approximate procedures have wider applications. Also, the extension to the time domain would raise some difficulties. We discuss this aspect of the problem below.

e. Dilution and Distortion

We now recall that

$$\rho_a(j\omega) = \rho_a\,[\rho_1(j\omega), \rho_2(j\omega)] \tag{34}$$

Then we adopt the view that the $D.C.$ or zero frequency solutions are a convenient reference. Thus, set

$$\rho_1(j\omega) = \rho_1(0)\,[1 + \delta_1(j\omega)] \tag{35}$$

$$\rho_2(j\omega) = \rho_2(0)\,[1 + \delta_2(j\omega)] \tag{36}$$

and

$$\rho_3(j\omega) = \rho_a(0)\,[1 + \delta_a(j\omega)] \tag{37}$$

where δ_1, δ_2 and δ_a can be regarded as dispersion functions which vanish as $\omega \to 0$. We now employ a MacLaurin series expansion so that in effect

$$\rho_a(1 + \delta_a) = \sum_{n=0}^{N-1} \frac{1}{n!} \left[\rho_1\delta_1 \frac{\partial}{\partial\rho_1} + \rho_2\delta_2 \frac{\partial}{\partial\rho_2}\right]^n \rho_a(\rho_1, \rho_2) + R_N \tag{38}$$

where R_N is a suitably defined remainder term [Sokolnikoff 1939]. It is to be noted that the derivatives in (38) involve only DC resistivities. To be explicit, we should note that

$$\frac{\partial\rho_a}{\partial\rho_1} = \lim_{\substack{\delta_1 \to 0 \\ \delta_2 \to 0}} \left[\frac{\partial\rho_a(\rho_1(1+\delta_1), \rho_2(1+\delta_2))}{\partial(\rho_1(1+\delta_1))}\right] \tag{39}$$

with a similar convention for the other derivatives.

In accordance with the form of (38) we may write

$$\delta_a(j\omega) = B_1\delta_1(j\omega) + B_2\delta_2(j\omega) + B_{1,1}\delta_1^2(j\omega) + B_{2,2}\delta_2^2(j\omega) + B_{1,2}\delta_1(j\omega)\delta_2(j\omega) + \cdots \tag{40}$$

where, to be explicit,

$$B_1 = \frac{\rho_1(0)}{\rho_a(0)}\frac{\partial\rho_a(0)}{\partial\rho_1(0)} = \frac{\rho_1}{\rho_a}\frac{\partial\rho_a}{\partial\rho_1} = \frac{\partial \ln\rho_a}{\partial \ln\rho_1} \tag{41}$$

is, by definition, a dilution factor. Similarly

$$B_2 = \frac{\rho_2}{\rho_a}\frac{\partial\rho_a}{\partial\rho_2} = \frac{\partial \ln\rho_a}{\partial \ln\rho_2} \tag{42}$$

is also a dilution factor. Both B_1 and B_2 as defined involve only DC resistivity functions and such a convention conforms with the original works of Siegel [1959]. As indicated, the dilution concept refers to the first order diminuition of the responses of the constitutive regions* On the other hand, the higher order terms in (42) produce a more complicated change of the apparent dispersion function [Wait 1981]. Thus, we call these coefficients distortion factors and the second order forms are defined by

$$B_{1,1} = \frac{1}{2}\frac{\rho_1^2}{\rho_a}\frac{\partial^2\rho_a}{\partial\rho_1^2} \tag{43}$$

$$B_{2,2} = \frac{1}{2}\frac{\rho_2^2}{\rho_a}\frac{\partial^2\rho_a}{\partial\rho_2^2} \tag{44}$$

and

$$B_{1,2} = \frac{\rho_1\rho_2}{\rho_a}\frac{\partial^2\rho_a}{\partial\rho_1\partial\rho_2} \tag{45}$$

where again only DC (real) resistivity functions are used.

---

* From Webster: Dilute — to make thinner, to diminish,.....
Distort — to twist out of regular shape,.....

Exercise Using the "homogeneity" property stated by (18), show that the following identities exist [Wait 1986b]

$$B_1 = 1 - B_2 \tag{46}$$

$$B_{1,1} + B_{1,2} + B_{2,2} = 0 \tag{47}$$

and

$$B_{1,1} = B_{2,2} = -\frac{1}{2}B_{1,2} \tag{48}$$

Also show that

$$B_{1,2} = \frac{\partial B_2}{\partial \ln \rho_1} + B_1 B_2 \tag{49}$$

f. Extension to Time Domain

The series expansion of the dispersion function, involving only DC resistivities, is particularly suitable for dealing with the time-domain or transient response [Wait 1982, 1986b]. We discuss this problem here in the context of the quasi-static theory.

When a step current $I_0 u(t)$ is injected into the current electrodes, the corresponding voltage response $v(t)$ is expressible in the form

$$v(t) = I_0 \rho_a(0) A(t) \tag{50}$$

where $\rho_a(0)$ is the DC apparent resistivity and $A(t)$ is the normalized step response (i.e. $A(t) \to 1$ as $t \to \infty$). Then from linear system theory

$$A(t) = \frac{1}{\rho_a(0)} \mathcal{L}^{-1} \frac{\rho_a(s)}{s} \tag{51}$$

where $\mathcal{L}^{-1}$ is the inverse of the Laplace transform operator. Alternatively, we can write

$$\rho_a(s)/s = \rho_a(0) \mathcal{L} A(t) \tag{52}$$

Clearly, if $\rho_a(s)$ could be replaced by $\rho_a(0)$, corresponding to non-dispersion, $A(t)$ would simply be the unit step function $u(t)$.

If we now use (51) in conjunction with (40), it is evident that the step function response is given by

$$\begin{aligned} A(t) = & u(t) + B_1 \mathcal{L}^{-1} \frac{\delta_1(s)}{s} + B_2 \mathcal{L}^{-1} \frac{\delta_2(s)}{s} + B_{1,1} \mathcal{L}^{-1} \frac{\delta_1{}^2(s)}{s} \\ & + B_{2,2} \mathcal{L}^{-1} \frac{\delta_2{}^2(s)}{s} + B_{1,2} \mathcal{L}^{-1} \frac{\delta_1(s)\delta_2(s)}{2} + \cdots \end{aligned} \tag{53}$$

The functions $B_1, B_2, B_{1,1} \cdots$ etc are real and time independent.

To discuss the time domain responses in a more explicit manner, it is desirable to introduce the "decay function" $M(t)$ which for $t > 0$ is defined by

$$M(t) = 1 - A(t) \tag{54}$$

Clearly, this corresponds to the response at the potential electrodes *following* the cessation of a steady current I_0 applied to the current electrodes. Then we may write

$$\begin{aligned} M(t) =& B_1 m_1(t) + B_2 m_2(t) + B_{1,1} m_{1,1}(t) + B_{2,2} m_{2,2}(t) \\ &+ B_{1,2} m_{1,2}(t) + \cdots \end{aligned} \tag{55}$$

where

$$m_1(t) = -\mathcal{L}^{-1}\delta_1(s)/s \tag{56}$$

$$m_2(t) = -\mathcal{L}^{-1}\delta_2(s)/s \tag{57}$$

$$m_{1,1}(t) = -\mathcal{L}^{-1}\delta_1{}^2(s)/s \tag{58}$$

$$m_{2,2}(t) = -\mathcal{L}^{-1}\delta_2{}^2(s)/s \tag{59}$$

$$m_{1,2}(t) = -\mathcal{L}^{-1}\delta_1(s)\delta_2(s)/s \tag{60}$$

It is certainly evident from the form of (55) that the first two terms on the R.H.S. represent pure "dilution" of the response. The succeeding second order terms lead to "distortion" or mutilation of the decay curve shapes.

By a simple application of the convolution theorem for Laplace transforms, we may express (55) in the explicit form [Wait, 1986b]:

$$\begin{aligned} M(t) =& B_1 m_1(t) + B_2 m_2(t) \\ &- B_{1,1}\left[\int_0^t m_1'(t-\tau) m_1(\tau) d\tau + m_1(0) m_1(t)\right] \\ &- B_{2,2}\left[\int_0^t m_2'(t-\tau) m_2(\tau) d\tau + m_2(0) m_2(t)\right] \\ &- B_{1,2}\left[\int_0^t m_1'(t-\tau) m_2(\tau) d\tau + m_1(0) m_2(t)\right] + \cdots \end{aligned} \tag{61}$$

Clearly higher order terms involve multiple convolution integrals that represent further distortion of the decay curves.

Exercise Choose $m_1(t) = m_1 e^{-\alpha t} u(t)$ and $m_2(t) = m_2 e^{-\beta t} u(t)$ where

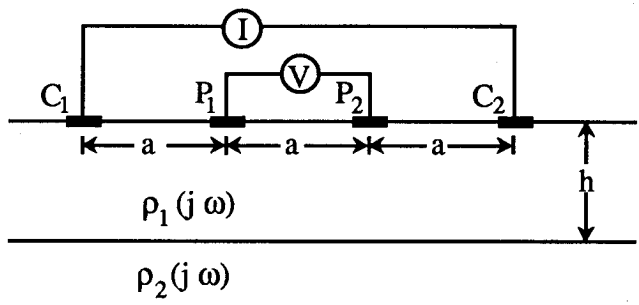

Figure 1.2.2 Four electrode Wenner array over a two layer polarizable earth.

$m_1 = m_1(0)$ and $m_2 = m_2(0)$ and where α and β are decay constants for the assumed exponential responses. Then show that [Wait 1986b]:

$$\begin{aligned} M(t) =& B_1 m_1 e^{-\alpha t} + B_2 m_2 e^{-\beta t} - B_{1,1} m_1^2 (1 - \alpha t) e^{-\alpha t} \\ & - B_{2,2} m_2^2 (1 - \beta t) e^{-\beta t} - B_{1,2} m_1 m_2 \frac{1}{\beta - \alpha} \left[\beta e^{-\beta t} - \alpha e^{-\alpha t}\right] \\ & + \cdots \end{aligned} \tag{62}$$

g. Two Layer Polarizable Earth Model

To illustrate the concept of dilution and distortion, it is desirable to adopt a concrete model which involves two well-defined regions. Such an example is a two layer flat earth model as illustrated in Fig. 1.2.2. For convenience, a four electrode array is shown with the current electrodes, C_1 and C_2, outside the potential electrodes, P_1 and P_2. The common spacing between the electrodes of this so-called Wenner array is a. The current injected into the electrodes, C_1 and C_2, is $I \exp(j\omega t)$. The resulting open circuit voltage at the potential electrodes is $V \exp(j\omega t)$. The apparent complex resistivity $\rho_a(j\omega)$ is defined according to

$$\frac{V}{I} = \frac{\rho_a(j\omega)}{2\pi a} \tag{63}$$

Assuming the validity of potential theory (i.e. electromagnetic coupling is negligible), it follows that

$$\frac{\rho_a(j\omega)}{\rho_1(j\omega)} = 1 + 2y \sum_{m=1}^{\infty} [N(j\omega)]^m \Omega(y,m) \tag{64}$$

where

$$y = a/h = \text{electrode spacing/upper layer thickness}$$

$$N(j\omega) = \frac{\rho_2(j\omega) - \rho_1(j\omega)}{\rho_2(j\omega) + \rho_1(j\omega)} \tag{65}$$

and

$$\Omega(y,m) = \frac{1}{m}\left[\frac{1}{[1+(y^2/4m^2)]^{\frac{1}{2}}} - \frac{1}{[1+(y^2/m^2)]^{\frac{1}{2}}}\right] \tag{66}$$

Exercise Derive the preceding expression for ρ_a/ρ_1 assuming DC theory is relevant using an image method. Note, C_1 can be treated as a current point source and C_2 a current point sink [e.g. Wait, 1982, Chap. 1].

In order to show explicit results, we need to specify a dispersion model for two polarizable regions. We follow current practice and adopt the Cole-Cole representation which is a versatile four-parameter model. In the present context,

$$\rho_1(j\omega) = \rho_1(\infty) + \frac{\rho_1(0) - \rho_1(\infty)}{1 + (j\omega\tau_1)^{k_1}} \tag{67}$$

and

$$\rho_2(j\omega) = \rho_2(\infty) + \frac{\rho_2(0) - \rho_2(\infty)}{1 + (j\omega\tau_2)^{k_2}} \tag{68}$$

where $\rho_i(0)$ and $\rho_i(\infty)$ are the zero and infinite frequency limits, respectively, of the complex resistivity of the ith layer ($i = 1, 2$), τ_i is a relaxation time constant, and k_i is a dispersion index. The index k_j would be 1 for a pure polar liquid but for geological materials it would range typically from 0.6 to 0.1.

Using the basic definitions for the dilution factors as given by (41) and (42), we may deduce the "first order" approximation

$$\rho_a(j\omega) \cong \rho_a(0)[1 + \delta_a(j\omega)] \tag{69}$$

where

$$\delta_a(j\omega) = B_1\delta_1(j\omega) + B_2\delta_2(j\omega) \tag{70}$$

The "second order" approximation is given by

$$\begin{aligned}\delta_a(j\omega) =& B_1\delta_1(j\omega) + B_2\delta_2(j\omega) + B_{1,1}\delta_1{}^2(j\omega) \\ &+ B_{2,2}\delta_2{}^2(j\omega) + B_{1,2}\delta_1(j\omega)\delta_2(j\omega)\end{aligned} \tag{71}$$

where the indicated distortion factors are deduced from (43), (44) and (45). Explicit expressions for the dilution and distortion factors are given by Gruszka and Wait [1985] for this particular configuration.

For the numerical example, we choose the "chargeability" $m_2 = [\rho_2(0) - \rho_2(\infty)]/\rho_2(0) = 0.8$ and $\rho_1(j\omega) = \rho_1(0)$. In other words, the lower region is polarizable but the upper layer (i.e. the overburden) is taken to be non-polarizable. To be representative of an actual field situation, the dispersion index k_2 for the lower region is taken to be $1/2$. Then, we specify three values of the $D.C.$ resistivity ratios of the two regions; namely,

$$C = \rho_2(0)/\rho_1(0) = 0.1,\ 1.0 \text{ and } 10$$

For the conditions indicated above, we graph the complex values of $\rho_a(j\omega)/\rho_1(0)$ in the plane in Fig. 1.2.3. The "exact" version corresponds to using (64) with the corresponding Cole-Cole form for $\rho_2(j\omega)$ given by (68). The parameter $\omega\tau$ ranges through all values from 0 to ∞ for each value of C indicated. For purpose of comparison, the curves for the first approximation given by (69) and (70) are also shown. In addition, we show the second order approximation given by (69) and (71). All curves are arcs or approximately arcs of circles in accordance with the expected behavior for a Cole-Cole model [Daniel 1949, Wait 1984]. But more significantly, it is seen that the first order and even the second order approximated curves may diverge significantly from the exact form. This discrepancy is most notable for the case where $C = 0.1$ corresponding to a relatively well-conducting overburden. When the lower region is better conducting than the upper layer, the divergence of the curves is almost insignificant.

Actually, the numerical example we have chosen is rather extreme in the sense that the polarization (i.e. dispersion) in the lower layer is very high. When m_2 is reduced from 0.8 to say 0.2, the first order approximation, involving just the real dilution factors, B_1 and B_2, is very good for all values of the resistivity contrast. Some further examples are given by Gruszka and Wait [1985].

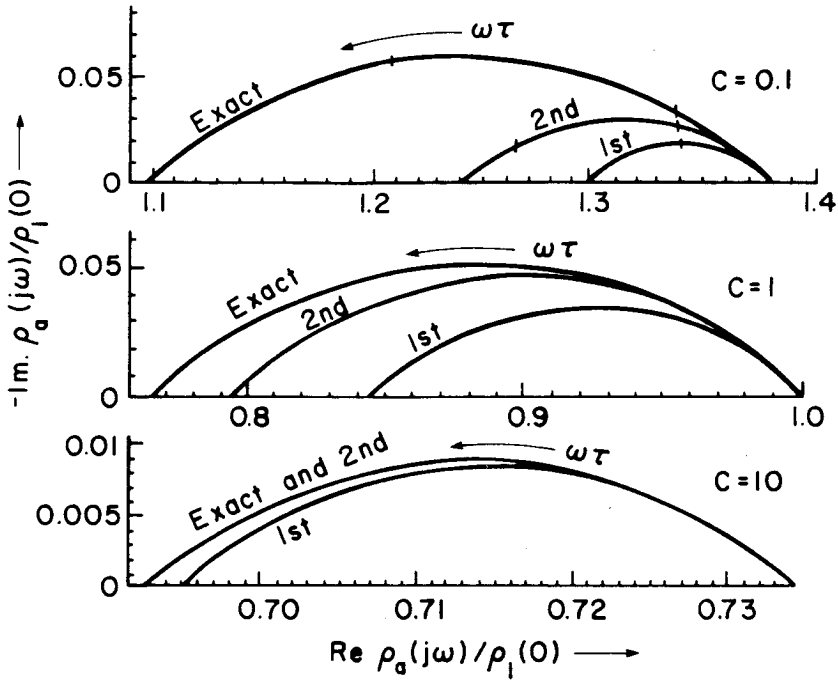

Figure 1.2.3 Complex resistivity trajectories in Argand plane for two layer polarizable earth model.

Exercise Consider a multi-region model [Wait, 1982] where

$$\rho_a(j\omega) = \rho_a[\rho_1(j\omega),\ \rho_2(j\omega),\ \rho_3(j\omega),\ \cdots \rho_J(j\omega)] \tag{72}$$

where $\rho_i(j\omega)$ is the complex resistivity of the ith homogeneous region (and $i = 1, 2, 3 \cdots J$). In analogy, to the two region cases, show that

$$\rho_a(j\omega) = \rho_a(0)\,[1 + \delta_a(j\omega)] \tag{73}$$

where

$$\delta_a(j\omega) \simeq \sum_{i=1}^{J} B_i \delta_i(j\omega) \tag{74}$$

when the dilution factors are defined in terms of the *D.C.* resistivities such that

$$B_i = \frac{\rho_i}{\rho_a}\frac{\partial \rho_a}{\partial \rho_i} = \frac{\partial \ln \rho_a}{\partial \ln \rho_i} \tag{75}$$

and

$$\sum_{i=1}^{J} B_i = 1 \tag{76}$$

h. An Alternative Approach

A further approximate representation follows from the fact that for a two-region problem, we can write

$$\rho_a(j\omega) = \rho_1(j\omega) f\left(\frac{\rho_2(j\omega)}{\rho_1(j\omega)}\right) \tag{77}$$

where f is a function of the complex ratio of the two complex resistivities. An equivalent statement of (77) is

$$\frac{\rho_a(0)[1+\delta_a(j\omega)]}{\rho_1[1+\delta_1(j\omega)]} = f\left(\frac{\rho_2}{\rho_1}[1+\delta_\tau(j\omega)]\right) \tag{78}$$

where

$$1+\delta_\tau(j\omega) = \frac{1+\delta_2(j\omega)}{1+\delta_1(j\omega)} \tag{79}$$

and where it is understood that $\rho_1 = \rho_1(0)$ and $\rho_2 = \rho_2(0)$ are the *D.C.* resistivity values.

Following Gruszka [1987], we now expand the right hand side of (78) about $\delta_\tau = 0$. Thus

$$\begin{aligned}\frac{\rho_a(0)[1+\delta_a(j\omega)]}{\rho_1[1+\delta_1(j\omega)]} =& f\left(\frac{\rho_2}{\rho_1}\right) + \frac{\rho_2}{\rho_1} f^{(1)}\delta_\tau + \frac{1}{2!}\left(\frac{\rho_2}{\rho_1}\right)^2 f^{(2)}\delta_\tau^2 \\ &+ \frac{1}{3!}\left(\frac{\rho_2}{\rho_1}\right)^3 f^{(3)}\delta_\tau^3 + \cdots + \frac{1}{n!}\left(\frac{\rho_2}{\rho_1}\right)^n f^{(n)}\delta_\tau^n + \cdots\end{aligned} \tag{80}$$

where

$$f^{(n)} = f^{(n)}\left(\frac{\rho_2}{\rho_1}\right) = \left.\frac{d^n f(x)}{dx^n}\right|_{x=\rho_2/\rho_1} \tag{81}$$

A similar expansion was also employed by Guptasarma [1984]. As Gruszka [1987] points out, we can solve for $\delta_a(j\omega)$ by inserting the expression for $\delta_r(j\omega)$, given by (79), into (80) to yield

$$\delta_a(j\omega) = \delta_1(j\omega) + \beta_1\left(\frac{\rho_2}{\rho_1}\right)(\delta_2 - \delta_1) + \beta_2\left(\frac{\rho_2}{\rho_1}\right)\frac{(\delta_2 - \delta_1)^2}{1+\delta_1} + \cdots + \beta_n\left(\frac{\rho_2}{\rho_1}\right)\frac{(\delta_2 - \delta_1)^n}{(1+\delta_1)^{n-1}} \tag{82}$$

where

$$\beta_n(x) = \frac{1}{n!}\, x^n\, \frac{f^{(n)}(x)}{f(x)} \tag{83}$$

$$\delta_1 = \delta_1(j\omega) \qquad \text{and} \qquad \delta_2 = \delta_2(j\omega)$$

Actually, (82) is a compact version of (71) as can be verified by expanding the terms of the form $(1+\delta_1)^{-m}$ about δ_1 and then collecting terms in the same order of δ_1 and δ_2. This process yields the identities

$$B_1 = 1 - \beta_1,\ B_2 = \beta_1,\ B_{11} = B_{22} = \beta_2, \text{ and } B_{12} = -2\beta_2$$

While (82) is more compact than (71), it is not as convenient for application to time domain responses as displayed by (61).

Another extension leads to expansion coefficients β_1, β_2, $\cdots$ which are complex. In this case, again following Gruszka [1987], we begin by noting that

$$\rho_a(j\omega) = |\rho_a(j\omega)|\ \exp(j\phi_a) \tag{84}$$

$$\rho_1(j\omega) = |\rho_1(j\omega)|\ \exp(j\phi_1) \tag{85}$$

and

$$\rho_2(j\omega) = |\rho_2(j\omega)|\ \exp(j\phi_2) \tag{86}$$

Thus, (78) with obvious contraction of notation can be written

$$\left|\frac{\rho_a(j\omega)}{\rho_1(j\omega)}\right| e^{j(\phi_a - \phi_1)} = f\left(\left|\frac{\rho_2(j\omega)}{\rho_1(j\omega)}\right| e^{j\phi_r}\right) \tag{87}$$

where

$$\phi_r = \phi_2 - \phi_1$$

We now take the natural logarithm of both sides of (83) to give

$$\ln\left|\frac{\rho_a(j\omega)}{\rho_1(j\omega)}\right| + j(\phi_a - \phi_1) = \ln f(\cdots) \tag{88}$$

Then, on expanding the right hand side of (88) about $\phi_r = 0$, we obtain

$$\begin{aligned}\ln\left|\frac{\rho_a(j\omega)}{\rho_1(j\omega)}\right| + j(\phi_a - \phi_1) &= \ln f(|z|) + j\beta_1(|z|)\phi_r \\ &\quad -[\beta_2(|z|) + \frac{1}{2}\beta_1(|z|) - \frac{1}{2}\beta_1^2(|z|)]\phi_r^2 + \cdots\end{aligned} \tag{89}$$

where

$$z = \rho_2(j\omega)/\rho_1(j\omega)$$

$$\beta_1(x) = \frac{x}{f(x)}\frac{\partial f(x)}{\partial x} \text{ and } \beta_2(x) = \frac{x^2}{2}\frac{\partial^2 f(x)}{\partial x^2}\frac{1}{f(x)}$$

where $x = |z|$ is real !

The definitions of $\beta_1(|z|)$ and $\beta_2(|z|)$, as a function of amplitude $|z|$, are consistent with (83), but note here $\beta_1(|z|)$ and $\beta_2(|z|)$ are frequency dependent real functions. If we now equate the real and imaginary parts of (89), it follows that the leading terms are

$$\begin{aligned}|\rho_a(j\omega)| &\simeq |\rho_1(j\omega)| f(|z|) \\ &\quad \exp\left\{-\left[\beta_2(|z|) + \frac{1}{2}\beta_1(|z|) - \frac{1}{2}\beta_1{}^2(|z|)\right](\phi_2 - \phi_1)^2\right\}\end{aligned} \tag{90}$$

and

$$\phi_a(j\omega) \simeq \phi_1 + \beta_1(|z|)(\phi_2 - \phi_1) \tag{91}$$

where, as implied above, $\phi_1 = \phi_1(j\omega)$ and $\phi_2 = \phi_2(j\omega)$ and $|z| = |\rho_2(j\omega)/\rho_1(j\omega)|$ are real functions of frequency.

As Gruszka [1987] points out, (90) can be further simplified if β_1 is near 0 or 1 and β_2 is small, the exponential term can be replaced by 1. The resulting expressions for the amplitude and phase of $\rho_a(j\omega)$ can be called the "G approximation": it bears some similarity with the form given by Guptasarma [1984] but there are some subtle differences. For example, here β_1 is conveniently a *real* function of the frequency.

It is an interesting and instructive exercise to compare three approximations for the complex resistivity $\rho_a(j\omega)$ over a specific two

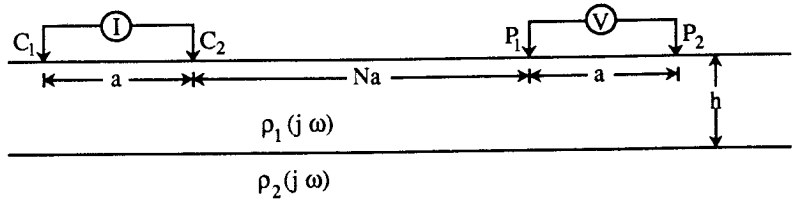

Figure 1.2.4 The dipole-dipole array over a two layer polarizable earth model.

layer model as shown in Fig. 1.2.4. Again, we are abstracting from Gruszka [1987] who used the dipole-dipole array. He gives explicit formulas for the functions β_1 and β_2 which we will not reproduce here* but they can be obtained from the prescription given by (83). The three approximations are summarized as follows

$$\rho_a(j\omega)/\rho_1 = \text{RHS (Right Hand Side)}$$

where, for the S (for Seigel) approximation,

$$\text{RHS} \simeq 1 + \delta_1(j\omega) + \beta_1 \left(\frac{\rho_2}{\rho_1}\right) [\delta_2(j\omega) - \delta_1(j\omega)] \tag{92}$$

where, for the W (for Wait) approximation,

$$\begin{aligned} \text{RHS} \simeq & 1 + \delta_1(j\omega) + \beta_1 \left(\frac{\rho_2}{\rho_1}\right) [\delta_2(j\omega) - \delta_1(j\omega)] \\ & + \beta_2 \left(\frac{\rho_2}{\rho_1}\right) [\delta_2(j\omega) - \delta_1(j\omega)]^2 \end{aligned} \tag{93}$$

and where, for the G (for Gruszka) approximation,

$$\begin{aligned} \text{RHS} \simeq & \left|\frac{\rho_1(j\omega)}{\rho_1}\right| \frac{f(|\rho_2(j\omega)/\rho_1(j\omega)|)}{f(\rho_2/\rho_1)} \\ & \exp\left[j\left(\phi_1(j\omega) + \beta_1 \left|\frac{\rho_2(j\omega)}{\rho_1(j\omega)}\right| (\phi_2(j\omega) - \phi_1(j\omega))\right)\right] \end{aligned} \tag{94}$$

* Actually, $\beta_1 = B_2$ and $\beta_2 = B_{22}$, and explicit expressions are given for $B_2(x)$ and $B_{22}(x)$ by (101) and (103), respectively.

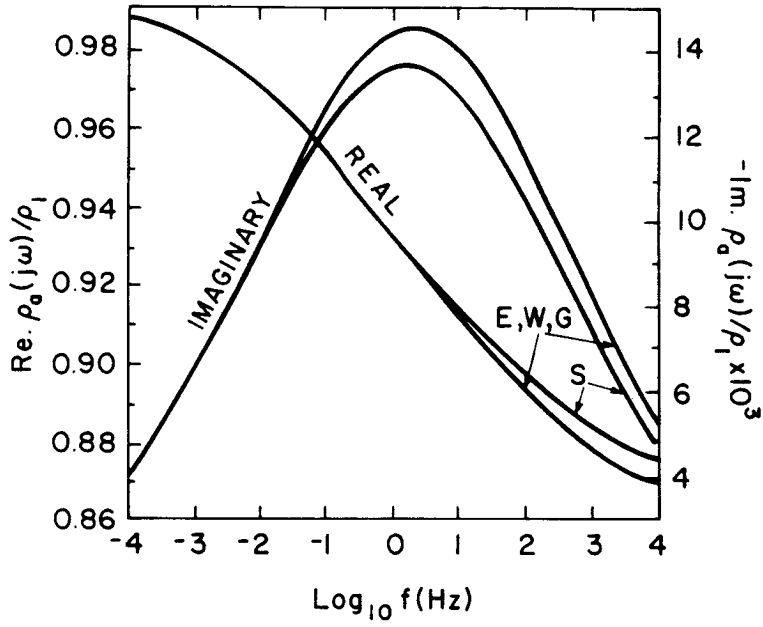

Figure 1.2.5 Real and imaginary parts of the normalized apparent resistivity for a dipole-dipole array over a two layer earth model where the lower layer is polarizable. Approximations S (Seigel), W (Wait) and G (Gruszka) are shown along with E (exact) curves. Parameters: $\rho_1 = 10^3$ **ohm m,** $m_2 = 0.2, \tau_2 = 0.1$ **sec.,** $k_2 = 0.25, N = 2, a = 20$ **m, and** $h = 10$**m .**

We characterize the two layers by Cole-Cole forms; thus

$$\rho_i(j\omega) = \rho_i \left[1 - m_i \left(1 - \frac{1}{1 + (j\omega\tau_i)^k}\right)\right] \tag{95}$$

where $i = 1, 2$. For the example illustrated here, we set $m_1 = 0$ so the upper layer is non polarizable, i.e. $\rho_1(j\omega) = \rho_1$.

Using (92), (93) and (94), we plot, in . 1.2.5, the real and imaginary parts of the normalized apparent resistivity as a function of frequency. For comparison, the corresponding "exact" results denoted by E, from Gruszka and Wait [1985] are also shown. The specific parameter values

are indicated in the caption to Fig. 1.2.5. As can be seen, only the Seigel or S approximation departs significantly from the exact calculations. Other more detailed comparisons have been given by Gruszka [1987].

Graphs of Dilution and Distortion Factors

We summarize here some results for the dilution factor B_2 and $B_{2,2}$ for dipole-dipole array located on the surface of a two-layer earth model. Electromagnetic coupling effects are not included so we may view one complication at a time. We also show analogous results for a borehole model.

The geometry of the two layer model is shown in Fig. 1.2.4 so the notation need not be discussed again. Also, the potential theory relevant to this model was already considered [Wait 1982]. Thus, we need only state the working formulas.

Following (77), we may write the *D.C.* limiting form as

$$\rho_a = \rho_1 f(\rho_2/\rho_1) \tag{96}$$

where

$$f(x) = \frac{1}{2\pi h} \sum_{i=1}^{2} \sum_{j=1}^{2} (-1)^{i+j+1} \cdot \frac{h}{x_{ij}} F(x) \tag{97}$$

and, following Gruszka (1987),

$$F(x) = 1 + \frac{2 \sum_{i=1}^{2} \sum_{j=1}^{2} (-1)^{i+j+1} \int_0^\infty \frac{K e^{-2g}}{1 - K e^{-2g}} J_0\left(g \frac{x_{ij}}{h}\right) dg}{\sum_{i=1}^{2} \sum_{j=1}^{2} (-1)^{i+j+1} \cdot \frac{h}{x_{ij}}} \tag{98}$$

where

$$K = \frac{\rho_2 - \rho_1}{\rho_2 + \rho_1} \tag{99}$$

Then to obtain the dilution factor β_2, we perform the operation

$$B_2 = \frac{\rho_2}{\rho_a} \frac{\partial \rho_a}{\partial \rho_2} \tag{100}$$

to yield

$$B_2 = \frac{\dfrac{4x}{(1+x)^2}\displaystyle\sum_{i=1}^{2}\sum_{j=1}^{2}(-1)^{i+j+1}\int_0^\infty \frac{e^{-2g}}{(1-Ke^{-2g})^2}J_0\left(g\frac{x_{ij}}{h}\right)dg}{F(x)\displaystyle\sum_{i=1}^{2}\sum_{j=1}^{2}(-1)^{i+j+1}\frac{h}{x_{ij}}} \tag{101}$$

A further differentiation is needed to obtain an explicit expression for the distortion factor $B_{2,2}$. Thus we use

$$B_{2,2} = \frac{1}{2}\frac{\rho^2}{\rho_a}\frac{\partial^2\rho_a}{\partial{\rho_2}^2} \tag{102}$$

to yield

$$B_{2,2} = \frac{\dfrac{8x^2}{(1+x)^4}\displaystyle\sum_{i=1}^{2}\sum_{j=1}^{2}(-1)^{i+j+1}\int_0^\infty \frac{e^{-4g}}{(1-Ke^{-2g})^3}J_0\left(g\frac{x_{ij}}{h}\right)dg}{F(x)\displaystyle\sum_{i=1}^{2}\sum_{j=1}^{2}(-1)^{i+j+1}\frac{h}{x_{ij}}} \tag{103}$$

As indicated, B_2 and B_{22} are real functions. Then, the second order approximation for the complex apparent resistivity is given by

$$\rho_a(j\omega) = \rho_a(1+\delta_a(j\omega)) \tag{104}$$

where

$$\begin{aligned}\delta_a(j\omega) = {} & B_1\delta_1(j\omega) + B_2\delta_2(j\omega) + B_{11}{\delta_1}^2(j\omega) \\ & + B_{12}\delta_1(j\omega)\delta_2(j\omega) + B_{22}{\delta_2}^2(j\omega)\end{aligned} \tag{105}$$

As we have indicated before $\delta_1(j\omega)$ and $\delta_2(j\omega)$ are defined in terms of the layer complex resistivities in accordance with

$$\rho_1(j\omega) = \rho_1[1+\delta_1(j\omega)] \tag{106}$$

and

$$\rho_2(j\omega) = \rho_2[1+\delta_2(j\omega)] \tag{107}$$

Also, as we indicated before,

$$B_1 = 1 - B_2 \tag{108}$$

and

$$B_{12} = -2B_{11} = -2\,B_{22} \tag{109}$$

Thus, computed data for B_2 and B_{22} provided by Gruszka [1987] are adequate to generate the complex (apparent) resistivity up to second order in δ_1 and δ_2.

The linear distances x_{ij} in (98), (101) and (103) are related to the electrode separations according to $x_{ij} = |P_j - C_i|$. Thus, for the dipole-dipole array shown in Fig. 1.2.4, $x_{11} = C_1P_1$, $x_{12} = C_1P_2$, $X_{21} = C_2P_1$ and $x_{22} = C_2P_2$ where $C_1P_1 = (N+1)a = C_2P_2$, $C_1P_2 = (N+2)a$ and $C_2P_1 = Na$ when the electrodes are all in line.

The graphical plots of B_2 and B_{22} as a function of the resistivity ration ρ_2/ρ_1 are shown in Figs. 1.2.6 and 1.2.7 for various a/h and N as indicated in the captions. Corresponding results for B_2 and B_{22}, as a function of a/h for various ρ_2/ρ_1 and N, are shown in Figs. 1.2.8 and 1.2.9. Then, the results for B_2 and B_{22}, as a function of N for various ρ_2/ρ_1 and a/h are shown in Figs. 1.2.10 and 1.2.11. These results allow one to estimate how the frequency dependence of the measured complex resistivity for a subsurface polarizable region are diluted and/or distorted by the presence of an upper layer which may or may not be polarizable.

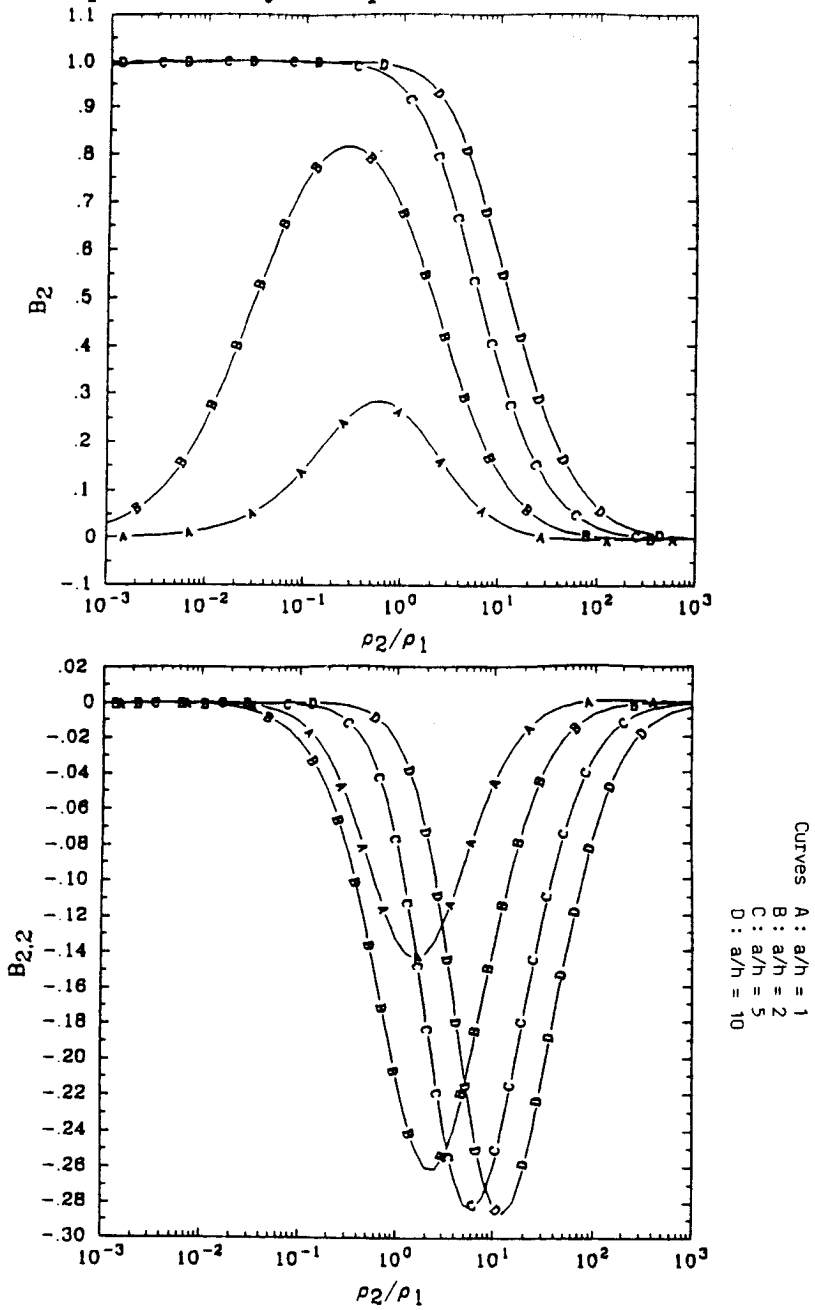

Figure 1.2.6 Dilution and distortion factors as a function of ρ_2/ρ_1 for various a/h for $N = 2$.

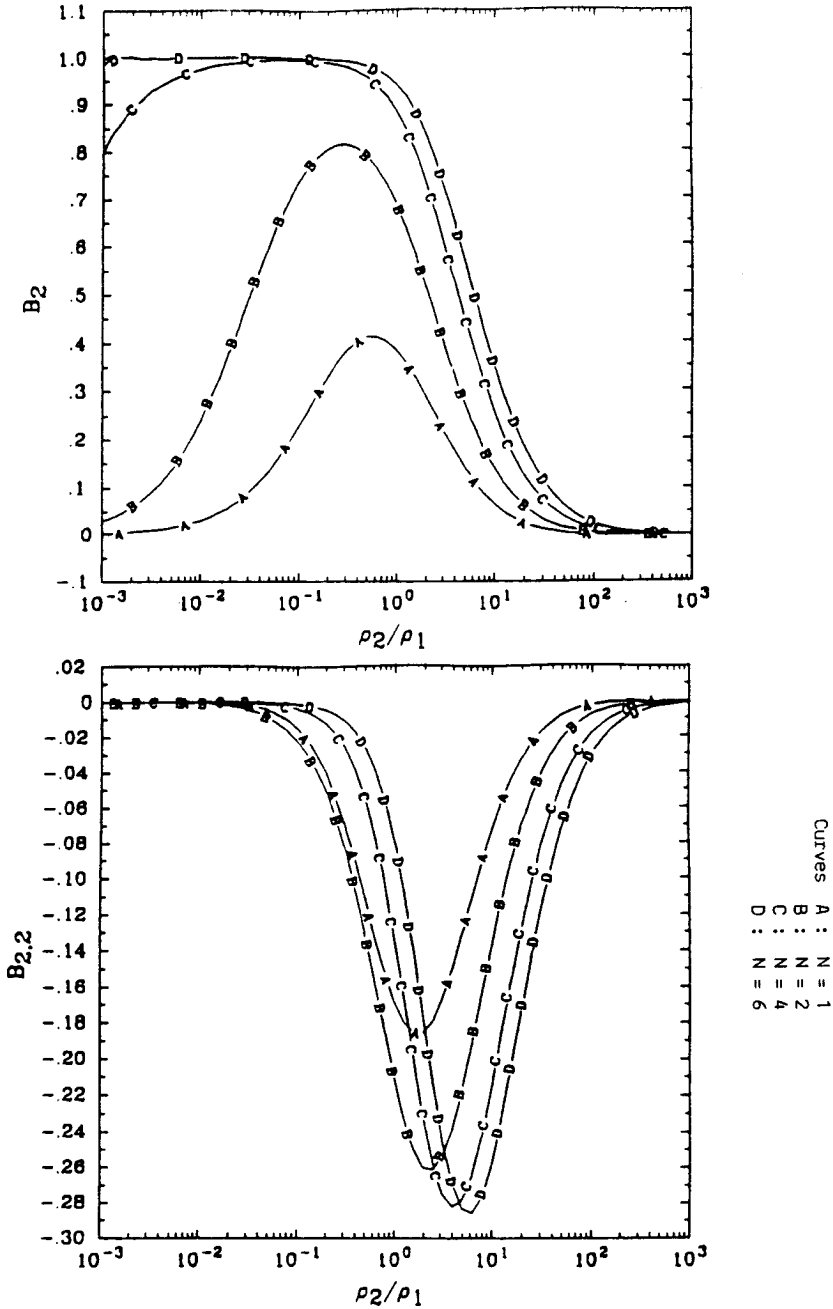

Figure 1.2.7 Dilution and distortion factors as a function of ρ_2/ρ_1 for $a/h = 2$ and for various N.

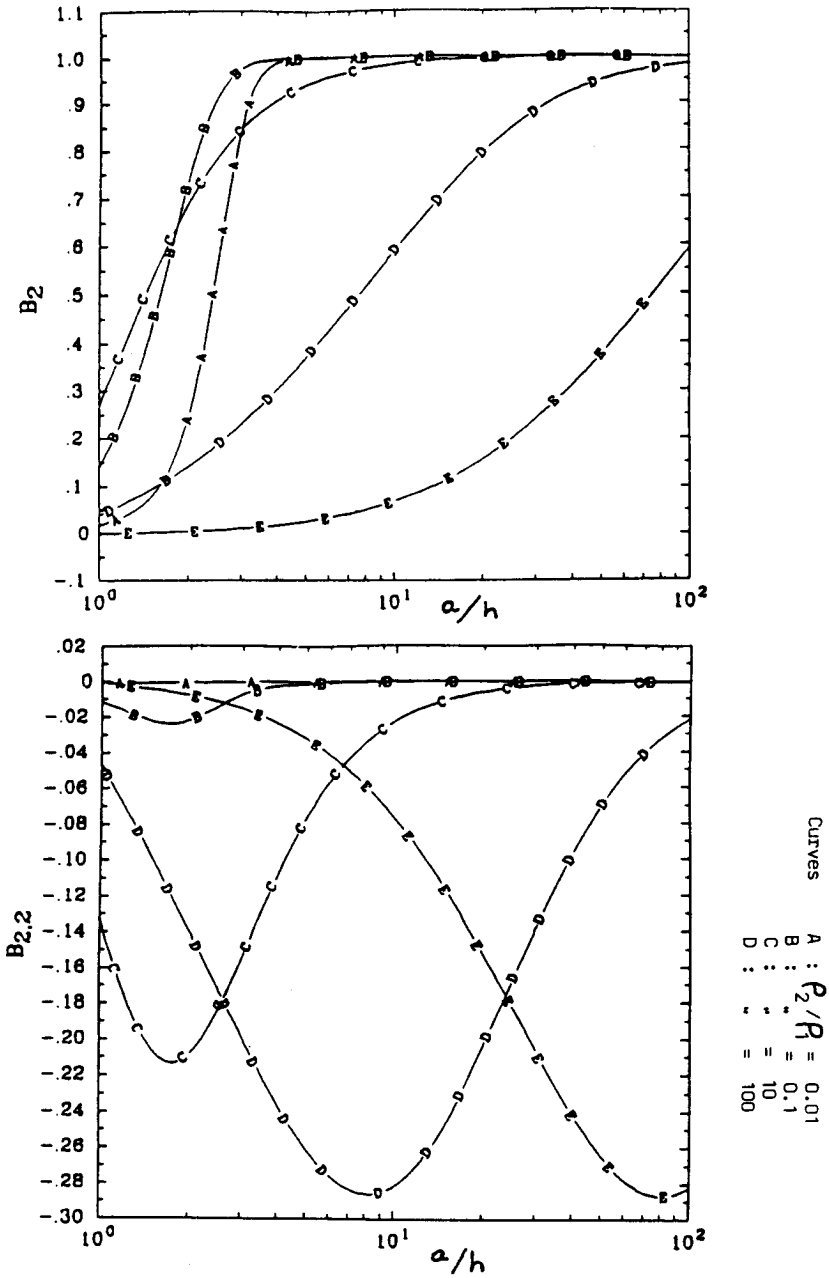

Figure 1.2.8 Dilution and distortion factors as a function of a/h for various ρ_2/ρ_1 for $N = 2$.

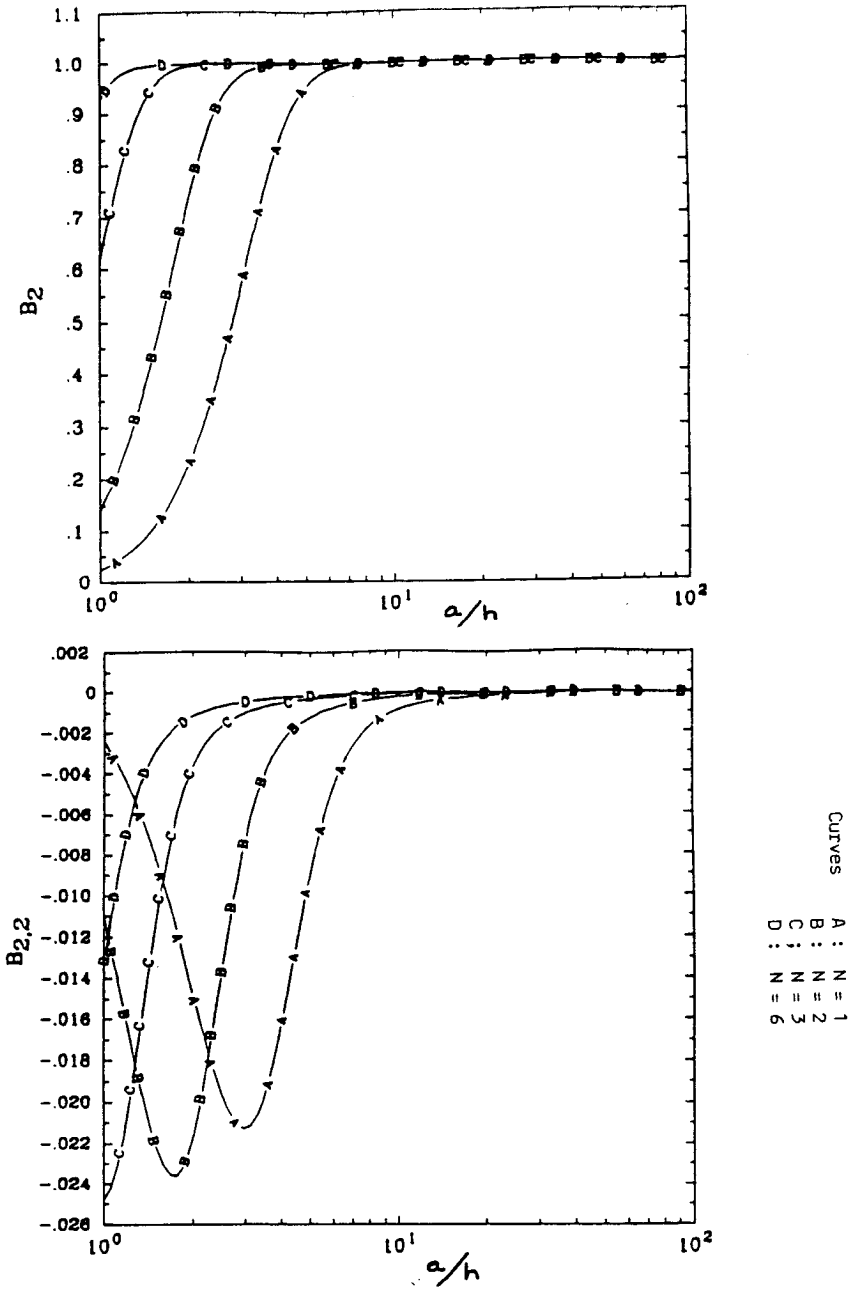

Figure 1.2.9 Dilution and distortion factors as a function of a/h for various N for ρ_2/ρ_1=0.1.

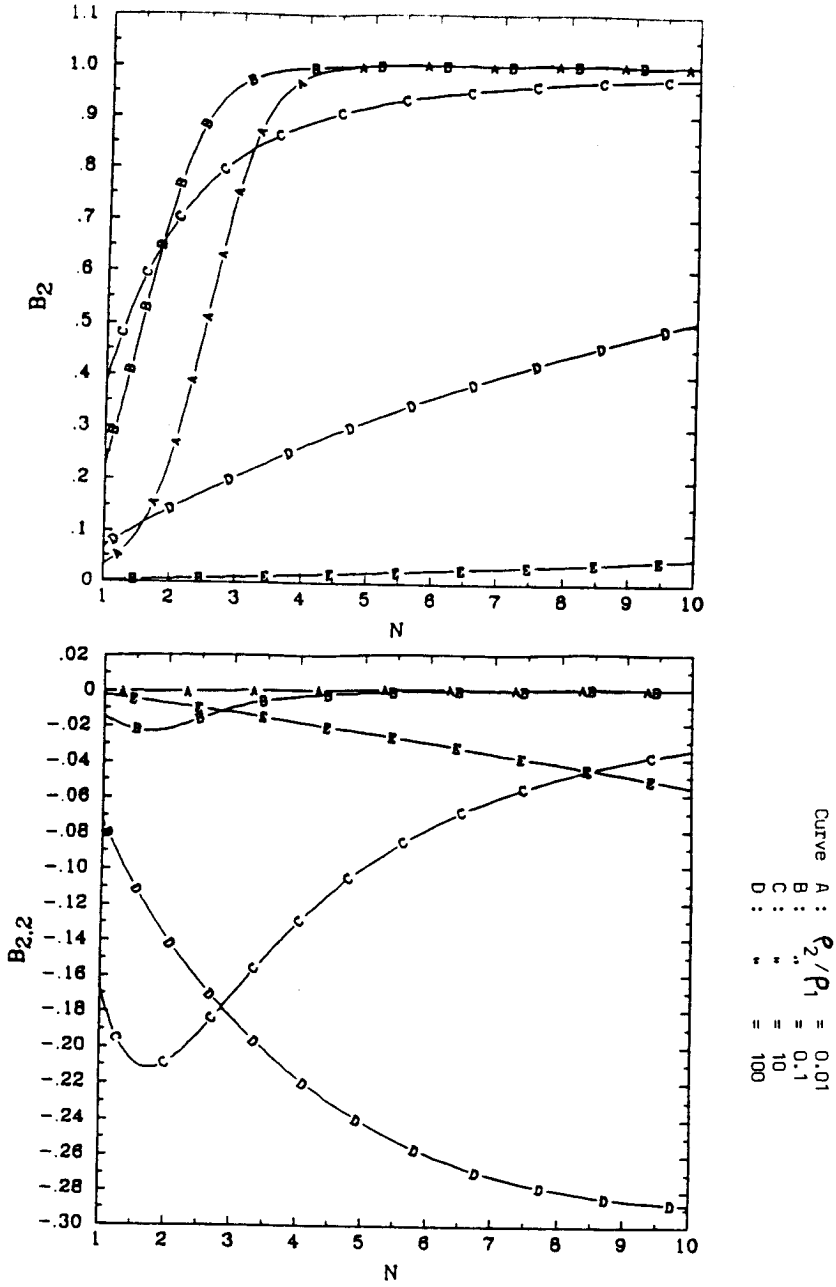

Figure 1.2.10 Dilution and distortion factors as a function of N for various ρ_2/ρ_1 for $a/h = 2$.

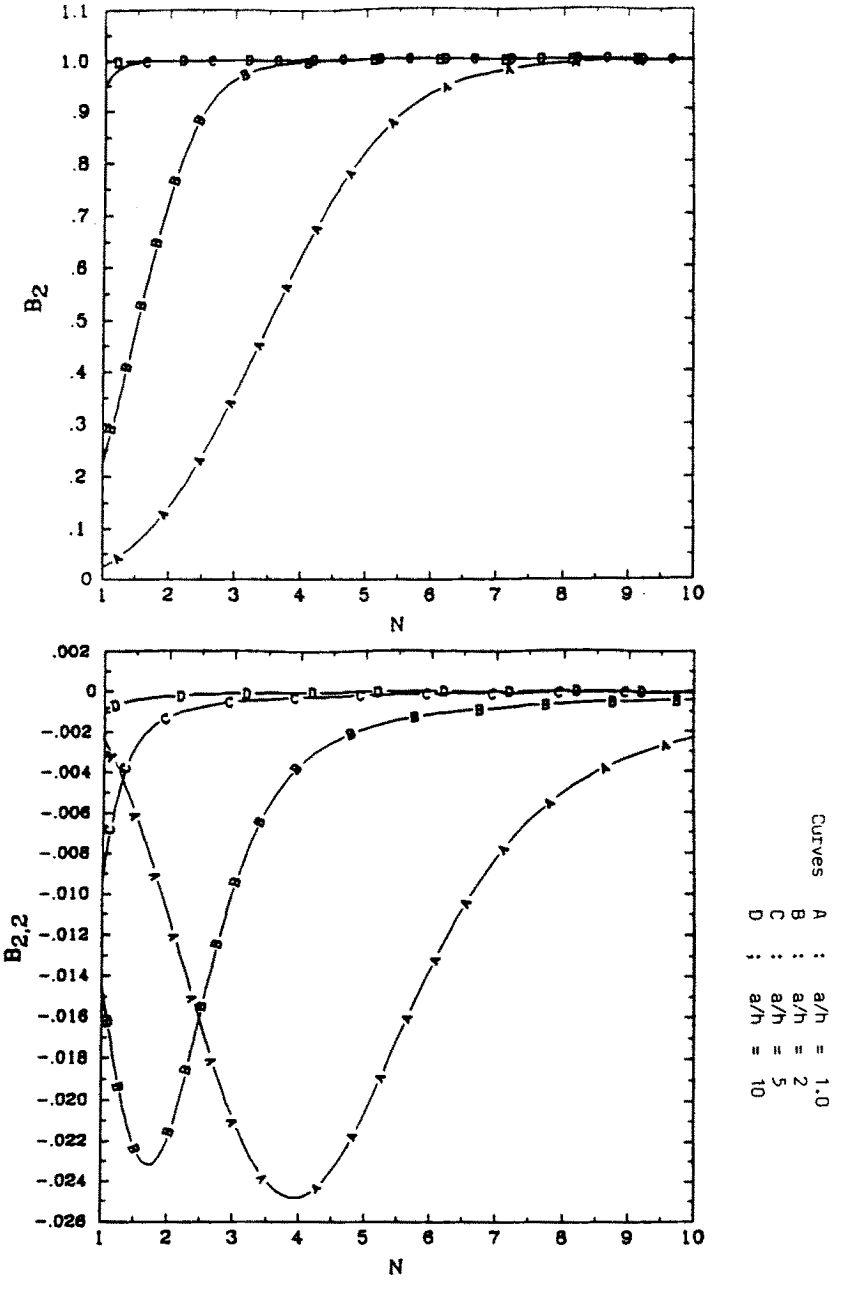

Figure 1.2.11 Dilution and distortion factors as a function of N for various a/h for $\rho_2/\rho_1 = 0.1$.

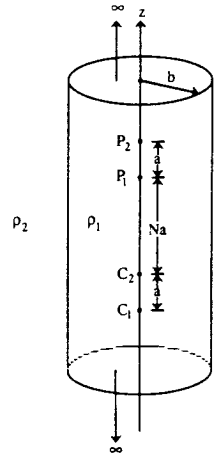

Figure 1.2.12 Dipole-dipole electrode array on the axis of a bore-hole.

We now locate the electrodes in a fluid filled bore-hole which is analogous to the two layer planar structure discussed above. The situation is shown in Fig. 1.2.12 where the electrodes are located on the axis of the cylindrical bore-hole of radius b. The resistivity of the fluid is ρ_1 and the resistivity of the external region or formation is ρ_2.

The relevant potential theory solution for this type of problem is outlined elsewhere [Chap. 1, Wait 1982, and Wait and Gruszka 1987] so we will state the working expressions without further ado. For the model shown in Fig. 1.2.12, the normalized apparent resistivity is given by

$$\frac{\rho_a}{\rho_1} = 1 + \left(\frac{2}{\pi} \sum_{j,i=1}^{2} (-1)^{i+j+1} \int_0^\infty A(\lambda b)\, \cos(\lambda x_{ij}) d\lambda \right) \Big/ \text{Den} \quad (110)$$

where

$$A(\lambda b) = -\frac{\lambda b(k-1) K_0(\lambda b) K_1(\lambda b)}{1 + \lambda b(k-1) I_0(\lambda b) K_1(\lambda b)} \quad (111)$$

where

$$k = \rho_1/\rho_2 \quad (112)$$

and

$$\text{Den} = \sum_{i=1}^{2} \sum_{j=1}^{2} (-1)^{i+j+1} \frac{1}{z_{ij}} \quad (113)$$

For the dipole-dipole array:

$$z_{11} = C_1P_1 = z_{22} = C_2P_2 = (N+1)a$$
$$z_{12} = C_1P_2 = (N+2)a \text{ and } z_{21} = C_2P_1 = Na$$

The dilution factor is obtained from

$$B_2 = \frac{\rho_2}{\rho_a}\frac{\partial \rho_a}{\partial \rho_2}$$

giving

$$B_2 = \frac{\left[k\frac{2}{\pi}\sum_{i=1}^{2}\sum_{j=1}^{2}(-1)^{i+j+1}\int_0^\infty A'(\lambda b)\,\cos(\lambda z_{ij})d\lambda\right] \Big/ \text{Den}}{1+\left[\frac{2}{\pi}\sum_{i=1}^{2}\sum_{j=1}^{2}(-1)^{i+j+1}\int_0^\infty A(\lambda b)\,\cos(\lambda z_{ij})d\lambda\right] \Big/ \text{Den}} \tag{114}$$

where

$$A'(\lambda b) = \frac{\lambda b\, K_0(\lambda b)\, K_1(\lambda b)}{[1+\lambda b(k-1)I_0(\lambda b)\, K_1(\lambda b)]^2} \tag{115}$$

The distortion factor is obtained from

$$B_{22} = \frac{{\rho_2}^2}{\rho_a}\frac{\partial^2 \rho_a}{\partial {\rho_2}^2} \tag{116}$$

which is conveniently written in the form

$$B_{22} = B_2 - 1 + \frac{\left[k^2\frac{2}{\pi}\sum_{i=1}^{2}\sum_{j=1}^{2}(-1)^{i+j+1}\int_0^\infty A''(\lambda b)\,\cos(\lambda z_{ij})d\lambda\right] \Big/ \text{Den}}{1+\left[\frac{2}{\pi}\sum_{i=1}^{2}\sum_{j=1}^{2}(-1)^{i+j+1}\int_0^\infty A(\lambda b)\,\cos(\lambda z_{ij})d\lambda\right] \Big/ \text{Den}} \tag{117}$$

where

$$A''(\lambda b) = \frac{(\lambda b)^2\, I_0(\lambda b)\, K_0(\lambda b)\, {K_1}^2(\lambda b)}{[1+\lambda b(k-1)\, I_0(\lambda b)\, K_1(\lambda b)]^3} \tag{118}$$

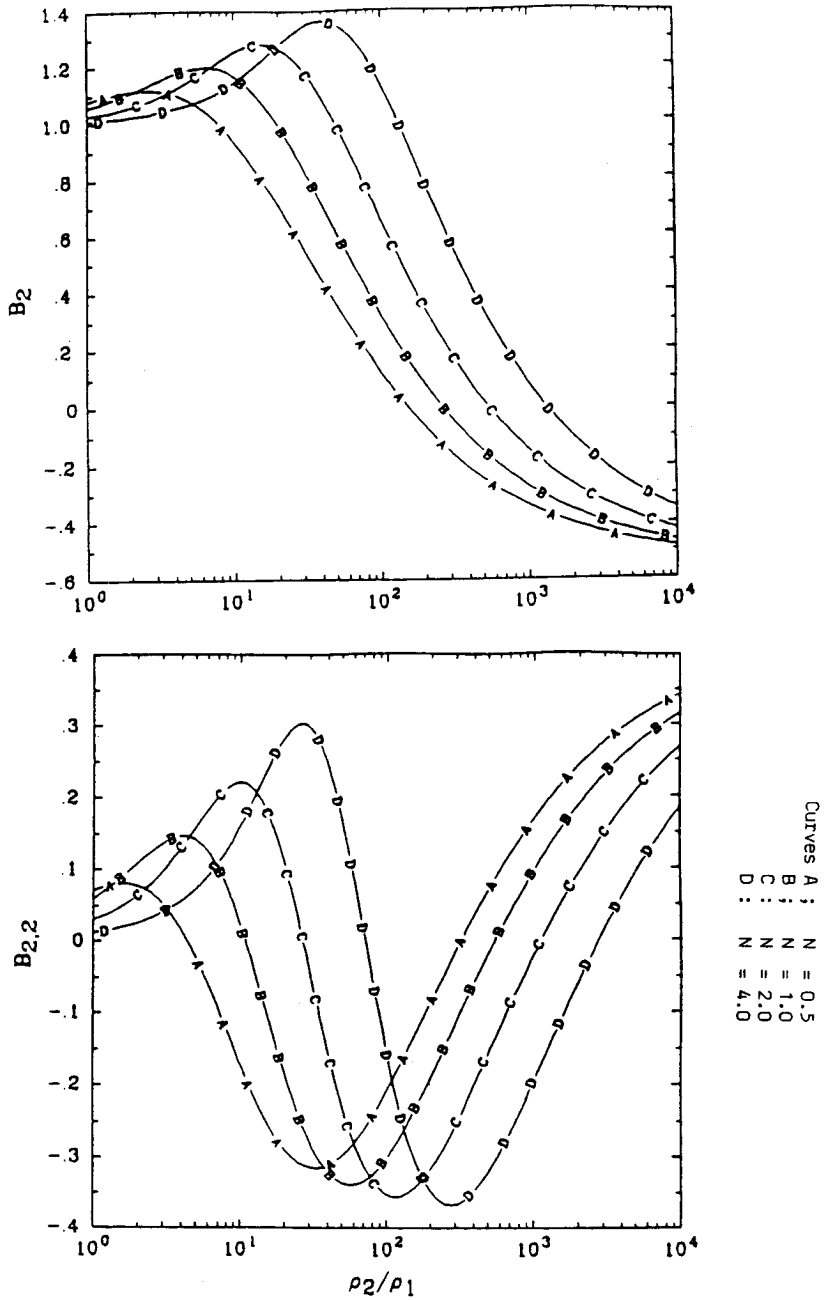

Figure 1.2.13 Dilution and distortion factors as a function of ρ_2/ρ_1 for various N for $a/b = 10$.

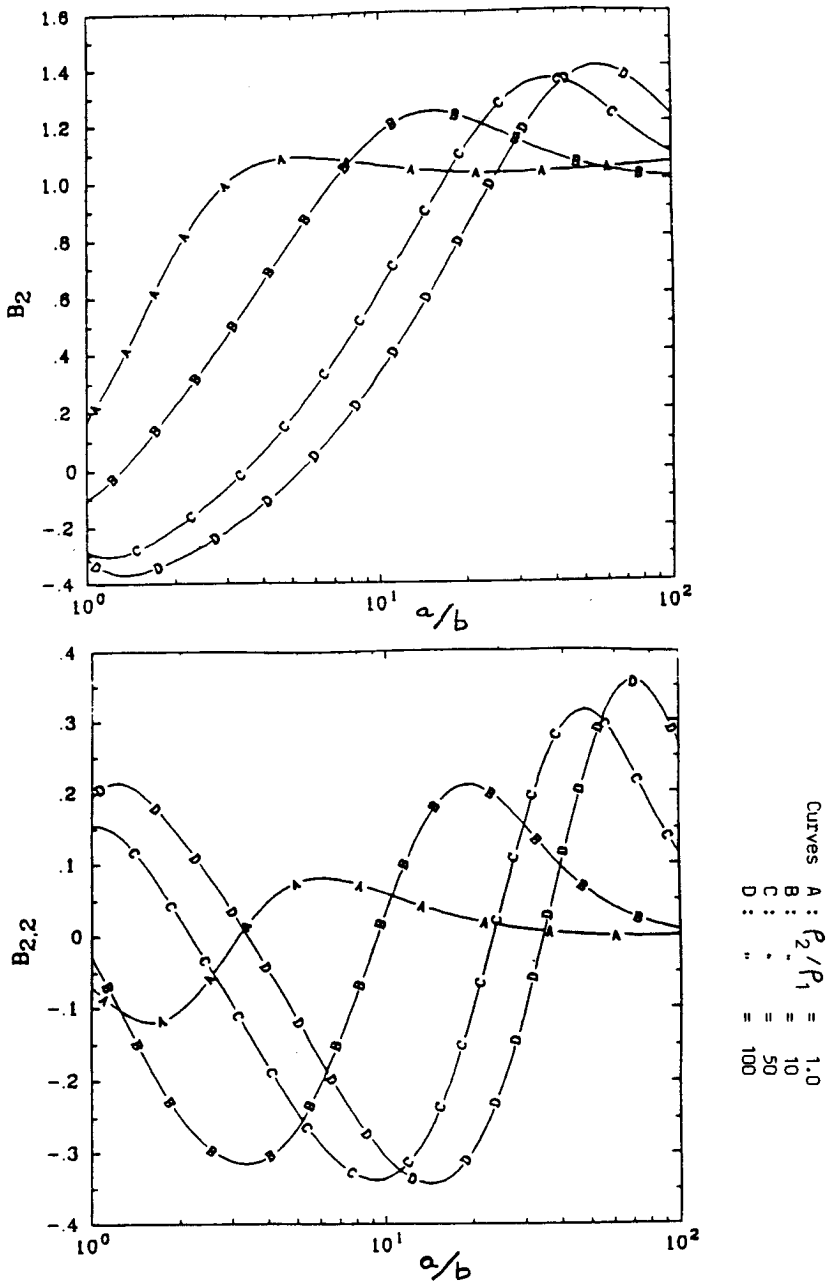

Figure 1.2.14 Dilution and distortion factors as a function of a/b for various ρ_2/ρ_1 for $N = 1.0$.

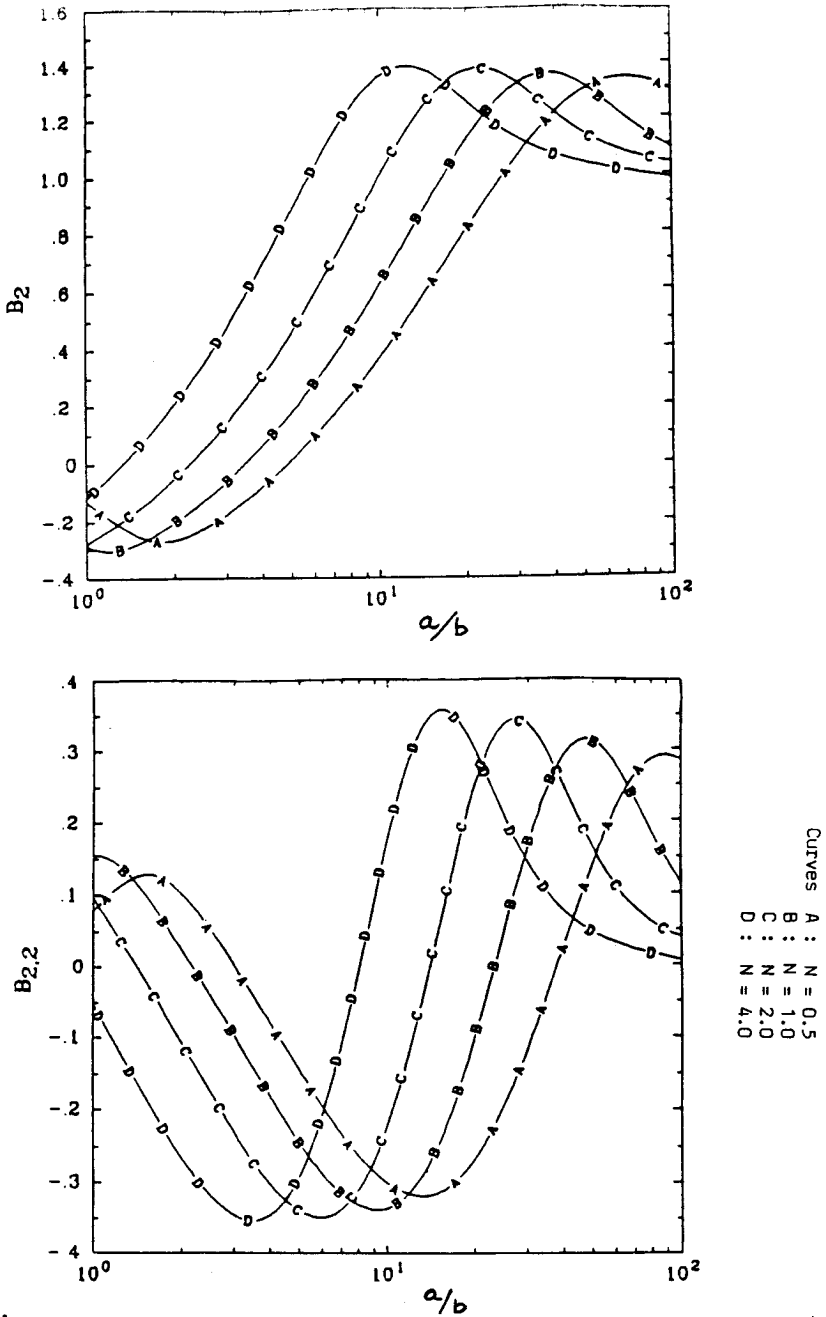

Figure 1.2.15 Dilution and distortion factors as a function of a/b for various N for $\rho_2/\rho_1 = 50$.

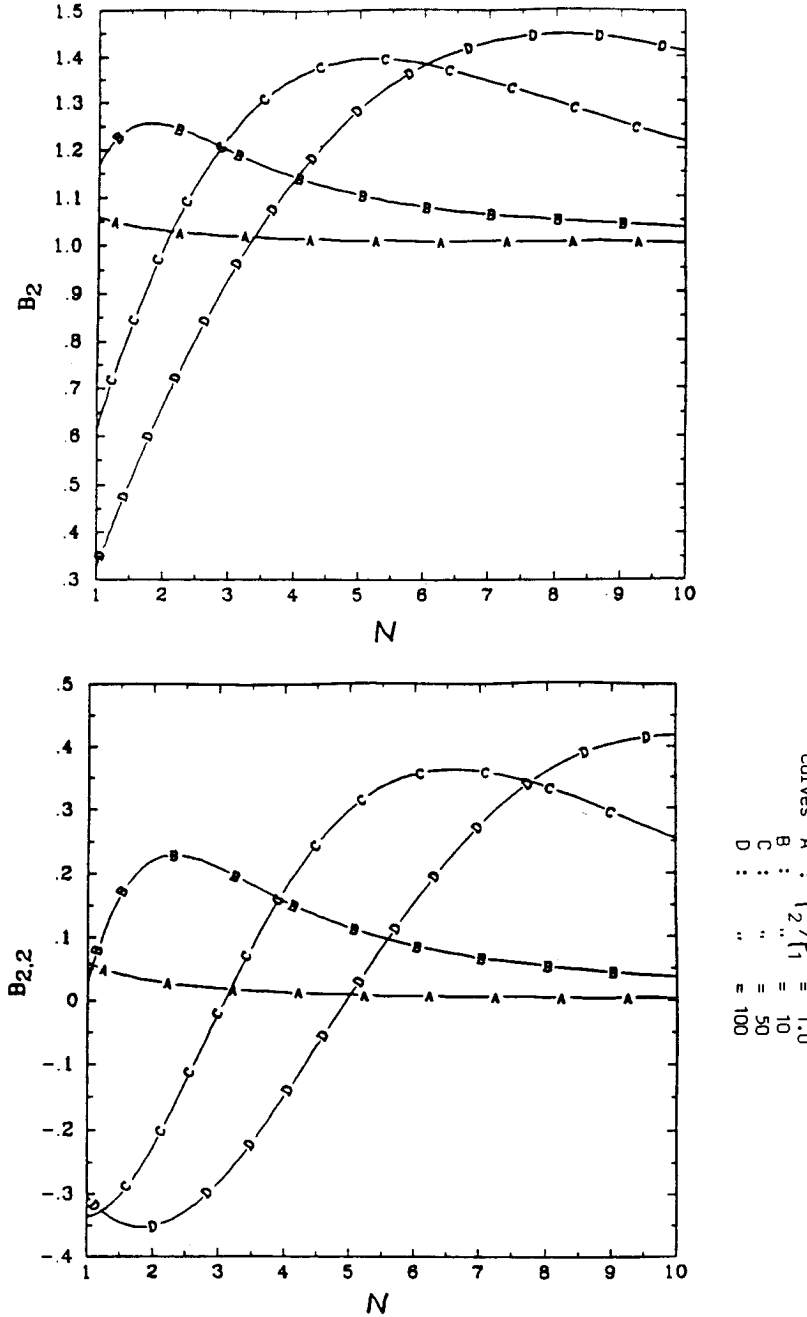

Figure 1.2.16 Dilution and distortion factors as a function of N for a/b =10 for various ρ_2/ρ_1.

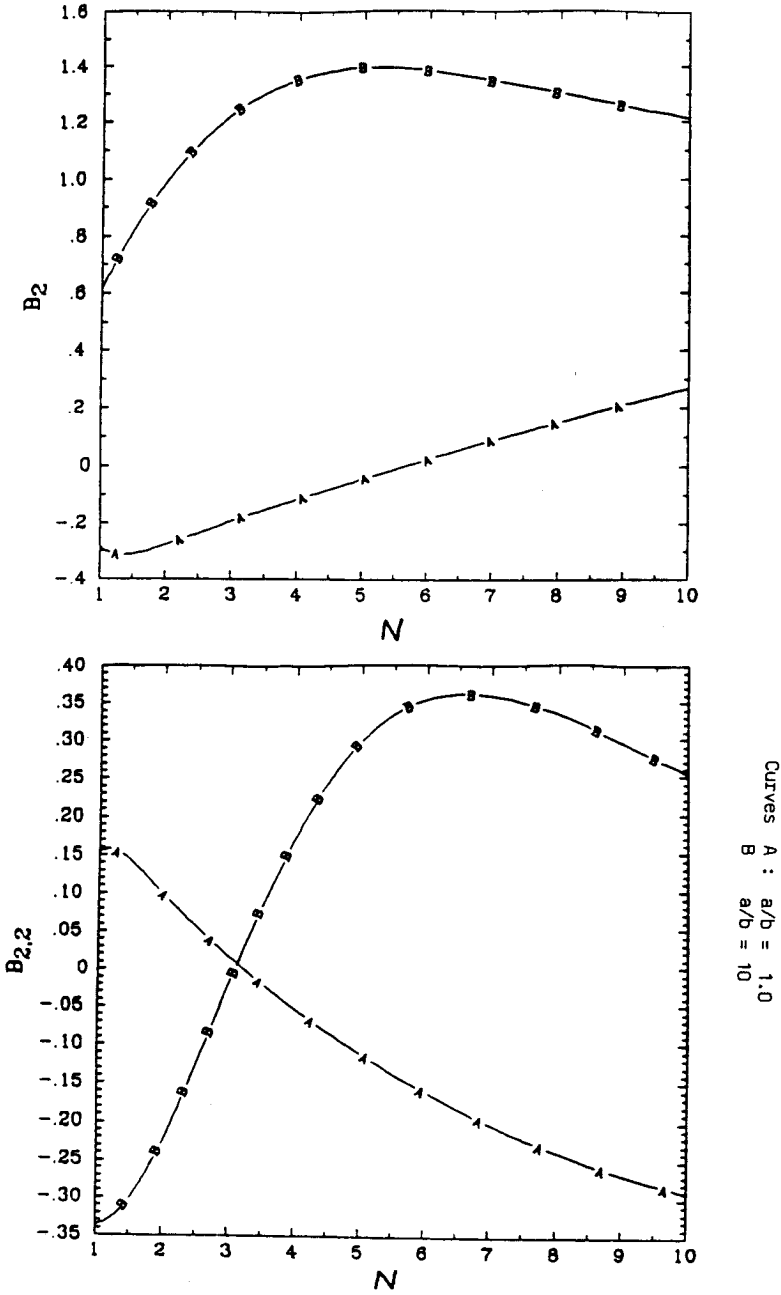

Figure 1.2.17 Dilution and distortion factors as a function of N for various a/b for $\rho_2/\rho_1 = 50$.

We present graphical results for B_2 and B_{22} for this borehole configuration using a similar format to the case above for the two layer planar model. The curves are shown in Figs. 1.2.13 to 1.2.17 where the parameters are the resistivity ratio ρ_2/ρ_1, spacing/hole radius ratio a/b, and spacing number N. Here, it is of interest to note that the dilution factor B_2 can become negative (e.g. as in Fig. 1.2.14). This property is consistent with the observed property that the slope of $\ln \rho_a$ vs. $\ln \rho_2$ of the classical resistivity departures are indeed negative in some cases.

References

[1] Daniel, V., *Dielectric Relaxation*, Academic Press 1967.

[2] Gruszka, T. P. and J. R. Wait, "Dilution and distortion effects in the IP response of a two layer earth," *IEEE Trans.*, **GE-23**, 606-609, 1985.

[3] Gruszka, T. P., "PhD Thesis, Applied Math.Prog.," Univ. of Arizona, Dec. 1987.

[4] Guptasarma, 3 D., "True and apparent spectra of buried polarizable targets," *Geophysics*, **49**, 171–176, 1984

[5] Seigel, H. O., "Mathematical formulation and type curves for IP," *Geophysics*, **24**, 547–565, 1985.

[6] Sokolnikoff, I., *Advanced Calculus*, McGraw-Hill, 1939.

[7] Song, L. and K. Vozoff, "The complex resistivity spectra of models consisting of two polarizable media of different intrinsic properties," *Geophysical Prospecting*, **33**, 1029–1062, 1985.

[8] Wait, J. R., "Towards a general theory of IP in geophysical exploration," *IEEE Trans.*, **GE-19**, 231–234, 1981.

[9] Wait, J. R., *GeoElectromagnetism*, Academic Press, New York, 1982.

[10] Wait, J. R., "Relaxation Phenomena and IP, Geoexploration," **22**, 107–127, 1984.

[11] Wait, J. R., *Electromagnetic Wave Theory*, Harper and Row/ Wi-

ley, New York 1985.

[12] Wait, J. R., *Introduction to Antennas and Propagation*, Peter Peregrinus Ltd.,UK/IEEE Service Center, New York, 1986a.

[13] Wait, J. R., "Extensions to the phenomenological theory of IP," *IEEE Trans.*, **GE-24**, 409–414, 1986b.

[14] Wait, J. R. and T. P. Gruszka, "Resistivity and IP response for a borehole model," *IEEE Trans.*, **GE-25**, 368–372, 1987.

1.3 Resistivity and I.P. Response for an Electrode Near an Interface

a. Introduction

There are a number of instances where it is desirable to measure the complex resistivity of a geological structure near a plane interface or fault plane. A notable example is when the current and potential electrodes are located in a bore hole where the latter intersects the plane of the formation at an angle. Another example is when an in-line surface-based electrode array crosses an outcropping vertical contact at an oblique angle.

Our purpose here is to present explicit results for both the resistivity and the induced polarization response for a two-electrode or normal array in the vicinity of a plane interface between two homogeneous regions. We will describe the problem in the context of a borehole geometry but later we indicate the equivalence to the surface based scheme. The relevant frequencies are assumed to be sufficiently low that all electromagnetic propagation and coupling effects can be neglected. Also the influence of the borehole, whether empty or fluid filled, is also ignored.

b. Basic Formulation

The generic problem is really a standard one in potential theory which is usually phrased in the context of an electrostatic point charge located over a plane interface $(z = 0)$ between two dielectric half-spaces. We begin with the case where a point source C of current I is located at a height h over a plane interface separating two homogeneous conducting half-spaces of complex resistivities ρ_1 and ρ_2. The situation is illustrated in Fig. 1.3.1a and 1.3.1b. The potential Ψ at P can be measured either in the upper region $(z > 0)$ or in the lower region $(z < 0)$ as indicated in Fig. 1.3.2a or 1.3.2b, respectively. There is an obvious symmetry about the z axis so the potential $\Psi(r, z)$ is only a function of r and z.

For the region $z > 0$, we deduce directly from image theory that

$$\Psi = \frac{I\rho_1}{4\pi}\left[\frac{1}{R} + K\frac{1}{R'}\right] \tag{1}$$

where

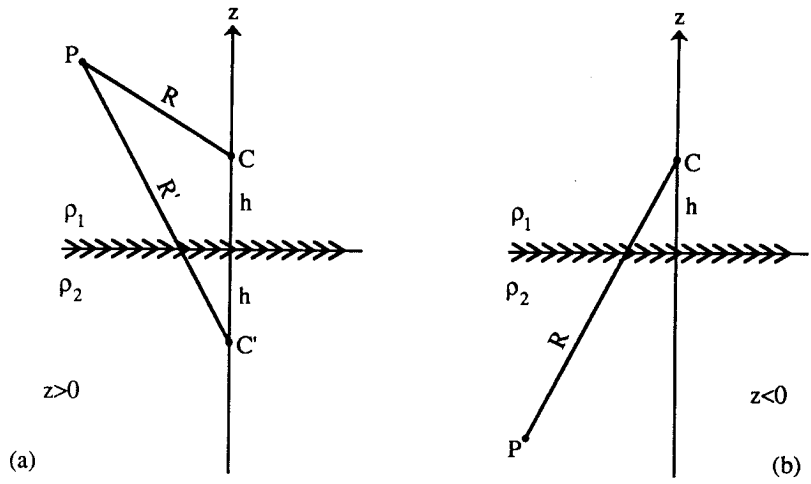

Figure 1.3.1 Generic problem of current electrode at C over a plane interface between two homogeneous regions.

$$R = \left[r^2 + (z-h)^2\right]^{\frac{1}{2}} \tag{2}$$

$$R' = \left[r^2 + (z+h)^2\right]^{\frac{1}{2}} \tag{3}$$

$$K = (\rho_2 - \rho_1)/(\rho_2 + \rho_1) \tag{4}$$

Clearly R is the distance from the source (at $r = 0, z = h$) to the observer at (r, z). On the other hand, R' is the distance from the image at $(0, -h)$ to the observer. For the region $z < 0$,

$$\Psi = \frac{I\rho_1\rho_2}{2\pi(\rho_2 + \rho_1)R} \tag{5}$$

where R is given by (2).

We can readily verify that the potential Ψ and the normal current density J_z are indeed continuous at $z = 0$. In the latter case we should note that, for $z > 0$,

$$J_z = -(1/\rho_1)\partial\Psi/\partial z \tag{6}$$

while, for $z < 0$,

$$J_z = -(1/\rho_2)\partial\Psi/\partial z \tag{7}$$

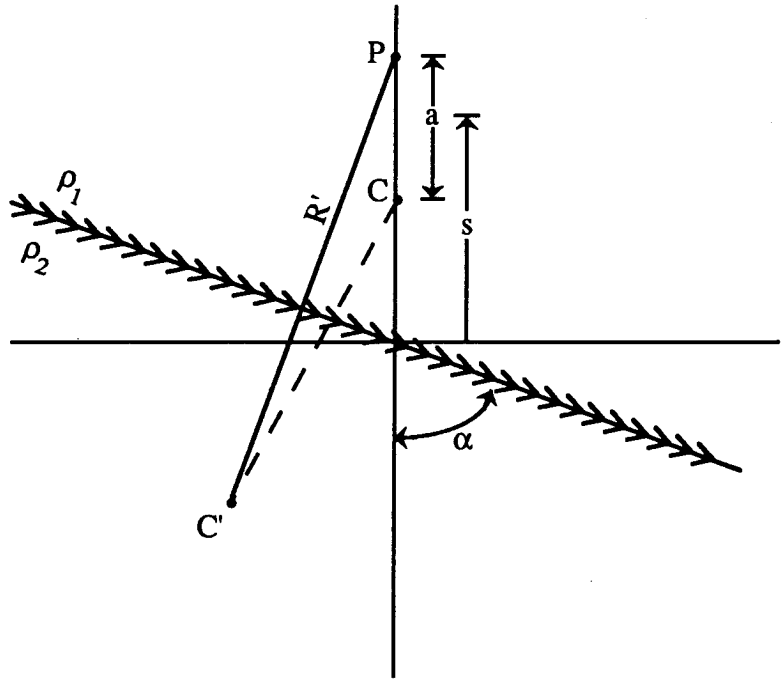

Figure 1.3.2 Geometry for borehole axis intersecting interface at an angle α.

Subject to the low frequencies, the above expressions for the potential are valid functions of frequency $\omega/(2\pi)$ when we insert the appropriate forms for the complex resistivities $\rho_1(i\omega)$ and $\rho_2(i\omega)$ for the appropriate time factor $\exp(i\omega t)$.

We now allow the borehole axis to intersect the planar interface at an angle α where $0° < \alpha < 90°$. Furthermore, the current electrode C and the potential electrode P are located on the axis of the borehole. The situation is illustrated in Fig. 1.3.2 for the case where the electrodes are both located in region 1 where the complex resistivity is $\rho_1(i\omega)$. The distance R between C and P is now denoted by a, the inter-electrode spacing. The distance R' from P to the image source C' is obtained from trigonometry and given by

$$R' = \left[2s^2(1 - \cos 2\alpha) + \frac{a^2}{2}(1 + \cos 2\alpha)\right]^{1/2} \tag{8}$$

where s is the distance from the center of the array to the interface

shown in Fig. 1.3.2.

In the case where the electrodes straddle the interface, (5) is still valid where we merely replace R by a. When the electrodes are both in the lower region, the expression for the potential at P, for a current source at C, are symmetric to the case where the electrodes are in the upper region (i.e. we interchange subscripts 1 and 2). In summary, we may write

$$\Psi = \begin{cases} \dfrac{I\rho_1}{4\pi}\left[\dfrac{1}{a} + \dfrac{\rho_2 - \rho_1}{\rho_2 + \rho_1}\dfrac{1}{R'}\right] & ; s > \dfrac{a}{2} \\ \dfrac{I\rho_1\rho_2}{2\pi(\rho_1 + \rho_2)a} & ; -\dfrac{a}{2} < s < \dfrac{a}{2} \\ \dfrac{I\rho_2}{4\pi}\left[\dfrac{1}{a} + \dfrac{\rho_1 - \rho_2}{\rho_1 + \rho_2}\dfrac{1}{R'}\right] & ; s < -\dfrac{a}{2} \end{cases} \tag{9}$$

where R' is given by (8) and it is now valid for $(-\infty < s < \infty)$.

c. *Apparent Resistivity*

Following tradition, it is convenient and desirable to define an apparent complex resistivity $\rho_a(i\omega)$ for all values of s such that

$$\Psi = I\rho_a(i\omega)/(4\pi a) \tag{10}$$

In other words, if the region were effectively homogeneous and of infinite extent, ρ_a would be the actual resistivity.

Now we are specifically interested in knowing how the ratio ρ_a/ρ_1 varies with the normalized distance s/a for various values of the ratio ρ_1/ρ_2. The explicit functional forms are

$$\frac{\rho_a}{\rho_1} = \begin{cases} 1 + \dfrac{(\rho_2 - \rho_1)/(\rho_2 + \rho_1)}{2(s/a)^2(1 - \cos 2\alpha) + (1/2)(1 + \cos 2\alpha)} & ; \dfrac{s}{a} > \dfrac{1}{2} \\ 2\rho_2/(\rho_2 + \rho_1) & ; -\dfrac{1}{2} < \dfrac{s}{a} < \dfrac{1}{2} \\ \dfrac{\rho_2}{\rho_1}\left[1 + \dfrac{(\rho_1 - \rho_2)/(\rho_1 + \rho_2)}{2(s/a)^2(1 - \cos 2\alpha) + (1/2)(1 + \cos 2\alpha)}\right] & ; \dfrac{s}{a} < -\dfrac{1}{2} \end{cases} \tag{11}$$

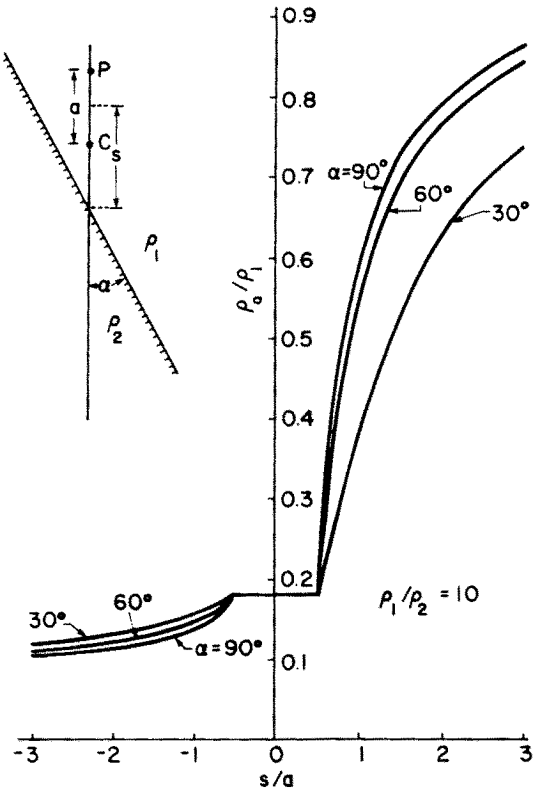

Figure 1.3.3 Apparent resistivity as a function of the vertical distance above or below the tilted interface for $\rho_1/\rho_2 = 10$.

To illustrate the results, we regard ρ_1/ρ_2 as real. In other words any relative phase shifts are ignored. Thus the normalized apparent resistivity ρ_a/ρ_1 is also real. We later show some results relevant to the case where ρ_1/ρ_2 is complex.

Using the tripartite expression (11), ρ_a/ρ_1 is plotted as a function of the normalized spacing s/a in Figs. 1.3.3 to 1.3.8 for various angles α and real values of ρ_1/ρ_2. In Fig. 1.3.3, for $\rho_1/\rho_2 = 10$, three angles $\alpha = 90°, 60°$, and $30°$ are selected. As indicated, ρ_a/ρ_1 asymptotically approaches 1.0 for large values of s/a and approaches 0.1 for large negative values of s/a. The limiting forms are approached most rapidly for $\alpha = 90°$ when the borehole intersects the interface at right angles. Very similar curves are shown in Fig. 1.3.4 where $\rho_1/\rho_2 = 0.1$. Now the limiting values of ρ_a/ρ_1 are 1.0 for large positive s/a and 10 for

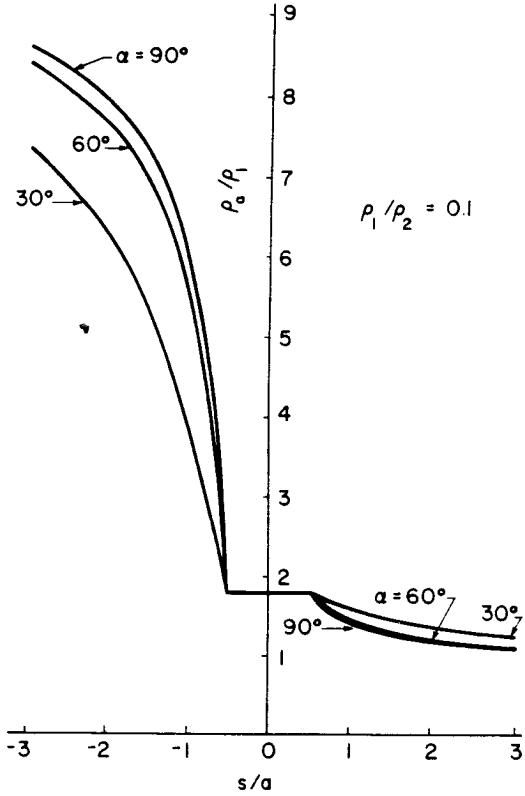

Figure 1.3.4 Apparent resistivity as a function of the vertical distance above or below the tilted interface for $\rho_2/\rho_1 = 0.1$.

large negative values of s/a. Actually the curves in Fig. 1.3.4 have a mirror symmetry with those in Fig. 1.3.3.

The influence of changing the resistivity ratio ρ_1/ρ_2 is illustrated in Fig. 1.3.5 for the case $\alpha = 90°$ only. As indicated, ρ_a/ρ_1 approaches 1.0 for large positive s/a but ρ_a/ρ_1 approaches 3, 5 and 10 for large negative s/a for $\rho_1/\rho_2 = 1/3$, $1/5$ and $1/10$, respectively.

An attempt to illustrate the symmetry of the curves when the ratio ρ_1/ρ_2 is inverted is shown in Fig. 1.3.6. In the conventional manner, we plot ρ_a/ρ_1 as a function of s/a with $\rho_1/\rho_2 = 3$ for various α values. The same curves apply to the case $\rho_1/\rho_2 = 1/3$ if the abscissa $[s/a]$ at the top and the ordinate $[\rho_a/\rho_1]$ on the right of the figure are used. Many other results could also be presented in this format at the slight risk that the reader would be confused. The curves in Fig. 1.3.6 are

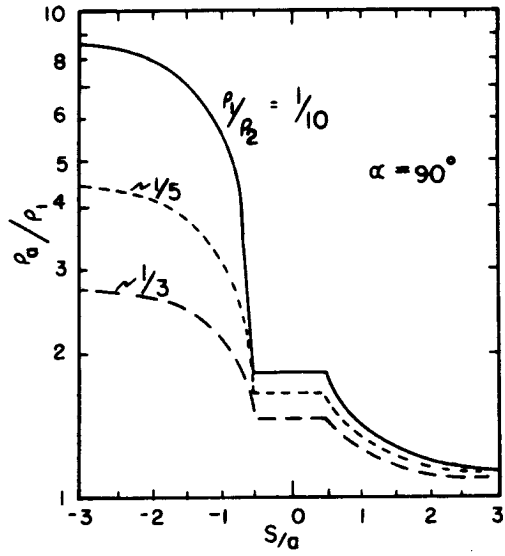

Figure 1.3.5 Apparent resistivity as a function of the distance above or below the horizontal interface for several resistivity ratios.

also intended to show the effect of a highly oblique intersection of the borehole axis with the interface. For example, at $\alpha = 5°$, the change in ρ_a/ρ_1 is within 10% over the range of s/a from -3 to $+3$. Of course, in the limit $\alpha \to 0°$, the ratio ρ_a/ρ_1 degenerates to a straight line given by

$$\rho_a/\rho_1 = 2\rho_2/(\rho_1 + \rho_2) \tag{12}$$

corresponding to the unlikely case when the borehole is coincident with the interface.

To illustrate the effect of a high resistivity contrast on each side of the interface, we choose $\rho_1/\rho_2 = 100$ and $\rho_1/\rho_2 = 0.01$. These results are shown in Figs. 1.3.7 and 1.3.8, respectively.

d. Induced Polarization and Dilution

We now wish to touch briefly on the case where one or both of the half-space regions are polarizable in the sense that the frequency dependencies of the resistivities are to be accounted for. Here, we will employ a first order theory. To this end, we write

$$\rho_a(i\omega) = \rho_a(0)[1 + \delta_a(i\omega)] \tag{13}$$

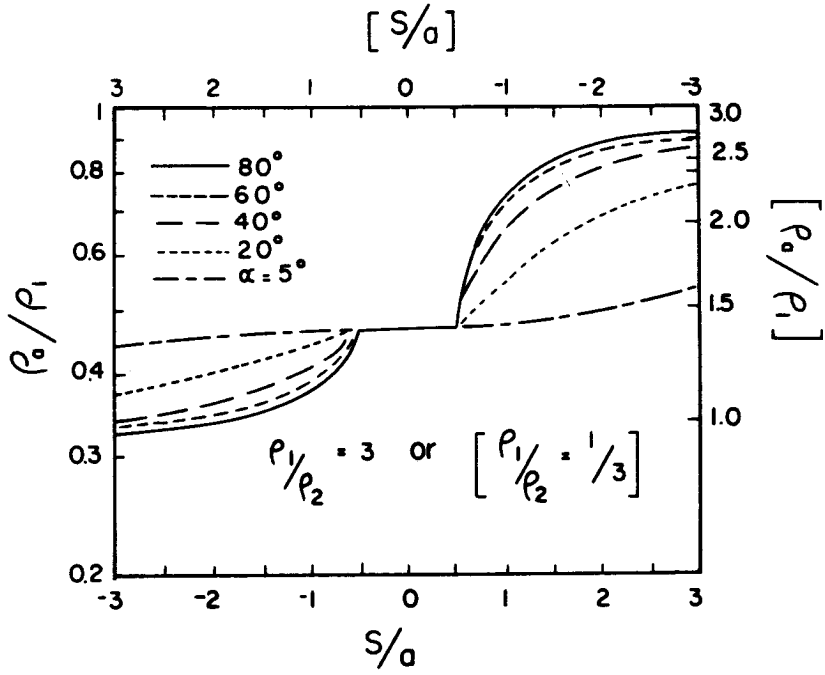

Figure 1.3.6 Apparent resistivity as a function of the distance s for a range of tilt angles for $\rho_1/\rho_2 = 3$; the results are also applicable to the case $\rho_1/\rho_2 = 1/3$ if the top and right hand scales are employed.

$$\rho_1(i\omega) = \rho_1(0)[1 + \delta_1(i\omega)] \tag{14}$$

$$\rho_2(i\omega) = \rho_2(0)[1 + \delta_2(i\omega)] \tag{15}$$

where $\delta_a(i\omega)$, $\delta_1(i\omega)$ and $\delta_2(i\omega)$ are the departures of the complex resistivities from their DC or zero-frequency values. By making an appropriate Taylor expansion, it is evident that

$$\delta_a(i\omega) \simeq B_1\delta_1(i\omega) + B_2\delta_2(i\omega) \tag{16}$$

where

$$B_1 = \left[\frac{\partial \ln \rho_a(i\omega)}{\partial \ln \rho_1(i\omega)}\right]_{\omega\to 0} \tag{17}$$

and

$$B_2 = \left[\frac{\partial \ln \rho_a(i\omega)}{\partial \ln \rho_2(i\omega)}\right]_{\omega\to 0} \tag{18}$$

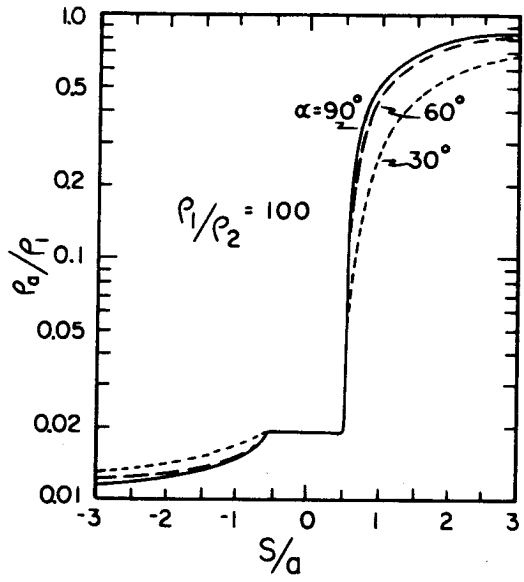

Figure 1.3.7 Apparent resistivity as a function of the vertical distance above or below the tilted interface for $\rho_1/\rho_2 = 100$.

Equivalent definitions of these dilution factors are

$$B_1 = \frac{\partial \ln \rho_a}{\partial \ln \rho_1} = \frac{\rho_1}{\rho_a}\frac{\partial \rho_a}{\partial \rho_1} \tag{19}$$

and

$$B_2 = \frac{\partial \ln \rho_a}{\partial \ln \rho_2} = \frac{\rho_2}{\rho_a}\frac{\partial \rho_a}{\partial \rho_2} \tag{20}$$

where we employ DC resistivities. It can also be shown that

$$B_1 + B_2 = 1 \tag{21}$$

so it is only necessary to compute one of these coefficients.

It should be realized that the simple representation given by (16) is only valid in a first order sense; higher order terms containing higher powers of δ_1 and δ_2 are neglected. We will not pursue this matter here. Suffice it to say that we are dealing with weakly dispersive media where $|\delta_1|$ and $|\delta_2| \ll 1$.

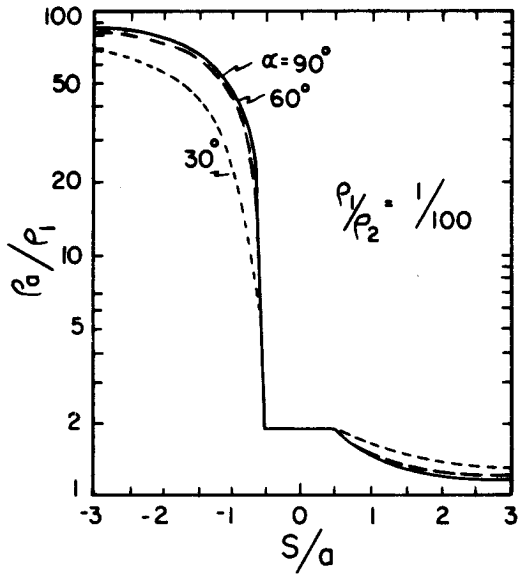

Figure 1.3.8 Apparent resistivity as a function of the vertical distance above or below the tilted interface for $\rho_1/\rho_2 = 0.01$.

Using (20) in conjunction with (12), it is easy to show that

$$B_2 = \begin{cases} \dfrac{2\rho_1\rho_2}{(R'/a)(\rho_1+\rho_2)^2+\rho_2{}^2-\rho_1{}^2} & ;\dfrac{s}{a} > \dfrac{1}{2} \\ \rho_1/(\rho_1+\rho_2) & ;-\dfrac{1}{2} > \dfrac{s}{a} > \dfrac{1}{2} \\ \dfrac{(R'/a)(\rho_1+\rho_2)+\rho_1-\rho_2-2\rho_1\rho_2/(\rho_1+\rho_2)}{(R'/a)(\rho_1+\rho_2)+\rho_1-\rho_2} & ;\dfrac{s}{a} < -\dfrac{1}{2} \end{cases} \tag{22}$$

where $R' = R'(s)$ is given by (8).

Some examples of the dilution factor B_2 are shown in Fig 1.3.9a, 1.3.9b, 1.3.10a and 1.3.10b. To facilitate the presentation, we choose a linear-log format. Also positive and negative values of s/a are displayed separately. In Fig. 1.3.9a, we plot B_2 as a function of s/a from $+0.3$ to $+10$ where it is evident that B_2 is approaching zero as the array moves away from medium (2) into medium (1). Of course, the corresponding value of $B_1 = (1 - B_2)$ would then approach 1.0. The values of B_2 for negative s/a are shown in Fig. 1.3.9b for the same conditions. As expected, B_2 approaches 1.0 as the array moves away

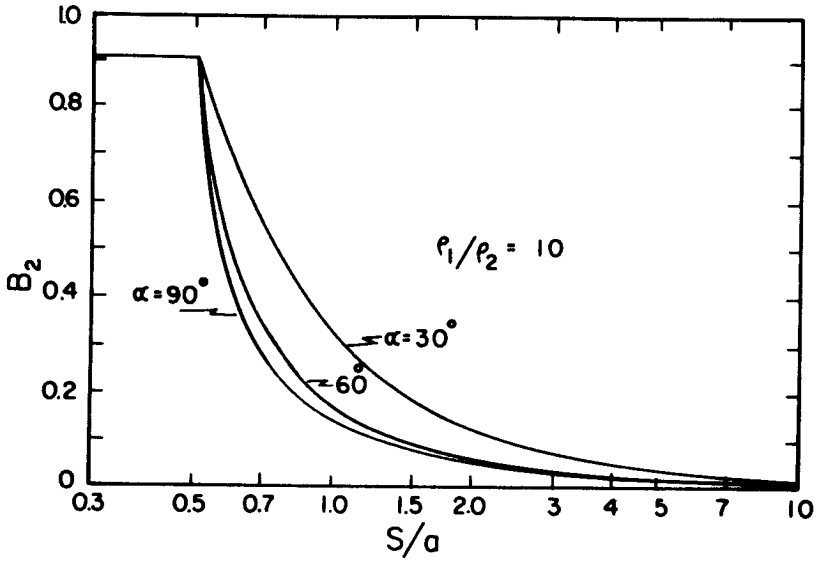

Figure 1.3.9a The dilution factor (relevant to the induced polarization response) for several tilt angles, $\rho_1/\rho_2 = 10$, and positive values of the distance s.

from the interface into medium (2). For the region from $s/a = +0.5$ to -0.5 where the electrodes are straddling the interface, B_2 has a constant value 0.909. The corresponding dilution factor B_2 for $\rho_1/\rho_2 = 0.1$ is shown in Figs. 1.3.10a and 1.3.10b for positive and negative values, respectively. Similar limiting behavior is noted. Also the constant value of B_2, in the range $s/a = +0.5$ to -0.5, is now 0.091.

e. Concluding Remarks

We have adopted a very simple model here in order to illustrate the interesting phenomena when the resistivity and the induced polarization are measured near an interface between two homogeneous regions. The problem is formulated in the context of a drill hole intersecting the plane interface. Actually, the problem is fully equivalent to the case where the two electrodes C and P are located on the surface of plane earth where there is vertical contact between two homogeneous regions (i.e. quarter spaces). For example, in Fig. 1.3.2, we can visualize the

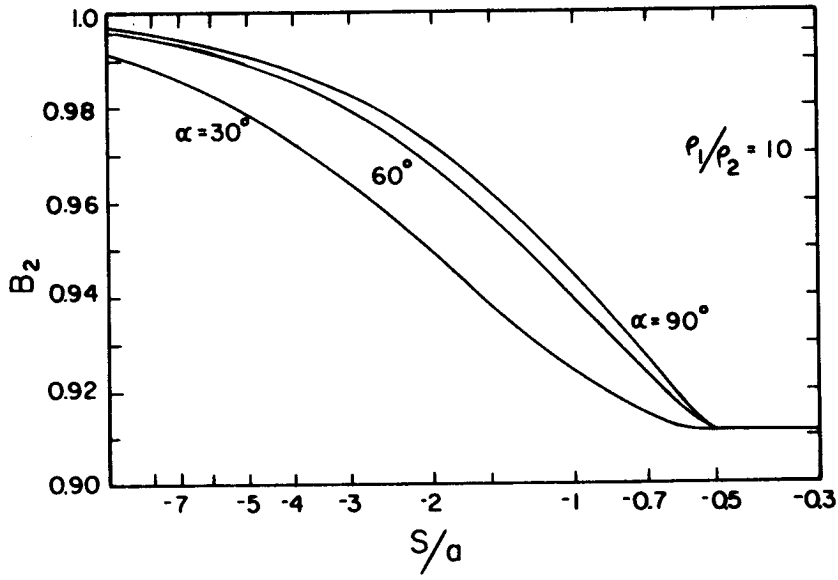

Figure 1.3.9b The dilution factor (relevant to the induced polarization response) for several tilt angles, $\rho_1/\rho_2 = 10$, and negative values of the distance s.

plane of the paper as the surface of the earth and where the array is to be moved along a line making an angle α with the trace of the contact. All the apparent resistivity curves and the dilution factor results are valid for this case under the initial quasi-static assumptions.

f. Exercises

Exercise 1: Consider a two-electrode array on the surface of a two-layer earth. The spacing between the electrodes C and P is denoted by a. The thickness of the upper layer is d and its conductivity is σ_1. The conductivity of the lower homogeneous half-space is σ. Beginning with the exact expression for the potential at P, derive an expression for the apparent resistivity ρ_a in the limiting case where the upper layer thickness is vanishingly thin and the conductivity is indefinitely large in such a manner that their product g, in mhos, is finite. Plot the apparent resistivity as function of the electrode spacing in normalized form.

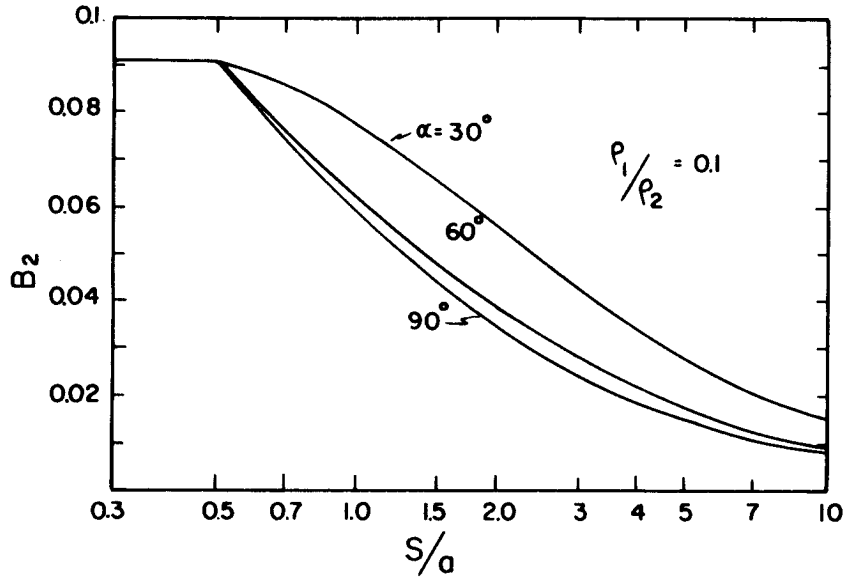

Figure 1.3.10a The dilution factor (relevant to the induced polarization response) for several tilt angles, $\rho_1/\rho_2 = 0.1$, and positive values of the distance s.

Solution 1: The exact expression for the potential at P, assuming DC conditions, is

$$\Psi = \frac{1}{2\pi\sigma_1}\left[\int_0^\infty J_0(\lambda a)d\lambda + 2\int_0^\infty \frac{(\sigma_1-\sigma)e^{-2d\lambda}J_0(\lambda a)}{(\sigma_1+\sigma)-(\sigma_1-\sigma)e^{-2d\lambda}}d\lambda\right] \tag{1}$$

Now noting that $\sigma/\sigma_1 \to 0, \sigma_1 d \to g$, and $e^{-2d\lambda} \to 1 - 2d\lambda$, we see that

$$\Psi = \frac{1}{2\pi g}\int_0^\infty \frac{J_0(\lambda a)}{\lambda + (\sigma/g)}d\lambda \tag{2}$$

This integral will now be evaluated by first inserting the identity

$$\frac{1}{\lambda+(\sigma/g)} = \int_0^\infty e^{-(\lambda+(\sigma/g))x}dx \tag{3}$$

into the integrand. Then the potential is given by

$$\Psi = \frac{1}{2\pi g}\int_0^\infty \int_0^\infty e^{-(\sigma/g)x}e^{-\lambda x}J_0(\lambda a)d\lambda dx \tag{4}$$

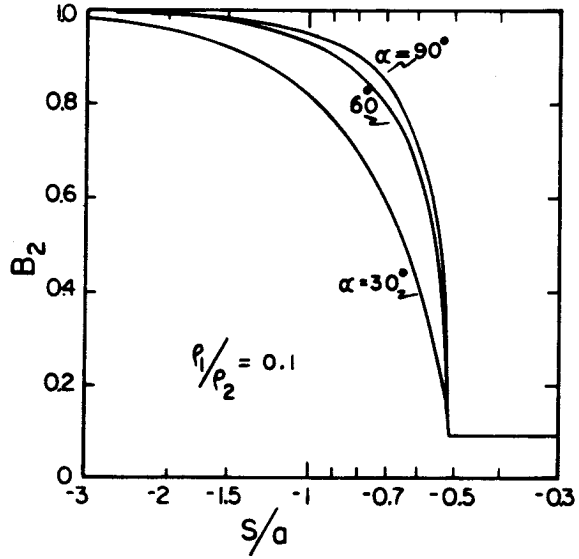

Figure 1.3.10b The dilution factor (relevant to the induced polarization response) for several tilt angles, $\rho_1/\rho_2 = 0.1$, and negative values of the distance s.

The integration over λ can be readily performed to give

$$\Psi = \frac{1}{2\pi g}\int_0^\infty \frac{e^{-(\sigma/g)x}}{(x^2+a^2)^{1/2}}dx$$

$$= \frac{1}{4g}\left[\frac{2}{\pi}\int_0^\infty \frac{\exp\left[-\frac{\sigma a}{g}\left(\frac{x}{a}\right)\right]}{\left[1+\left(\frac{x}{a}\right)^2\right]^{1/2}}d\left(\frac{x}{a}\right)\right] \tag{5}$$

The integral can now be expressed in terms of Struve's function H_0 and the Bessel function Y_0, both of order 0, by using an identity given by Watson [pg. 331, #3 with $\omega = 0$ and $\nu = 0$]. Thus

$$\Psi = \frac{1}{4g}\left[H_0\left(\frac{a\sigma}{g}\right) - Y_0\left(\frac{a\sigma}{g}\right)\right] \tag{6}$$

We now define an apparent resistivity ρ_a or an apparent conductivity σ_a according to

$$\Psi = 1/2\pi\sigma_a a = \rho_a/2\pi a \tag{7}$$

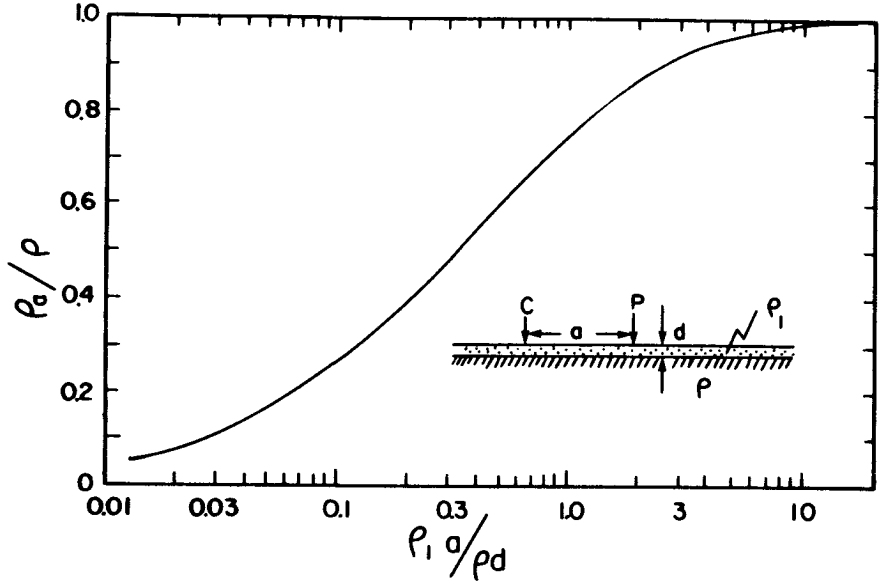

Figure 1.3.11 Normalized apparent resistivity as a function of the normalized electrode spacing for a two electrode array and a thin conductive sheet on the surface of a homogeneous half space.

Then, using dimensionless forms, we write

$$\frac{\rho_a}{\rho} = \frac{\sigma}{\sigma_a} = \pi \frac{\sigma a}{2g}\left[H_0\left(\frac{a\sigma}{g}\right) - Y_0\left(\frac{a\sigma}{g}\right)\right] \tag{8a}$$

$$= \pi \frac{a\rho_1}{2d\rho}\left[H_0\left(\frac{a\rho_1}{d\rho}\right) - Y_0\left(\frac{a\rho_1}{d\rho}\right)\right] \tag{8b}$$

Using tabulated values of H_0 and Y_0, we plot the normalized resistivity ratio ρ_a/ρ as a function of the normalized spacing parameter $\rho_1 a/\rho d$ for a range of values from 0.01 to 20. As it should, the ordinate approaches 1.0 as the spacing parameter becomes sufficiently large. Thus, we have a convenient single universal curve to estimate the importance of thin conductive surface layer on resistivity measurements.

Exercise 2: Using the same model as in the previous exercise, deduce the sensitivity functions B_1 and B_2 for the same two-

electrode array C and P. The relevant quantities are

$$B_1 = \frac{\partial \ln \rho_a}{\partial \ln \rho_1} \tag{1}$$

and

$$B = \frac{\partial \ln \rho_a}{\partial \ln \rho} \tag{2}$$

Plot these parameters as a function of the normalized spacing parameter used in the preceding exercise.

Solution 2: To simplify the development, we write

$$\frac{\rho_a}{\rho} = F(y) = \frac{\pi}{2} y [H_0(y) - Y_0(y)] \tag{3}$$

where $y = a\rho_1/d\rho$ is the spacing parameter. Now clearly

$$B_1 = \frac{\partial \ln F(y)}{\partial \ln y} = \frac{y}{F(y)} \frac{\partial F(y)}{\partial y} \tag{4}$$

where

$$\frac{\partial F(y)}{\partial y} = \frac{\pi}{2} \left\{ H_0(y) - Y_0(y) - y \left[\frac{2}{\pi} - H_1(y) + Y_1(y) \right] \right\} \tag{5}$$

Here, we have used the identities

$$\frac{dH_0(y)}{dy} = \frac{2}{\pi} - H_1(y) \tag{6}$$

and

$$\frac{dY_0(y)}{dy} = -Y_1(y) \tag{7}$$

where H_1 and Y_1 are Struve and Bessel functions of order one, respectively. Then, the explicit expression to calculate B_1 is

$$B_1 = 1 + y \frac{(2/\pi) - H_1(y) + Y_1(y)}{H_0(y) - Y_0(y)} \tag{8}$$

and

$$B = 1 - B_1 \tag{9}$$

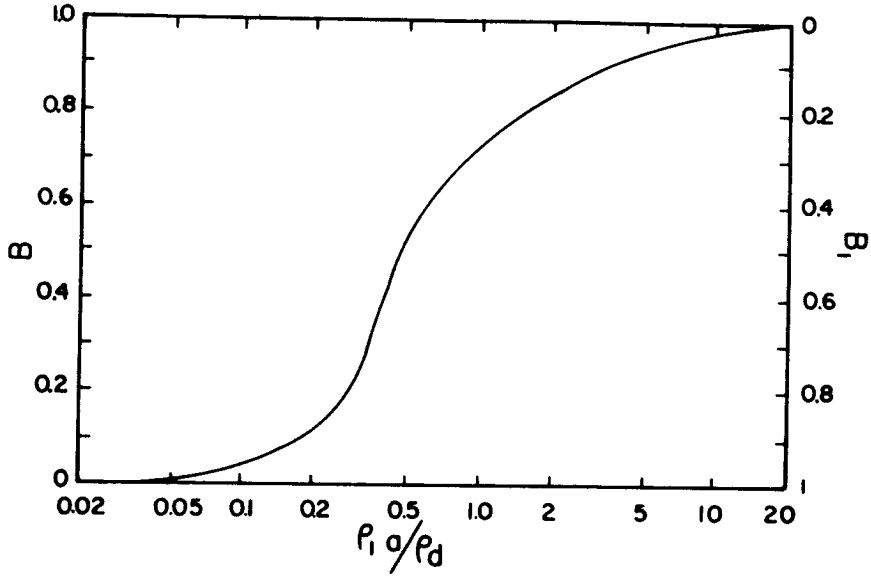

Figure 1.3.12 Sensitivity or dilution factors B and B_1.

Using tabulated values of the Struve and Bessel functions, the functions B and B_1 are plotted as a function of the spacing parameter in Fig 1.3.12. As indicated, for large values of the spacing parameter, the sensitivity factor (i.e. B) for the lower half space tends to 1 meaning that the masking effect of the conductive surface layer is negligible. On the other hand, for small values of the spacing parameter, the surface layer is dominating the response.

Acknowledgments

Most of the numerical results presented are due to Alan Peters in connection with an assignment for the Graduate Course ECE 586. Some results were also included from Gerardo Aguirre's assignment. Alan Peters also contributed to the analysis.

I would like to thank Hulya Akman for her assistance with the calculations in the exercises in subsection 1.3.f.

References

[1] Wait, J. R., *GeoElectromagnetism*, Academic Press, chapters 1 and 2, 1982.

[2] Watson, G.N., *Theory of Bessel Functions, Cambridge University Press*, 2nd. Ed., 1944.

1.4 Low Frequency Electromagnetic Response

a. Introduction

A basic problem in electrical prospecting is how the currents are injected into the earth from a horizontal current-carrying cable grounded at its end points. The basic building block for this analysis is the horizontal electric dipole of current moment $I\,ds$ located in the air-earth interface. Such a solution was given by Sommerfeld [1909-1926] many years ago for the case where the earth was idealized as a homogeneous isotropic half-space. An exhaustive treatment of dipoles in the presence of a conducting half-space was published by Banos [1966] in a textbook. It is our purpose here to outline the solution of the problem in the context of induced polarization. We also consider cylindrical geometry which is relevant to borehole measurements.

b. Basis Anisotropic Half-Space Model

We choose a model of an anisotropic but homogeneous half-space as indicated in Fig. 1.4.1. To facilitate the solution, the source dipole is located at height h over the interface at $z = 0$ and oriented in the x direction. We later allow h to tend to zero corresponding to a grounded electric circuit. The upper region ($z > 0$) is taken to be free space with electrical properties ϵ_o and μ_o (i.e. permittivity and permeability). The lower region, $z < 0$, has a complex resistivity $\rho_h(\omega)$ in the horizontal direction and a complex resistivity $\rho_v(\omega)$ in the vertical direction. As indicated these complex resistivities are functions of the angular frequency ω for an implied time factor $\exp(j\omega t)$. However to abbreviate the subsequent discussion, we shall designate these frequency dependent complex resistivities by ρ_h and ρ_v.

Ohm's law for the lower region can be succinctly stated as follows

$$\overline{J} = \overline{\overline{\sigma}} \cdot \overline{E} \tag{1}$$

where $\overline{J}$ is the current density vector, $\overline{E}$ is the electric field vector, and $\overline{\overline{\sigma}}$ is the (complex) conductivity tensor. The latter quantity takes the form

$$\overline{\overline{\sigma}} = \begin{pmatrix} \rho_h^{-1} & 0 & 0 \\ 0 & \rho_h^{-1} & 0 \\ 0 & 0 & \rho_v^{-1} \end{pmatrix} \tag{2}$$

where the off-diagonal elements are zero. To be specific, we are saying that

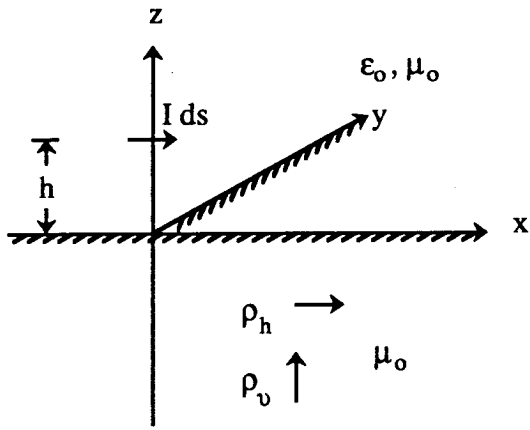

Figure 1.4.1 Horizontal electric dipole over an anisotropic half-space.

$$J_x = (\rho_h)^{-1} E_x \tag{3a}$$

$$J_y = (\rho_h)^{-1} E_y \tag{3b}$$

and

$$J_z = (\rho_z)^{-1} E_z \tag{3c}$$

Then Maxwell's equations for $z < 0$ are

$$\text{curl } \overline{H} = \overline{\overline{\sigma}}\,\overline{E} \tag{4}$$

and

$$\text{curl } \overline{E} = -j\mu_o\omega\overline{H} \tag{5}$$

excluding any source regions and the corresponding forms for $z > 0$ are identical if $\overline{\overline{\sigma}}$ is replaced by $j\epsilon_o\omega$.

c. *Vector Potential Formulation*

To solve the boundary value problem, we find it convenient to introduce the vector potential $\overline{A}$ and a scalar potential Ψ such that

$$\overline{H} = \text{curl } \overline{A} \tag{6}$$

and

$$\overline{E} = -j\mu_o\omega\overline{A} - \text{grad } \Psi \tag{7}$$

which clearly are consistent with (4) and (5).

We now choose the gauge condition [Wait 1966a]

$$\mathrm{div}\overline{A} + (\rho_h)^{-1}\Psi = 0 \tag{8}$$

for $z < 0$ and

$$\mathrm{div}\overline{A} + j\epsilon_o\omega\Psi = 0 \tag{9}$$

for $z > 0$. Then it is not difficult to show that for $z > 0$

$$\nabla^2 A_x - \gamma^2 A_x = 0 \tag{10}$$

$$\nabla^2 A_y - \gamma^2 A_y = 0 \tag{11}$$

and

$$\nabla^2 A_z - \left(\frac{1}{\rho_h} - \frac{1}{\rho_v}\right)\rho_h \frac{\partial}{\partial z}(\mathrm{div}\overline{A}) - \frac{\rho_h}{\rho_v}\gamma^2 A_z = 0 \tag{12}$$

where

$$\gamma^2 = (j\mu_o\omega/\rho_h) \tag{13}$$

On the other hand, for $z > 0$, we simply have

$$(\nabla^2 - \gamma_o^2)A_x = 0 \tag{14}$$

$$(\nabla^2 - \gamma_o^2)A_y = 0 \tag{15}$$

and

$$(\nabla^2 - \gamma_o^2)A_z = 0 \tag{16}$$

where $\gamma_o^2 = (j\epsilon_o\omega)(j\mu_o\omega) = -\epsilon_o\mu_o\omega^2$.

In order to solve the problem, we need to choose the vector potential to have both a component A_x in the direction of the dipole and component A_z normal to the interface. However, we can set $A_y = 0$ and still be able to satisfy all the boundary conditions (i.e. tangential field components E_x, E_y, H_x, and H_y must be continuous at the interface $z = 0$). Another condition is that A_x, for the region $z > 0$, must have the proper singularity at the source; that is

$$A_x \to (I\,ds/4\pi r_o)e^{-\gamma_o r_o} \tag{17}$$

as $\rho = (x^2 + y^2)^{1/2} \to 0$ and $z \to h$ where $r_o = [\rho^2 + (z-h)^2]^{1/2}$. This fact is incorporated neatly into the analysis by noting that

$$\frac{e^{-\gamma_o r_o}}{r_o} = \int_0^\infty \frac{\lambda}{u_o} e^{-u_o|z-h|} J_o(\lambda\rho)\,d\lambda \tag{18}$$

where $u_o = (\lambda^2 + \gamma_o^2)^{1/2}$. This "Sommerfeld Integral" is the key for solving many such problems involving localized sources in the presence of layered media [Wait, 1966a; Kong, 1976].

For $z < 0$, we write

$$A_x = \frac{I\,ds}{4\pi} \int_0^\infty F(\lambda, z) J_o(\lambda\rho) d\lambda \tag{19}$$

and

$$A_z = \frac{I\,ds}{4\pi} \frac{\partial}{\partial x} \int_0^\infty G(\lambda, z) J_o(\lambda\rho) d\lambda \tag{20}$$

where $\rho = (x^2 + y^2)^{1/2}$ and where F and G satisfy

$$\frac{\partial^2 F}{\partial z^2} - (\lambda^2 + \gamma^2) F = 0 \tag{21}$$

and

$$\frac{\partial^2 G}{\partial z^2} - (\lambda^2 K^2 + \gamma^2) G = (K - 1) \frac{\partial F}{\partial z} \tag{22}$$

where $K = \rho_v / \rho_h$. Solutions of (21) and (22) have the form

$$F(\lambda, z) = A(\lambda) e^{uz} \tag{23}$$

and

$$G(\lambda, z) = B(\lambda) e^{vz} - (u/\lambda^2) A(\lambda) e^{uz} \tag{24}$$

where $u = (\lambda^2 + \gamma^2)^{1/2}$ and $v = (\lambda^2 K + \gamma^2)^{1/2}$ and where $A(\lambda)$ and $B(\lambda)$ are yet to be determined.

d. Statement of the Formal Solution

It is important to observe that (21) and (22) are coupled differential equations which, in effect, mean that the solutions for A_x and A_z are coupled by virtue of the anisotropy (i.e. $K \neq 1$) even within the homogeneous region.[+] Of course, in the upper anisotropic region ($z > 0$), this complication does not arise. In fact, for $z > 0$, we write the solution in the somewhat more familiar form

$$A_x = \frac{I\,ds}{4\pi} \int_0^\infty \frac{\lambda}{u_o} \left[e^{-u_o|z-h|} + R_\perp(\lambda) e^{-u_o(z+h)} \right] J_o(\lambda\rho) d\lambda \tag{25}$$

[+] An alternative approach to the problem is to follow Kong [1976] and use Debye potentials or z directed electric and magnetic hertz vectors.

and

$$A_z = \frac{I\,ds}{4\pi}\frac{\partial}{\partial x}\int_0^\infty S(\lambda)e^{-u_o(z+h)}J_o(\lambda\rho)d\lambda \tag{26}$$

where $R_\perp(\lambda)$ and $S(\lambda)$ are also to be determined by the boundary conditions at $z = 0$.

As it turns out [Wait, 1982]:

$$A(\lambda) = \frac{\lambda}{u_o}[1 + R_\perp(\lambda)]\,e^{-u_o h} \tag{27}$$

$$R_\perp(\lambda) = \frac{u_o - u}{u_o + u} \tag{28}$$

$$S(\lambda) = \left[B(\lambda) - \frac{u}{\lambda^2}A(\lambda)\right]e^{u_o h} \tag{29}$$

$$B(\lambda) = \frac{1}{\lambda^2}\left[\frac{\gamma_o^2 + u_o u + \lambda^2}{u_o + (\gamma_o^2/\gamma^2)v}\right]A(\lambda) \tag{30}$$

which constitute the complete formal solution of the problem.

e. Quasi-Static Limiting Forms

We now do two things. First of all, we let $h \to 0$ corresponding to having the dipole lying in the interface. Then we proceed to the quasi-static limit and set $\gamma_o = 0$. The latter approximation or idealization is valid when all significant distances ℓ satisfy $|\gamma_o \ell| \ll 1$. In the limit, where $z = h = 0$, we then find that

$$E_x = -j\mu_o\omega A_x - \frac{\partial \Psi}{\partial x} \tag{31}$$

and

$$E_y = -\frac{\partial \Psi}{\partial y} \tag{32}$$

where

$$A_x = \frac{I\,ds}{2\pi}\int_0^\infty \frac{\lambda}{\lambda + u}J_o(\lambda\rho)d\lambda \tag{33}$$

$$= \frac{I\,ds}{2\pi\gamma^2\rho^3}\left[1 - (1 + \gamma\rho)e^{-\gamma\rho}\right] \tag{34}$$

and

$$\Psi = -\rho_h\left(\frac{\partial A_x}{\partial x} + \frac{\partial A_z}{\partial z}\right)_{z=0} \tag{35}$$

$$= -\frac{I\,ds}{2\pi}\rho_h\frac{\partial}{\partial x}\int_0^\infty \left[\frac{v - u}{\lambda} + 1\right]J_o(\lambda\rho)d\lambda \tag{36}$$

The expression above for A_x is the same as that for an isotropic half-space [Wait, 1961] and it depends only on ρ_h the complex resistivity in the horizontal direction. On the other hand, the surface potential Ψ depends on both ρ_h and ρ_v. To clarify this point, we write

$$\Psi = \Psi_1 + \Psi_2 \tag{37}$$

where

$$\Psi_1 = -\frac{I\,ds}{2\pi}\rho_h \frac{\partial}{\partial x}\frac{1}{\rho} = \frac{I\,ds}{2\pi}\rho_h \frac{x}{\rho^3} \tag{38}$$

and

$$\Psi_2 = \frac{I\,ds}{2\pi}\rho_h \int_0^\infty (v-u) J_1(\lambda\rho) d\lambda \frac{x}{\rho} \tag{39}$$

where we have employed the identities

$$\int_0^\infty J_o(\lambda\rho) d\lambda = \frac{1}{\rho} \tag{40}$$

$$\frac{\partial}{\partial x} J_o(\lambda\rho) = -J_1(\lambda\rho)\lambda \frac{x}{\rho} \tag{41}$$

In the isotropic limit, Ψ_2 vanishes and the limiting form $\Psi = \Psi_1$ corresponds to the expected result.

Actually, Ψ_2 can also be evaluated in closed form [Wait, 1982] and the result is given by

$$\Psi_2 = -\frac{I\,ds}{2\pi}\rho_h \frac{x}{\rho^3}\left[\exp(-\gamma\rho) - K^{1/2}\exp(-\gamma\rho K^{-1/2})\right] \tag{42}$$

In the static limit (i.e. $|\gamma\rho| \to 0$), we see that

$$\Psi = \Psi_1 + \Psi_2 \to \frac{I\,ds}{2\pi}(\rho_h\rho_v)^{1/2}\frac{x}{\rho^3} \tag{43}$$

which is the expected DC solution. Another interesting observation is that $\Psi_2 \to 0$ if $|\gamma\rho| \gg 1$. Then, in this asymptotic limit

$$\Psi \to \Psi_1 = \frac{I\,ds}{2\pi}\rho_h \frac{x}{\rho^3} \tag{44}$$

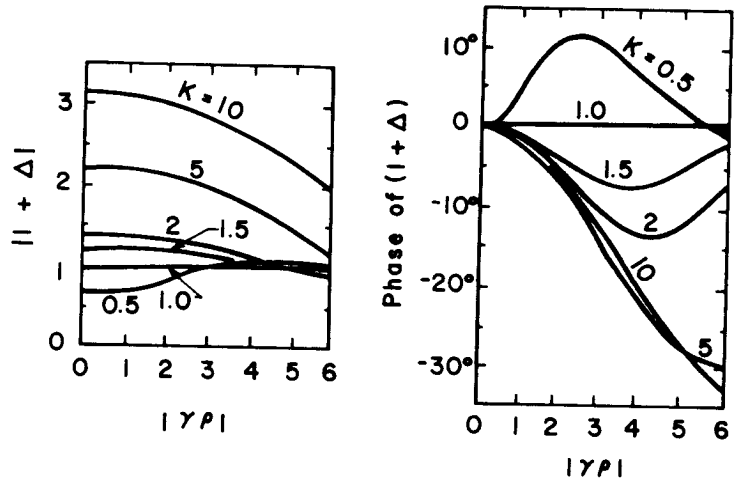

Figure 1.4.2 Amplitude and phase of the E_y field component for an x directed electric dipole on the surface ($z = 0$) of an anisotropic homogeneous half-space model of the earth.

which depends only on the horizontal resistivity.

The key point in the above development is that the potential function Ψ is dependent on frequency as $|\gamma\rho|$ varies from 0 to ∞ unless the half-space is isotropic. An interesting demonstration of this point is seen when we look at E_y (for $z = h = 0$) for the x directed electric dipole source. Using (32), (37), and (42), we deduce that

$$E_y = \frac{3(I\,ds)xy}{2\pi}\rho_h(1 + \Delta) \tag{45}$$

where

$$\Delta = \frac{1}{3}\left[(3K^{1/2} + \gamma\rho)\,\exp\,(-\gamma\rho K^{-1/2}) - (3 + \gamma\rho)\,\exp\,(-\gamma\rho)\right] \tag{46}$$

Clearly, in the isotropic limit, Δ vanishes. Also, if $|\gamma\rho| \gg 1$, Δ vanishes.

To illustrate the frequency dependence of E_y, as given by (45), we plot the amplitude and phase of $(1 + \Delta)$ in Figs. 1.4.2a and 1.4.2b, as a function of $|\gamma\rho|$ for the cases where $K = 0.5, 1.0, 2, 5$, and 10. In this example, all displacement currents have been neglected. Thus

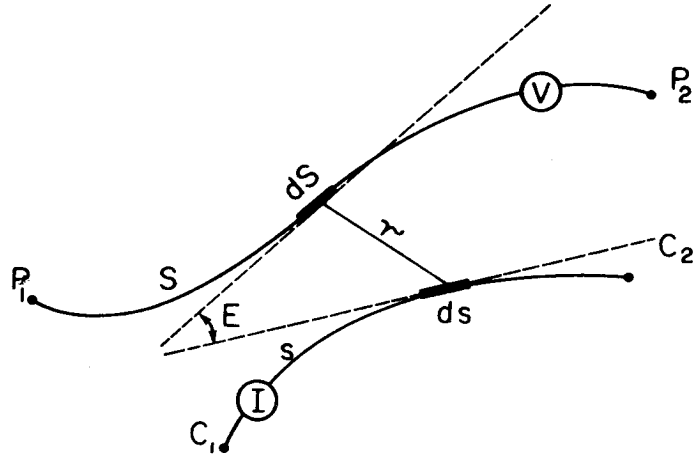

Figure 1.4.3 Plan view of the general non-intersecting current and potential cable configuration.

$|\gamma\rho| = (\mu_o\omega/\rho_h)^{1/2}$ is proportional to (frequency)$^{\frac{1}{2}}$ where ρ_h is real and frequency independent. Clearly the frequency dependence of the normalized field $1+\Delta$ is quite significant except in the isotropic limit where $K = 1$.

f. General Coupling Theory

Conceptually, it is evident that the tangential electric fields E_x and E_y of a horizontal electric dipole in the interface, can be used to deduce the mutual impedance between two grounded circuits. Such a configuration is illustrated in Fig. 1.4.3. For example, C_1 and C_2 could be the current electrodes which are connected by insulated wires to the generator which supplies the current I. The voltage V, induced in the potential circuit, is then the integrated electric field along the contour of the insulated wires connecting the "voltmeter" to the potential electrodes P_1 and P_2.

The first step is to regard the element $I\,ds$ in the current circuit as a source dipole at a distance s from C_1. The voltage V induced in the element dS is $-E_t dS$ where E_t is the tangential electric field at a distant r from ds. Here we designate ϵ as the angle subtended by ds and dS. The resulting induced voltage V is then obtained by integrating over both s and S. This procedure was illustrated by Sunde [1949] and generalized later [Wait, 1982]. In the present context,

we find that

$$\frac{V}{I} = Z_m = \int_{C_1}^{C_2} \int_{P_1}^{P_2} \left[P(r) \cos \epsilon + \frac{\partial^2 Q(r)}{\partial s \partial S} \right] ds\, dS \tag{47}$$

where

$$P(r) = \frac{j\mu_o \omega}{2\pi \gamma^2 r^3} \left[1 - (1 + \gamma r) e^{-\gamma r} \right] \tag{48}$$

and

$$Q(r) = \frac{\rho_h}{2\pi} \left[\frac{1}{r} + \int_0^\infty \left(\frac{v - u}{\lambda} \right) J_o(\lambda r) d\lambda \right] \tag{49}$$

At sufficiently low frequencies (i.e. where $|\gamma r| \ll 1$) we see that

$$P(r) \cong j\mu_0 \omega / 2\pi r \tag{50}$$

and

$$Q(r) \cong (\rho_h \rho_v)^{1/2} / 2\pi r \tag{51}$$

In this case $P(r)$ and the resulting integral in (47) has a purely inductive character while $Q(r)$ leads to a purely resistive contribution. In general, γr is arbitrary and the frequency dependence is more complicated and simple closed-form expressions are not possible. Nevertheless, it is useful to note that $Q(r)$ can be expressed in terms of exponential integrals. To show this, we observe that

$$\begin{aligned} \frac{\partial}{\partial r} \int_0^\infty \frac{v - u}{\lambda} J_0(\lambda r) d\lambda &= - \int_0^\infty (v - u) J_1(\lambda r) d\lambda \\ &= \left[K^{1/2} \exp\left(-\gamma \rho K^{-1/2}\right) - \exp\left(-\gamma \rho\right) \right] / \rho^2 \end{aligned} \tag{52}$$

Then we can write

$$\begin{aligned} Q(r) &= \frac{1}{2\pi} \left[\frac{1}{r} + \int_0^\infty \left[K^{1/2} e^{\left(-\gamma r K^{-1/2}\right)} - e^{(-\gamma r)} \right] \frac{1}{r^2} dr \right] \\ &= \frac{1}{2\pi} \left[\frac{1}{r} + K^{1/2} \frac{1}{r^2} E_2\left(\gamma r K^{-1/2}\right) - \frac{1}{r^2} E_2(\gamma r) \right] \end{aligned} \tag{53}$$

where

$$E_2(\alpha) = \int_{t=1}^\infty \frac{e^{-\alpha t}}{t^2} dt \tag{54}$$

is an exponential integral of order 2 as defined by Abramowitz and Stegun [1964].

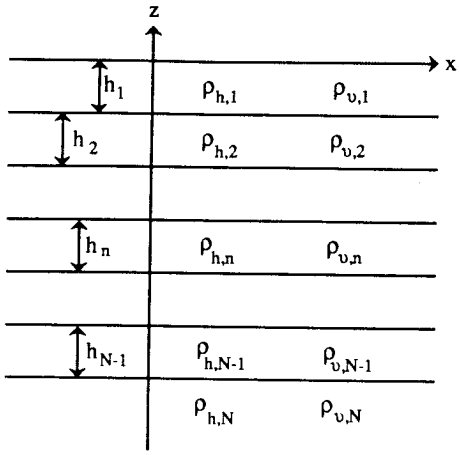

Figure 1.4.4 The N layered anisotropic half-space model of the earth.

g. Extensions to Layered Anisotropic Earth

There is some merit in extending the formulation of the electrocoupling to the case where the earth is represented as a layered half-space. Also it is desirable to let one or more of the layers be anisotropic. The situation is illustrated in Fig. 1.4.4. The solution of N-layer problem is carried through in a manner very similar to the homogenous half-space model. The details are given elsewhere [Wait 1966b, 1982]. As noted in Fig. 1.4.4, the n'th layer has a complex resistivity $\rho_{h,n}$ in the horizontal direction, and $\rho_{v,n}$ in the vertical direction. Here $n = 1, 2, 3, \ldots N$.

The mutual impedance formula given by (47) is still applicable but $P(r)$ and $Q(r)$ are now given by

$$P(r) = \frac{j\mu_o\omega}{2\pi}\int_o^\infty \frac{\lambda}{\lambda + j\mu_o\omega Y_1} J_0(\lambda r)d\lambda \tag{55}$$

and

$$Q(r) = \frac{1}{2\pi}\int_o^\infty \left[Z_1 - \frac{j\mu_o\omega}{\lambda + j\mu_o\omega Y_1}\right] \lambda J_0(\lambda r)d\lambda \tag{56}$$

where Y_1 and Z_1 are admittance and impedance functions defined as follows

$$Y_1 = N_1 \frac{Y_2 + N_1 \tanh u_1 h_1}{N_1 + Y_2 \tanh u_1 h_1} \tag{57}$$

$$Y_2 = N_2 \frac{Y_3 + N_2 \tanh u_2 h_2}{N_2 + Y_3 \tanh u_2 h_2} \tag{58}$$

$$\cdots$$

$$Y_n = N_n \frac{Y_{n+1} + N_n \tanh u_n h_n}{N_n + Y_{n+1} \tanh u_n h_n} \tag{59}$$

$$\cdots$$

$$Y_{N-1} = N_{N-1} \frac{N_N + N_{N-1} \tanh u_{N-1} h_{N-1}}{N_{N-1} + N_N \tanh u_{N-1} h_{N-1}} \tag{60}$$

where $N_n = u_n/(j\mu_o\omega)$ and $u_n = (\lambda^2 + \gamma_n^2)^{1/2}$ and $\gamma_n = (j\mu_o\omega/\rho_{h,n})^{1/2}$ for $n = 1, 2, 3, \ldots N$. The iterative formula for Z_1 has precisely the same form as (57) to (60) if the Y's are replaced by Z's, the N's are replaced by K's and the u's by v's, where

$$K_n = v_n \rho_{h,n} \quad \text{and} \quad v_n = \left(\lambda^2 \frac{\rho_{v,n}}{\rho_{h,n}} + \gamma_n^2\right)^{1/2}$$

In the limiting case of a homogeneous half-space (i.e. $h_1 \to \infty$ and $u_1 \to u$), $Y_1 \to u/j\mu_o\omega$ and $Z_1 \to v\rho_h$. Then $P(r)$ and $Q(r)$ reduce to the forms (48) and (49), respectively. We also recover the results derived by Hohmann [1973] for the 2-layer isotropic case.

Any general configuration of grounded wires connecting the electrodes can be handled with the above general forms for $P(r)$ and $Q(r)$ used in conjunction with (47). A rather extreme special case is the homogeneous half-space. It is often used as the basis for an electromagnetic coupling estimate in connection with induced polarization surveys. But, perhaps one should bear in mind here that the resistivity is complex and matters can become complicated; we illustrate the point below for a half-space of isotropic complex resistivity $\rho(\omega)$.

h. An Illustrative Example

The so called dipole-dipole array is considered as illustrated in the inset in Fig. 1.4.5a. The electrodes are on a common line and the spacing is such that $C_1C_2 = P_1P_2 = a$ and $P_2C_1 = na$. As shown by Wait and Gruszka [1986a], the mutual impedance for this case can be expressed in analytical form:

$$Z_m = \frac{\rho(\omega)}{4\pi}\gamma \left\{ \frac{2}{an(n+1)(n+2)\gamma} - 2G[\gamma a(n+1)] + G(\gamma an) + G[\gamma a(n+2)] \right\} \tag{61}$$

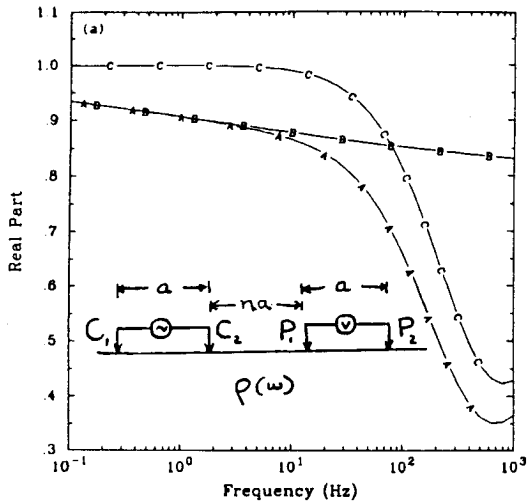

Figure 1.4.5a The real part of the complex resistivity for a dipole-dipole array as a function of frequency. Curve A – apparent resistivity, Curve B – pure IP, Curve C – pure EM.

where

$$\gamma = [j\mu_o\omega/\rho(\omega)]^{1/2} \tag{62}$$

and

$$G(z) = e^{-z}\left(\frac{1}{z} - 1\right) + zE_1(z) \tag{63}$$

in terms of the exponential integral [Abramowitz and Stegen, 1964] defined by

$$E_1(z) = \int_z^\infty \frac{e^{-v}}{v}dv = \int_1^\infty \frac{e^{-zt}}{t}dt \tag{64}$$

In the DC limit (i.e. $\omega \to 0$), we recover the expected form

$$Z_m \to R_0 = \frac{\rho(0)}{\pi an(n+1)(n+2)} \tag{65}$$

which is well known in resistivity formulations (e.g. [Chap. 1, Wait, 1982]).

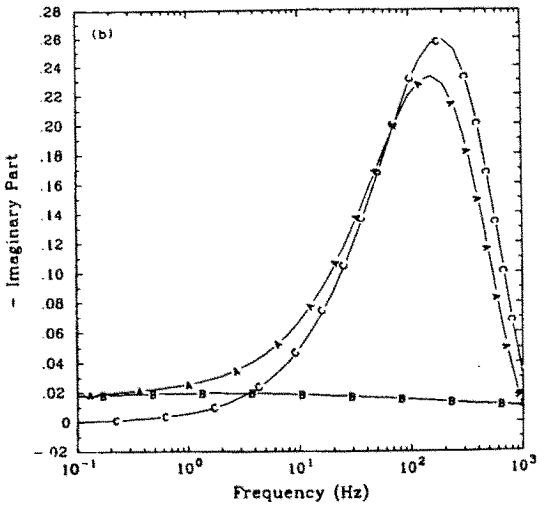

Figure 1.4.5b The imaginary part of the complex resistivity for a dipole-dipole array as a function of frequency.

We are now led to define an apparent (complex) resistivity as follows, for any frequency:

$$Z_m = \frac{\rho_a(\omega)}{\pi an(n+1)(n+2)} \tag{66}$$

Then clearly

$$\frac{\rho_a(\omega)}{\rho(0)} = \frac{Z_m}{R_0} = R(\omega) + jX(\omega) \tag{67}$$

where $R(\omega)$ and $X(\omega)$ are the real and imaginary parts of the apparent complex resistivity.

Actually, Z_m is valid for any frequency provided the appropriate frequency dependent form for $\rho(\omega)$ is employed. For purposes of illustration, we choose the Cole-Cole form [Pelton, 1978] given by

$$\rho(\omega) = \rho(0)\left[1 - m\left(1 - \frac{1}{1+(j\omega\tau)^k}\right)\right] \tag{68}$$

where $\rho(0)$ is the DC value, m is the chargeability, τ is a time constant, and k is a dispersion index. One should note that at a sufficiently high frequency $\rho(\omega) \to \rho(0)(1-m)$. Thus m is a good measure

of the total dispersion over the whole significant frequency range (i.e. 10^{-1} to 10^{3} Hz). The adjustable parameters τ and k are chosen to represent a particular rock or mineral type. For our numerical example, we choose $m = 0.2$, $n = 2$, $k = 1/4$, $\tau = 0.1$ sec., $\rho(0) = 10^{2}$ ohm-m and $a = 200$ m.

Using (61) and (68), we plot $R(\omega)$ and $X(\omega)$, as defined by (67), as a function of frequency in Hz in Figs. 1.4.5a and 1.4.5b respectively. The resulting curves are designated A. Then we plot what might be called pure induced polarization (IP) which, in the present context, would be defined by

$$R(\omega) + jX(\omega) = \frac{\rho(\omega)}{\pi a n(n+1)(n+2)R_0} = \frac{\rho(\omega)}{\rho(0)} \tag{69}$$

In other words, electromagnetic (EM) coupling is ignored. These curves are designated B. It is significant that the A and B curves begin to diverge even for frequencies as low as 1 Hz. This fact is not surprising when the pure EM coupling curves are also plotted. In this case we use (61) but $\rho(\omega)$ is replaced everywhere by $\rho(0)$. Clearly the EM coupling is dominating the response for frequencies above about 10 Hz. This fact should be borne in mind in interpreting such measurements. Wait and Gruszka [1986a,b] discuss a possible decoupling procedure where the actual or composite response function is "corrected" by subtracting out the pure EM coupling results. The method is not particularly effective at the higher frequencies.

In the applied geophysical literature [Wait 1959a, Dey and Morrison 1973, Brown 1985, Song 1985, Wynn and Zonge 1975, 1977, Wynn 1979], one finds various proposals to mitigate the annoying effects of electromagnetic coupling in induced polarization surveys. Some rather ingenious attempts to "remove" the EM coupling by special data processing techniques have been made. No attempt will be made here to evaluate these procedures which may be more "art" than science. Our purpose is merely to identify the nature of the problem and to illustrate the inherent complexity of the situation that confronts the exploration geophysicists.

Rather than attempting to remove or correct the resultant complex resistivity data for EM coupling, it might be better to carry out the interpretation using a dynamic formulation such as proposed earlier [Wait 1981]. Such an approach has been developed by Mahmoud et al [1987] which requires the use of two receiving grounded dipoles

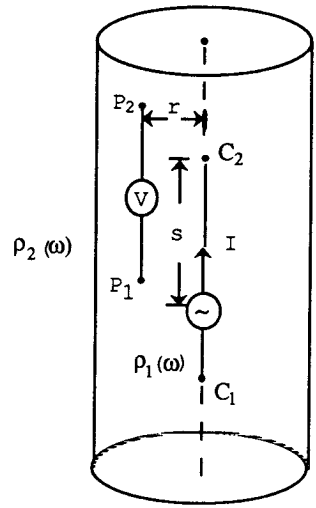

Figure 1.4.6 Four electrode array located in a bore-hole where potential circuit is offset by a distance r from the axis.

with special orientations relative to the source dipole. The procedure was applied to computer simulated data on a two layer earth with encouraging results.

i. Borehole Configuration

Here we wish to discuss the EM coupling problem when the electrodes are located in a borehole. The starting point is to deal with the electromagnetic field of an oscillating electric dipole located on the axis of the borehole. Such a solution, for a homogeneous cylinder of radius b of complex resistivity ρ_1 and an external homogeneous region of complex resistivity ρ_2, is straight forward. It is the special case of a general analysis for dipoles in the presence of cylindrical structures [Wait 1959b, Hill and Wait 1979]. A similar model was considered recently by Freedman and Vogiatzis [1986].

The special geometry is shown in Fig. 1.4.6. The current electrodes C_1 and C_2 are fed effectively by a generator on the axis of the borehole. The potential electrodes P_1 and P_2 are displaced from the axis

by a distance r. An expression for the mutual impedance Z is given in explicit form by Gruszka [1987] as follows:

$$Z = \frac{\rho_1}{4\pi}\sum_{i,j=1}^{2}(-1)^{i+j+1}\left\{\frac{e^{-\gamma_1 R_{ij}}}{R_{ij}} - \gamma_1^2\int_0^\infty \frac{\lambda}{u_1^2}e^{-u_1 z_{ij}}J_0(\lambda r)d\lambda \right.$$
$$\left. + \frac{2}{\pi}\int_0^\infty \frac{u_1^2 A(\lambda)I_0(u_1 r) - \gamma_1^2 A(0)I_0(\gamma_1 r)}{\lambda^2}\cos(\lambda z_{ij})d\lambda\right\}$$
$$- \frac{\gamma_1^2\rho_1 s}{2\pi}\left\{\int_0^\infty \frac{\lambda}{u_1^2}J_0(\lambda r)d\lambda + A(0)I_0(\gamma_1 r)\right\} \qquad (70)$$

where

$$A(\lambda) = -\left[\frac{u_1\rho_1 K_0(u_1 b) - u_2\rho_2\dfrac{K_0(u_2 b)}{K_1(u_2 b)}K_1(u_1 b)}{u_1\rho_1 I_0(u_1 b) + u_2\rho_2\dfrac{K_0(u_2 b)}{K_1(u_2 b)}I_1(u_1 b)}\right] \qquad (71)$$

$$u_1 = (\lambda^2 + \gamma_1^2)^{1/2} \quad , \quad Re\, u_1 > 0$$
$$u_2 = (\lambda^2 + \gamma_1^2)^{1/2} \quad , \quad Re\, u_2 > 0$$
$$R_{ij} = (r^2 + z_{ij}^2)^{1/2} \quad , \quad z_{ij} = |P_j - C_i|$$
$$\gamma_1 = (j\mu_1\omega/\rho_1)^{1/2} \quad , \quad \gamma_2 = (j\mu_2\omega/\rho_2)^{1/2}$$

and s is the overlap distance as indicated in Fig. 1.4.6.

A special case of the formulation is when we locate a dipole-dipole array on the axis of the bore-hole (i.e. $r = 0$). To illustrate this case, we let the borehole fluid have a dispersionless or non-polarizable resistivity ρ_1 while the external region of complex resistivity $\rho_2(\omega)$ is characterized by the Cole-Cole form given by (68). The particular parameter values are indicated in the caption for Fig. 1.4.7a.

The real and imaginary parts of the apparent complex resistivity are plotted as a function of frequency in Figs. 1.4.7a and 1.4.7b and identified as curve A in each figure. Curves B correspond to "pure IP" in the sense that the propagation constants γ_1 and γ_2 are set equal to zero. Then curves C are what we might call "pure EM" in the sense that $\rho_2(\omega)$ is replaced by its DC value $\rho(0)$. Curves D are obtained by subtracting the EM anomaly from the actual complex resistivity so the quantity plotted is

$$\frac{\rho_a(\omega)}{\rho_a(0)} - \left(\frac{\rho_a^{EM}}{\rho_a(0)} - 1\right)$$

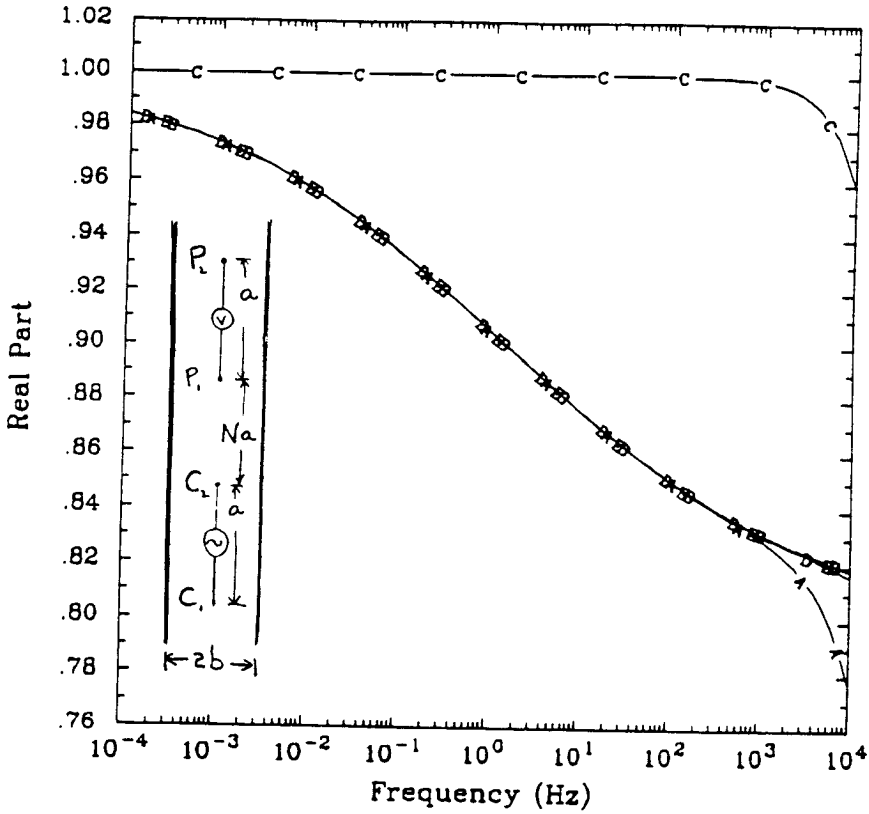

Figure 1.4.7a Dipole-dipole array located on the axis of a bore-hole with the following parameters: $\rho_1 = 1\ \Omega$m, $\rho_2/\rho_1 = 50$, $m_2 = 0.2$, $\tau = 0.1$ $k_2 = 0.25$, $N = 1.0$, $b = 0.1$ m, and $a = 10$ m. **The real part of the normalized complex resistivity is shown for the five cases listed below. Curve A –** $\rho_a(\omega)/\rho_a(0)$, **Curve B –** $\rho_a(\omega)/\rho_a(0)$ **for** $\gamma_1 = \gamma_2 = 0$, **Curve C –** $\rho_a(\omega)/\rho_a(0)$ **for** $m_2 = 0$, **Curve D – EM corrected, see text, Curve E –** $\rho_2(\omega)/\rho_2(0)$.

Finally, in Figs. 1.4.7a and 1.4.7b, curves E correspond to the complex resistivity ratio $\rho_2(\omega)/\rho_2(0)$ or "true IP" of the formation or external region.

It is evident that the electromagnetic coupling (curves C in Figs. 1.4.7a and 1.4.7b) is important at frequencies above about 100 Hz for the parameters chosen. Not surprisingly, the coupling is most noticeable in the imaginary part (i.e. the reactive part) of the apparent complex resistivity where, to the first order, we would expect the EM coupling to be proportional to $j\omega L$ where L is an inductance. In the

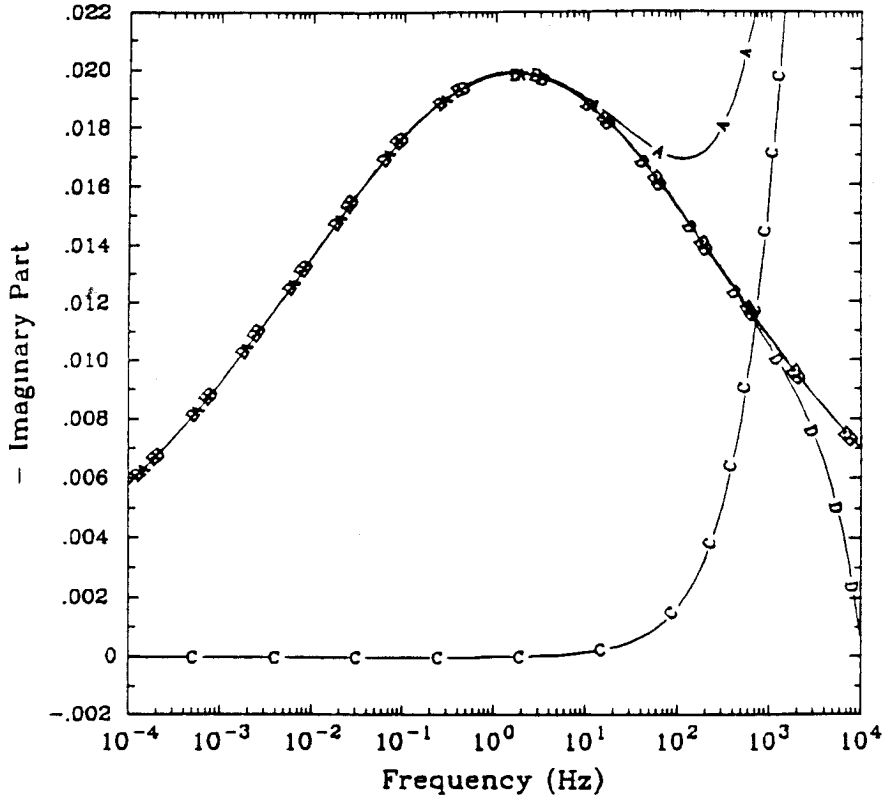

Figure 1.4.7b Dipole-dipole array located in a bore-hole with parameters indicated in caption for Fig. 1.4.7a. Here the imaginary part of the normalized complex resistivity is shown for the same five cases.

hypothetical case where the electromagnetic effects were absent (i.e. $\gamma_1 = \gamma_2 = 0$), we can see from the closeness of curves B and E that the resistivity of the formulation or external region would be almost identical to the measured or apparent resistivity.

To "correct" the apparent complex resistivity in the presence of EM coupling, we perform the single subtraction process indicated above. For the real part, we see from Fig. 1.4.7a that the resultant corrected resistivity coincides, within the graphical accuracy, with the actual resistivity of the external medium. However, the correction process is not so effective (i.e. curves A and D diverge at frequencies above about 200 Hz).

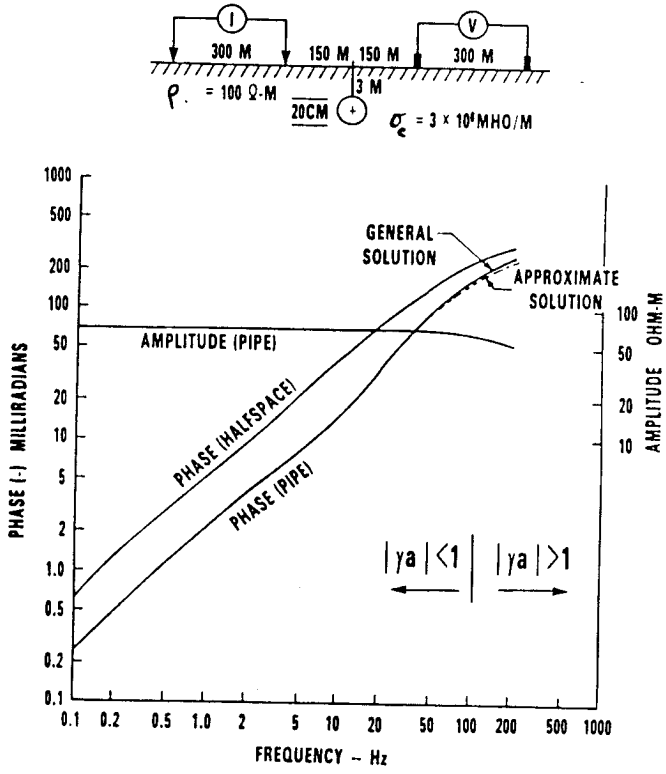

Figure 1.4.8a Amplitude and phase spectra, dipole-dipole array perpendicular to the pipe (spread $N = 1$).

j. More Complicated Cylindrical/Half-Space Problems

Often in dealing with complex resistivity data in the field, the so-called cultural problem arises. The best example is buried conductor such as a metallic pipe or cable that may be in the vicinity of the measuring electrodes. A case in point occurs when we employ a dipole-dipole array on the surface of a half space of the earth which is homogeneous except for a relatively thin conductor located at a fixed depth h. General formulations [Wait 1977a,b, 1978] for this type of problem have been published. The solutions are tractable under the following conditions: the buried conductor or cable is of infinite length, the conductor radius is small compared with other typical dimensions, and the conductor can be described by an axial (spatially dispersive) impedance. Parra [1984] has applied such a formulation to the case

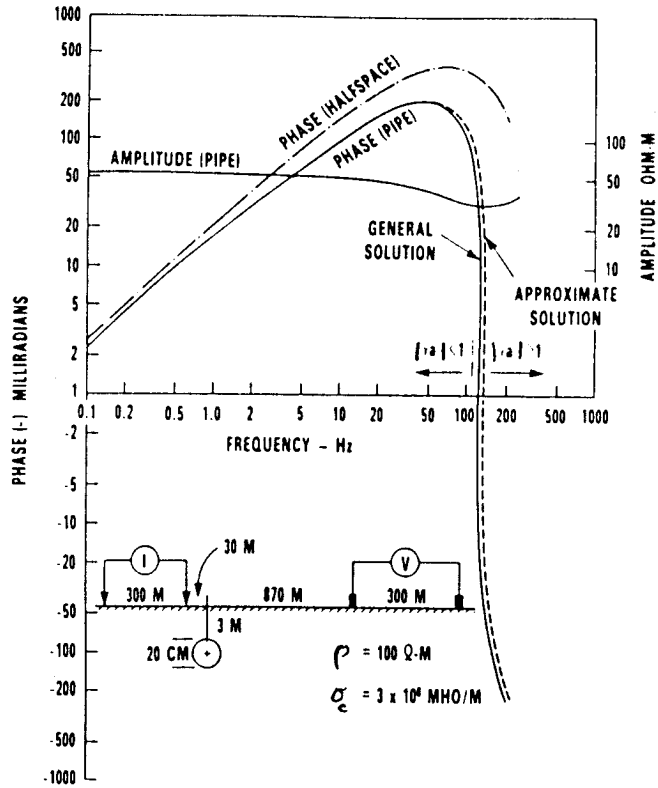

Figure 1.4.8b Amplitude and phase spectra, dipole-dipole array perpendicular to the pipe (spread $N = 3$).

of solid metal pipe of radius 10 cm buried at a depth of $h = 3\,\text{m}$. The half-space has a resistivity of $100\,\Omega\,\text{m}$ while the pipe has a real conductivity $\sigma_c = 3 \times 10^6$ mhos/m. Parra shows various results for a dipole-dipole array that may be oriented at any angle relative to the pipe. His results for two cases where the pipe is at right angles to the dipole-dipole array are shown in Figs. 1.4.8a and 1.4.8b. The amplitude and phase of the effectives complex resistivity are shown as a function of frequency from 0.1 to 10^3 Hz. For comparison, the phase is also shown for the half space in the absence of the pipe. In Fig. 1.4.8a, the pipe is located centrally between the dipoles and buried a distance of 3m. The electrode spacing $a = 300\,\text{m}$ and the spread factor $N = 1$. In Fig. 1.4.8b the pipe is located nearer the transmitting dipole and the spread factor $N = 3$. In the latter case, there is a

drastic change of the phase curve for frequencies greater than 100 Hz. This rapid change of phase seems to occur when $|\gamma a| > 1$ where γ is the propagation constant of the half-space. In Parra's calculations, the magnetic permeability of the pipe is assigned the free space value μ_o. Also, in the curves shown in Figs. 1.4.8a and 1.4.8b, the induced polarization at the pipe surface is neglected. Similar results were presented by Wait and Williams [1985] for the closely related problem of a vertical metal well casing in the vicinity of a surface-based dipole-dipole array. They allowed for the large magnetic permeability of the steel (e.g. $\mu/\mu_o \simeq 500$) and also the appropriate value of the interface impedance η at the steel/electrolyte boundary was incorporated into the calculations. In such a situation, both the eddy currents in the pipe or casing and the induced polarization contribute to the apparent complex resistivity.

Concluding Remarks

As we have demonstrated, the mutual impedance or apparent complex resistivity is a complicated function of the intrinsic complex resistivity of the medium. The influence of direct EM coupling, of the lead wires and effects of buried pipes and wires need to be estimated for a given situation. While it does not seem possible to mathematically justify claims to "remove" EM coupling, it is certainly not inconceivable that special data processing such as devised by Wynn and Zonge [1975, 1977] will emphasize the relative contribution of the induced polarization.

References

[1] Abramowitz, M., and I. A. Stegun (ed.), *Handbook of Mathematical Functions*, Dover, 1964.

[2] Brown, R. J., "EM coupling in multi-frequency IP and a generalization of the Cole-Cole impedance model," *Geophysical Prospection*, **33**, 282–302, 1985.

[3] Dey, A. and H.F. Morrison, "EM coupling in frequency and time domain IP surveys over a multi-layered earth," *Geophysics*, **38**,

380–405, 1973.

[4] Freedman, R. and J. P. Vogiatzis, "Theory of IP logging in a borehole," *Geophysics,* **51**, 1830–1849, 1986.

[5] Hill, D. A. and J. R. Wait, "Comparison of loop and dipole antennas in leaky feeder communication systems," *Int'l. Jour. of Electronics,* **47**, 155–166, 1979.

[6] Gruszka, T. P., "Induced polarization and electromagnetic coupling and their interaction in low frequency geophysical exploration," PhD Thesis, Univ. of Arizona, 1987.

[7] Hohmann, G. W., "EM coupling between grounded wires at the surface of a two-layer earth," *Geophysics,* **38**, 854–863, 1973.

[8] Mahmoud, S. F., S. G. Tantawi, and J. R. Wait, "Interpretation of multi-frequency complex resistivity data for a layered earth model," *IEEE Trans.,* **GE-26**, 399–408, 1988.

[9] Parra, J. O., "Effects of pipelines on spectral IP surveys," *Geophysics,* **49**, 1979–1992, 1984.

[10] Kong, J. A., *Theory of Electromagnetic Waves,* Wiley, 1976.

[11] Pelton, W. H., S. H. Ward, P. G. Hallof, W. R. Sill, and P. H. Nelson, "Mineral discrimination and the removal of inductive coupling with multi-frequency IP," *Geophysics,* 588–609, 1978.

[12] Sommerfeld, A. N., "The propagation of waves in wireless telegraphy," *Annalen der Physik,* Series 4, **28**, pp. 665 and 81, pp. 1135, 1909 and 1926, (in German).

[13] Song, L., "A new decoupling scheme," *Exploration Geophysics,* 1599–112, 1984.

[14] Sunde, E. D., *Earth Conduction Effects in Transmission Systems,* Van Nostrand, 1949.

[15] Wait, J. R., *Electromagnetic Radiation from Cylindrical Structures,* Pergamon, 1959b (reprinted with corrections, Peter Peregrinus Ltd. Stevenage UK, 1988).

[16] Wait, J. R., "EM fields of a horizontal dipole in the presence of a conducting half-space," *Can. Jour. Phys.,* **39**, 1017–1028, 1961.

[17] Wait, J. R., "The variable frequency method," *Overvoltage Research and Geophysical Applications* (edited by J. R. Wait), Perg-

amon Press, 1959a.

[18] Wait, J. R., "EM fields of a dipole over a stratified anisotropic half-space," *IEEE Trans. on Antennas and Propagat.*, **AP-14**, 790–792, 1966b.

[19] Banos, A., *Dipole Radiation in the Presence of a Conducting Half-space*, Pergamon, 1966.

[20] Wait, J. R., "Excitation of a coaxial cable or wire conductor located over the ground by a dipole radiator," *Archiv fur Elektronik und Electragungtechnik*, **31**, 121–127, 1977a.

[21] Wait, J. R., "Excitation of an ensemble of parallel cables by an external dipole over a layered ground," *A.E.U.*, **31**, 489–493, 1977b.

[22] Wait, J. R., "Towards a general theory of induced electric polarization in geophysical exploration," *IEEE Trans. on Geoscience and Remote Sensing*, **GE–19**, 231–234, 1981.

[23] Wait, J. R., "Excitation of currents on a buried insulated cable," *J. Appl. Phys.*, **49**, 876–880, 1978.

[24] Wait, J. R., *GeoElectromagnetism*, Academic Press, 1982.

[25] Wait, J. R. and T. P. Gruszka, "Interaction of EM and electrochemical effects in geophysical probing," *Electronics Letters*, **22**, 393–394, 1986b.

[26] Wait, J. R. and T.P. Gruszka, "On EM coupling removal from IP surveys," *Geoexploration*, **24**, 21–27, 1968a.

[27] Wait, J. R. and J. T. Williams, "EM and IP response of a steel well casing for a four electrode surface array," *Geophysical Prospecting*, **33**, 723–745, 1985.

[28] Wynn, J. C. and K. L. Zonge, "EM coupling," *Geophysical Prospecting*, **25**, 31–51, 1977.

[29] Wynn, J. C. and K. L. Zonge, "EM coupling, its intrinsic value, its removal and the cultural coupling problem," *Geophysics*, **40**, 831–850, 1975.

[30] Wynn, J. C., "EM coupling with a collinear array on a two layer earth," *US Geological Professional Paper 1077*, US Gov't Printing Office, 1979.

1.5 I.P. Response of Prolate Spheroidal Ore Grains

a. Introduction

In the induced polarization method of geophysical prospecting, one exploits the interfacial polarization at the surfaces of dissimilar material. The best example is the interface between a metallic conductor such as an ore grain and the adjacent electrolytic region. Here we will consider the alternating current response of an idealized spheroidal model of the ore grain which has a specified interface impedance $Z(j\omega)$ for a time-harmonic factor $\exp(j\omega t)$. We then consider an ensemble of such particles and obtain an expression for the apparent or effective complex resistivity $\rho_e(j\omega)$ as a function of volume loading and particle shape. We shall restrict attention to frequencies that are low enough to allow potential theory to be used.

The following theoretical development is based partly on previous publications [Wait 1982, 1983, Flanagan 1983, Flanagan and Wait 1985]. Essentially, it is a generalization of the spherical particle model which also utilized the interface impedance concept. We contrast our approach with the electrochemical formulation by Wong and Strangway [1981]. Not withstanding their diligence in fitting their theory to published experimental data, one could question their method in handling the infinite system of coupled mode equations for ionic perturbations. We discuss this point below.

b. Basic Formulation

To conform with the shape of the basic particle, we choose prolate spheroidal coordinates as indicated in Fig. 1.5.1. The relationships between the spheroidal system (η, δ, ϕ) and the cylindrical system (r, ϕ, z) are

$$r = c\left[(1-\delta^2)(\eta^2-1)\right]^{1/2} \tag{1}$$

$$z = c\eta\delta \tag{2}$$

$$\phi = \phi \tag{3}$$

where c is the semi-focal distance. The angular coordinate ranges from -1 to $+1$ while the radial coordinate ranges from 1 to ∞. As indicated in Fig. 1.5.2, the surface of the particle is defined by $\eta = \eta_0$ or, in terms

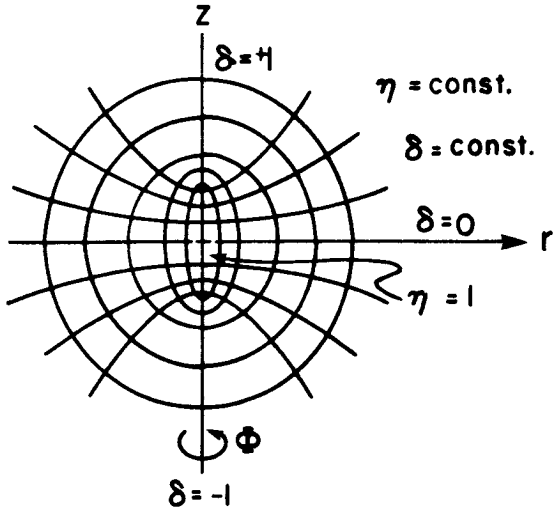

Figure 1.5.1 The prolate spheroidal coordinate system.

of cylindrical coordinates

$$\frac{r^2}{a^2} + \frac{z^2}{b^2} = 1 \tag{4}$$

where a and b are the semi-minor and semi-major axes, respectively. Confocal spheroidal coordinates are then

$$\frac{r^2}{c^2(\eta^2 - 1)} + \frac{z^2}{c^2\eta^2} = 1 \tag{5}$$

provided $a = c(\eta_0^2 - 1)^{1/2}$ and $b = c\eta_0$.

Initially, we assume $b > a$ corresponding to the prolate spheroidal geometry. Later, we indicate the extension to the oblate spheroidal case. In terms of a and b, we have $c = (b^2 - a^2)^{1/2}$ and $\eta_0 = b(b^2 - a^2)^{-1/2}$.

The particle is assigned a resistivity ρ_1 (for $\eta < \eta_0$) and the external region is homogeneous with resistivity ρ. The surface of the particle is characterized by an interface impedance $Z(j\omega)$. In this way, we account for the discontinuity of the potential across the surface.

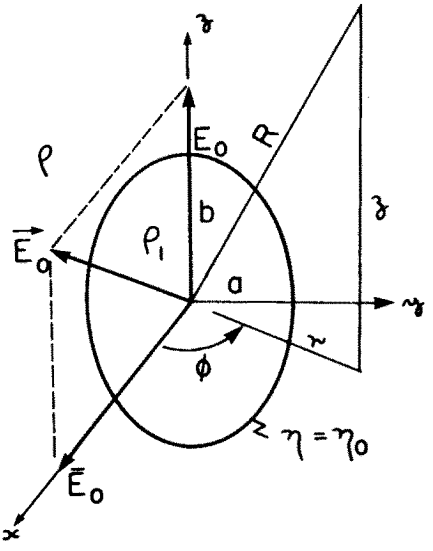

Figure 1.5.2 The spheroidal particle in a locally uniform applied field.

c. Spheroidal Harmonic Solution

Our objective is to determine the response of the spheroid when it is immersed in a uniform electric field $\vec{E}_0$. As indicated in Fig. 1.5.2, $\vec{E}_0$ is in the plane $\phi = 0$ or the (x, z) plane in the cartesian system. Thus, it is convenient to write

$$\vec{E}_0 = \hat{x}\overline{E}_0 + \hat{z}E_0 \tag{6}$$

where $\overline{E}_0$ and E_0 are the transverse and longitudinal components, respectively. Basically, we need to derive the response of the sphere to both transverse and longitudinal field excitations. The general case is then handled by superposition.

The electric fields are obtained from

$$\overline{E} = -\operatorname{grad} \Phi \tag{7}$$

where Φ, the resultant potential, satisfies

$$\nabla^2 \Phi = 0 \tag{8}$$

Solutions are of the form

$$\Phi = \begin{matrix} P_n^m(\eta)P_n^m(\delta)\cos m\phi \\ Q_n^m(\eta)Q_n^m(\delta)\sin m\phi \end{matrix} \tag{9}$$

where, in general, any linear combination is allowed. Here P_n^m and Q_n^m are Legendre polynomials of order m and degree n. The arguments are η for the radial functions and δ for the angular functions. To assure single-valueness, m is an integer. Also, because the field is finite at $\delta = \pm 1$, we can reject the $Q_n^m(\delta)$ functions. Furthermore, we recognize that for the interior (i.e. $\eta < \eta_0$), $Q_n^m(\eta)$ is singular as $\eta \to 1$ so it is not acceptable. Also, in the external region (i.e. $\eta > \eta_0$), we note that $P_n^m(\eta)$ does not vanish as $\eta \to \infty$.

In the case of purely axial excitation (i.e. $\overline{E}_0 = 0$), we write the resultant potentials in the following forms:

For $\eta > \eta_0$

$$\Phi = A^0 P_1(\eta)P_1(\delta) + \sum_{n=1,3,5\cdots}^{\infty} B_n{}^0 Q_n(\eta)P_n(\delta) \tag{10}$$

For $\eta < \eta_0$

$$\Phi = \sum_{n=1,3,5\cdots}^{\infty} C_n{}^0 P_n(\eta)P_n(\delta) \tag{11}$$

Here, A^0 is known while $B_n{}^0$ and $C_n{}^0$ are coefficients to be determined. We note that $m = 0$ because the problem has obvious axial symmetry. In fact, $A^0 = -cE_0$.

In the case of purely transverse excitation (i.e. $E_0 = 0$), the solution forms are as follows:

For $\eta > \eta_0$

$$\Phi = A^1 P_1{}^1(\eta)P_1{}^1(\delta)\cos\phi + \sum_{n=1,3,5\cdots}^{\infty} B_n{}^1 Q_n{}^1(\eta)P_n{}^1(\delta)\cos\phi \tag{12}$$

For $\eta < \eta_0$

$$\Phi = \sum_{n=1,3,5\cdots}^{\infty} C_n{}^1 P_n{}^1(\eta)P_n{}^1(\delta)\cos\phi \tag{13}$$

Here, A^1 is known while B_n^1 and C_n^1 are to be determined. Here, we have taken $m = 1$ and noted that Φ is an even function of ϕ. In fact, $A^1 = -c\overline{E}_0$.

In writing out (10) and (12), we have located the primary potential as the first expression on the R.H.S.(right hand side). In both cases, the summation term represents the secondary potential which vanishes as $\eta \to \infty$. More explicit details are given elsewhere [Wait, 1983].

The first boundary condition is that the normal current density J_η is continuous at the particle surface. To be specific,

$$\frac{1}{\rho_1}\frac{\partial \Phi}{\partial \eta}\Big|_{\eta=\eta_0-0} = \frac{1}{\rho}\frac{\partial \Phi}{\partial \eta}\Big|_{\eta=\eta_0+0} \tag{14}$$

The second boundary condition is that the potential drop across the interface is proportional to the product of the interface impedance $Z(j\omega)$ and the normal current density. This is equivalent to the statement

$$\Phi\Big|_{\eta=\eta_0-0} = \Phi\Big|_{\eta=\eta_0+0} - \frac{Z(j\omega)(\eta_0^2-1)^{1/2}}{\rho c(\eta_0^2-\delta^2)^{1/2}}\frac{\partial \Phi}{\partial \eta}\Big|_{\eta=\eta_0+0} \tag{15}$$

which must hold for $-1 \le \delta \le +1$ [Wait 1982, 1983].

On applying the boundary condition (14) to either (10) and (11) or to (12) and (13), we get

$$\frac{1}{\rho_1}\sum_n C_n{}^m \dot{P}_n^m(\eta_0) P_n{}^m(\delta) = \frac{1}{\rho} A^m P_1(\eta_0) P_1{}^m(\delta) + \frac{1}{\rho}\sum_n B_n{}^m \dot{Q}_n^m(\eta_0) P_n{}^m(\delta) \tag{16}$$

where

$$\dot{P}_n^m(\eta_0) = \frac{\partial}{\partial \eta} P_n{}^m(\eta)\Big|_{\eta=\eta_0} \tag{17}$$

and

$$\dot{Q}_n^m(\eta_0) = \frac{\partial}{\partial \eta} Q_n{}^m(\eta)\Big|_{\eta=\eta_0} \tag{18}$$

Here $m = 0$ or 1 corresponding to longitudinal or transverse excitation, respectively.

We now multiply both sides of (16) by $P_k^m(\delta)$ where k is an integer and then integrate over δ from -1 to $+1$. Making use of the orthogonality relation

$$\int_{-1}^{+1} P_n^m(\delta) P_k^m(\delta) d\delta = \begin{cases} \dfrac{2}{2k+1}\dfrac{(k+m)!}{(k-m)!} & \text{for } k = n \\ 0 & \text{for } k \neq n \end{cases} \tag{19}$$

we deduce that

$$C_k = A^m \frac{\rho_1}{\rho} \frac{P_1^m(\eta_0)}{\dot{P}_k^m(\eta_0)} \delta_{1,k} + B_k \frac{\rho_1}{\rho} \frac{\dot{Q}_k^m(\eta_0)}{\dot{P}_k^m(\eta_0)} \tag{20}$$

which holds for any value of k. Here

$$\delta_{1,k} = \begin{cases} 1 & \text{for } k = 1 \\ 0 & \text{for } k = 3, 5, 7 \cdots \end{cases}$$

Now, we apply the boundary condition (15) which leads to

$$\sum_n C_n^m P_n^m(\eta_0) P_n^m(\delta) = A^m P_1^m(\eta_0) P_1(\delta) + \sum_n B_n^m Q_n^m(\eta_0) P_n^m(\delta) - \frac{Z(j\omega)(\eta_0^2 - 1)^{1/2}}{\rho c (\eta_0^2 - \delta^2)^{1/2}} \left[A^m \dot{P}_1^m(\eta_0) P_1^m(\delta) + \sum B^m \dot{Q}_n^m(\eta_0) P_n^m(\delta) \right] \tag{21}$$

which holds for $-1 < \delta < +1$. We multiply both sides by $P_k^m(\delta)$ and integrate over δ from -1 to $+1$. With (19), this process yields

$$C_k^m P_k^m(\eta_0) = A^m P_1^m(\eta_0) \delta_{1,k} + B_k Q_k(\eta_0) - \frac{Z(j\omega)(\eta_0^2 - 1)^{1/2}}{\rho c} \left[A^m \dot{P}_1^m(\eta_0) a_{1,k} + \sum_{n=1,3\cdots}^{\infty} B_n^m \dot{Q}_n^m(\eta_0) a_{n,k} \right] \tag{22}$$

where

$$a_{n,k} = \frac{2k+1}{2} \frac{(k-m)!}{(k+m)!} \int_{-1}^{+1} \frac{P_n^m(\delta) P_k^m(\delta)}{(\eta_0^2 - \delta^2)^{1/2}} d\delta \tag{23}$$

Combining (20) and (22), we have the single equation set to determine B_k:

$$\frac{1}{A^m}\left[\sum_{n=1,3,\cdots}^{\infty} B_n{}^m \dot{Q}_n^m(\eta_0) a_{n,k} + B_k{}^m \Lambda F_k\right]$$
$$= -\dot{P}_1^m(\eta_0) a_{1,k} + \Lambda f_k \quad (\text{for } k = 1,3,5\cdots) \tag{24}$$

where

$$\Lambda = \frac{\rho c}{Z(j\omega)(\eta_0{}^2 - 1)^{1/2}} = \frac{a(b^2/a^2 - 1)\rho}{Z(j\omega)} \tag{25}$$

$$F_k = \frac{\rho_1}{\rho} P_k{}^m(\eta_0) \frac{\dot{Q}_k^m(\eta_0)}{\dot{P}_k^m(\eta_0)} - Q_k{}^m(\eta_0) \tag{26}$$

and

$$f_k = \left(1 - \frac{\rho_1}{\rho}\right) P_1{}^m(\eta_0)\delta_{1,k} \tag{27}$$

The reader, if you are still with us, is reminded that for the purely axial excitation, $m = 0$ while for the purely transverse excitation, $m = 1$.

d. The Confocal Model

Before discussing concrete results, it is useful to consider the nature of the equation set given by (24). Actually this system is complicated by the presence of the coupling integral given by (23). In our earlier work [Wait 1982, 1983], we have avoided the non-orthogonality by choosing an angle dependent form for the interface impedance. To illustrate this point, we allow the interface impedance to be $Z(\delta, j\omega) = Z_0(j\omega) f(\delta)$ where $f(0) = 1$. Thus, in the boundary condition (15), we replace $Z(j\omega)$ by $Z(\delta, j\omega)$ as defined. The equation set (24) has the same form but now

$$a_{n,k} = \frac{2k+1}{2}\frac{(k-m)!}{(k+m)!}\int_{-1}^{+1} \frac{P_n{}^m(\delta) P_k{}^m(\delta)}{(\eta_0{}^2 - \delta^2)^{1/2}} f(\delta)\, d\delta \tag{28}$$

We now choose the functional form of $f(\delta)$ such that

$$f(\delta) = (\eta_0{}^2 - \delta^2)^{1/2}/\eta_0 \tag{29}$$

over the range $-1 \le \delta \le +1$. In view of (19), we see that

$$a_{n,k} = \begin{cases} 1/\eta_0 & \text{if } n = k \\ 0 & \text{if } n \neq k \end{cases}$$

Then, (24) reduces to

$$\frac{1}{A^m} B_k{}^m \left[\dot{Q}_k^m(\eta_0) + \Lambda_0 F_k \right] = -P_1{}^m(\eta_0) + \Lambda_0 f_k \tag{30}$$

where Λ_0 is now a constant given by $\Lambda_0 = \rho c / Z_0(j\omega)$. Equation (30) can now be used to determine an explicit expression for B_k^m. In this case, the interface impedance can be regarded as a confocal sheath. Indeed, in accordance with (29)

$$f(\delta) = \left[1 - \delta^2 \left(1 - \frac{a^2}{b^2} \right) \right]^{1/2} \tag{29'}$$

which varies from $f(0) = 1$ at the waist to $f(\pm 1) = a/b$ at the tips of the particle. Essentially, this is the model considered by Wait [1983]. While this special angular variation may not be too realistic, it does lead to a simpler solution. Also, it is worth noting that other non-uniform models can be handled by modifying the form of $f(\delta)$.

e. Reduction of General Solution

The extension of the general solution given above for the prolate spheroidal geometry (i.e. $b > a$) to the oblate spheroidal case (i.e. $b < a$) is straight-forward. Analytically, the solutions are identical but we need to allow various parameters to pass from real to imaginary values in a consistent manner [Wait 1983]. We omit further discussion of this matter here.

To apply the general solution for the potential outside the particle, it is desirable to express the results in terms of spherical coordinates (R, θ, ϕ) as indicated in Fig. 1.5.2. Here, we will also restrict attention to the case where $R \gg a$ or b. Then, it is not difficult to show that for $n = 1$

$$Q_1(\eta) \simeq \frac{1}{3\eta^2} \simeq \frac{c^2}{3R^2} \tag{31}$$

$$Q_1{}^1(\eta) \simeq -\frac{2}{3\eta^2} \simeq -\frac{2c^2}{3R^2} \tag{32}$$

and, for $n = 3$

$$Q_3(\eta) \simeq \frac{2}{35\eta^4} \simeq \frac{2c^4}{35R^4} \tag{33}$$

$$Q_3{}^1(\eta) \simeq -\frac{8}{35\eta^4} \simeq -\frac{8c^4}{35R^4} \tag{34}$$

In general, we may note that for $\eta \gg 1$

$$Q_n{}^m(\eta) \simeq (-1)^m \frac{n!(n+m)!2^n}{(2n+1)!\eta^{n+1}}$$
$$\simeq (-1)^m \frac{n!(n+m)!2^n}{(2n+1)!R^{n+1}} c^{n+1} \tag{35}$$

In this sense, only the dipole term is significant. Also, in this same limit, we note that

$$P_1(\eta) \simeq R/c \tag{36}$$
$$P_1{}^1(\eta) \simeq R/c \tag{37}$$
$$P_1(\delta) \simeq z/R \tag{38}$$
$$P_1{}^1(\delta) \simeq z/R \tag{39}$$

We can now express (10) and (12) in convenient forms using the preceding approximations. For axial excitation

$$\Phi_z = -E_0 z + E_0 a^2 b M_z / R^3 \tag{40}$$

and for transverse excitation,

$$\Phi_x = -\overline{E}_0 r \cos\phi + \overline{E}_0 a^2 b (M_x/R^3) r \cos\phi \tag{41}$$

Here M and $\overline{M}$ are normalized dipole moments which are given by

$$M = \left(\frac{c^3}{a^2 b}\right) B_1{}^0 / A^0 \tag{42}$$

and

$$\overline{M} = -\left(\frac{2c^3}{3a^2 b}\right) B_1{}^1 / A^1 \tag{43}$$

This normalization, in effect, means that M and $\overline{M}$ both reduce to 1.0 in the limiting case of a perfectly conducting sphere with zero interface impedance and with the same volume.

f. The Normalized Induced Dipoles

At this stage, it is desirable to show some numerical results for the simpler confocal model formulated earlier [Wait 1982, 1983]. We restrict attention to the case of axial excitation. Thus we need to deduce

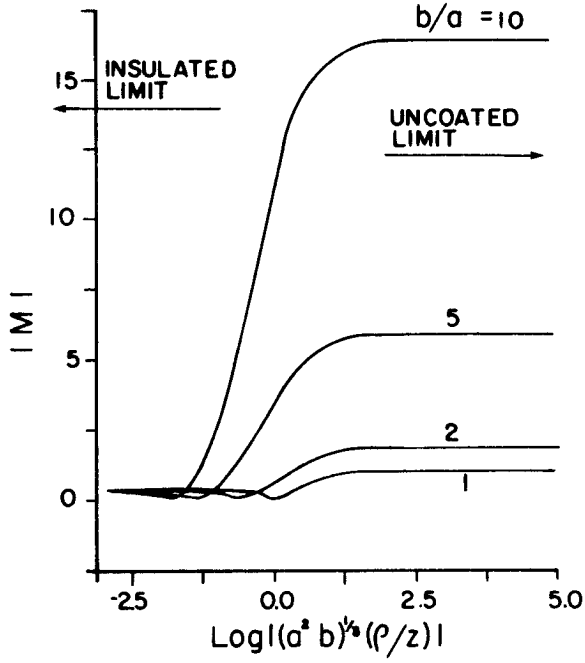

Figure 1.5.3a The magnitude of the normalized axial dipole moment for various spheroidicities calculated from the confocal model.

$B_1{}^m/A^m$ from (30) for $m = 0$, or use the relatively simpler but equivalent formula for M_z given by Wait [1982, 1983]. A useful formula for plotting purposes is the dimensionless quantity $(a^2b)^{1/3}\rho/Z(j\omega)$ which is proportional to (particle volume)$^{1/3}$ and inversely proportional to the interface impedance for a fixed value of the surrounding medium resistivity ρ. Here, we will let ρ be real but $Z(j\omega)$ is intrinsically complex. For purposes of illustration, the phase of $Z(j\omega)$ is taken to be 0.1 radian (i.e. 5.7°). Because we are thinking in terms of metallic particles, it is also permissible to set the particle resistivity $\rho_1 = 0$.

The results for $|M|$ and the phase of M for this confocal model are shown in Figs. 1.5.3a and 1.5.3b for values of $b/a = 1.1, 2, 5$, and 10. As the coating parameter $Z(j\omega)$ tends to zero, the amplitude of the dipole moment becomes very large for the elongated particle (i.e.

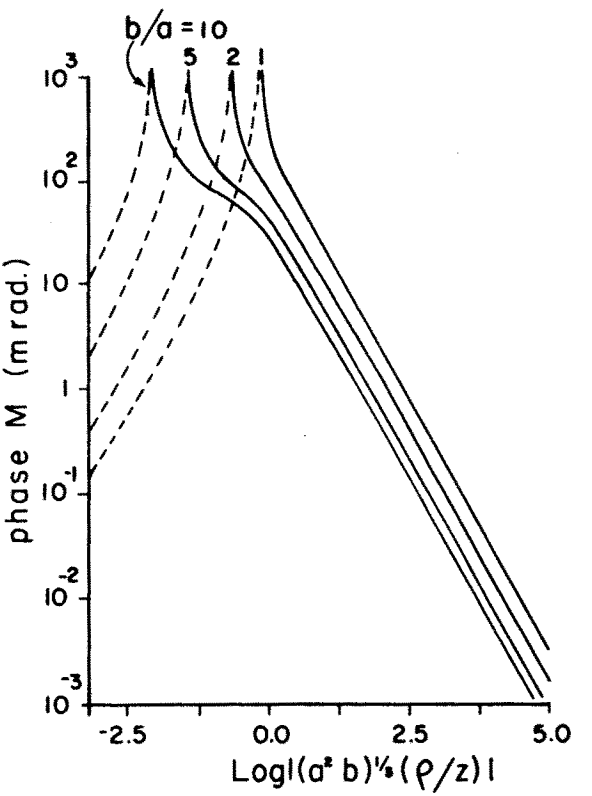

Figure 1.5.3b The phase of the normalized axial dipole moment for various spheroidicities calculated from the confocal model.

$b/a = 10$). This is a current channeling effect which is pronounced for axial excitation. However, the values of $|M|$ are greatly reduced as $Z(j\omega)$ is increased. In the limit of sufficiently large values of $Z(j\omega)$, the particle is acting as a prolate spheroidal void. In the intermediate range, interesting things happen. In fact, there is a point where $|M|$ becomes very small but not quite zero because $Z(j\omega)$ is complex. Here, there is also a rapid change in the phase as indicated in Fig. 1.5.3b.

To deal with the general case of a uniform coating (i.e. $f(\delta) = 1$), we must solve the system of equations given by (24). It is also necessary to evaluate the integral for $a_{n,k}$ given by (23). Both tasks have been implemented by Flanagan [1983] and described by Flanagan and Wait [1985] in detail. The main objective is to get a satisfactory numerical

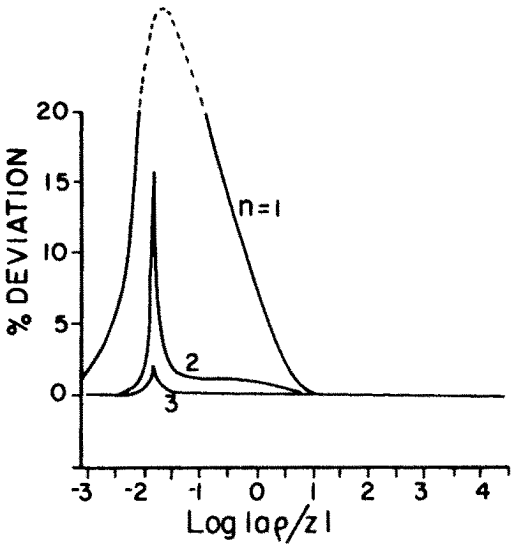

Figure 1.5.4a The convergence of the normal-axial dipole moment for various dimensions of the linear system involved.

solution for B_1/A. To this end, (24) is truncated at a sufficiently large value of n to simulate the infinite system. Not surprisingly, the highly elongated case requires a larger value of n. To illustrate the point, we choose $b/a = 10$ and successively increase n until there is no appreciable change in the solution for B_1/A and the corresponding value of the normalized dipole moment M. For $n = 4$, the error for $|M|$ was less than 1% (relative to the $n = 5$ case). To show the nature of the convergence of the solution process, we plot both the amplitude and the phase of M in Figs. 1.5.4a and 1.5.4b for this example, with $n = 1, 2,$ and 3 relative to the $n = 4$ case. The vertical scale is the percentage deviation so obtained. The convergence is very rapid. Of course, the $n = 1$ case corresponds to neglecting the higher order terms. This is akin to dealing with a confocal model where there is no such coupling.

The values of $|M|$ and the phase of M, are plotted in Figs. 1.5.5a and 1.5.5b using the (non-confocal) interface impedance which does not vary with δ. These results are compared with those in Figs. 1.5.3a and 1.5.3b where $f(\delta)$ is defined by (29). The general shapes and trends in the curves are remarkably similar in spite of the physically different

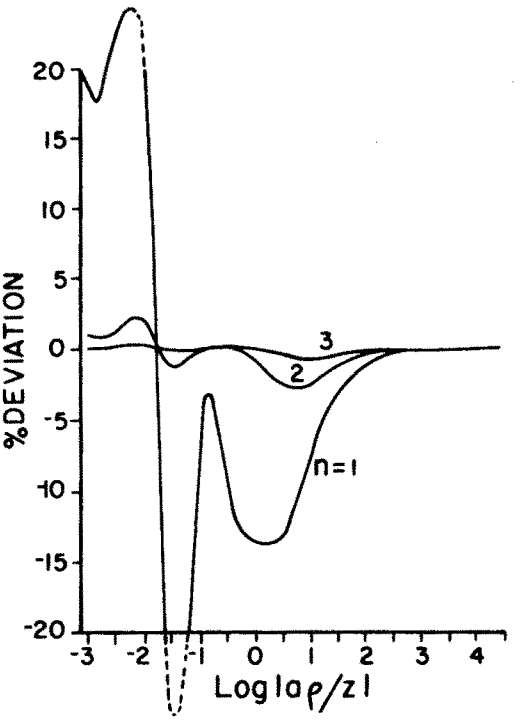

Figure 1.5.4b The convergence of the phase of the normalized axial dipole moment for various dimensions of the linear system involved.

models. In both cases, the phase of the interface impedance was taken to be 0.1 radians.

g. Effective Resistivity of Disseminated Particles

We now consider a uniform distribution of spheroidal particles in a bounded region. The objective is to determine the effective complex resistivity of the mixture. To simplify the problem, we will make a number of assumptions that will become clear in what follows.

As indicated in Fig. 1.5.6, we consider a spherical region of radius R_0. Within this volume there are N identical prolate spheroidal particles all aligned in the axial direction parallel to the applied electric field E_0. We assume that the particle locations are random.

At an external point $P(R, \theta)$ where $R \gg R_0$, we follow Maxwell

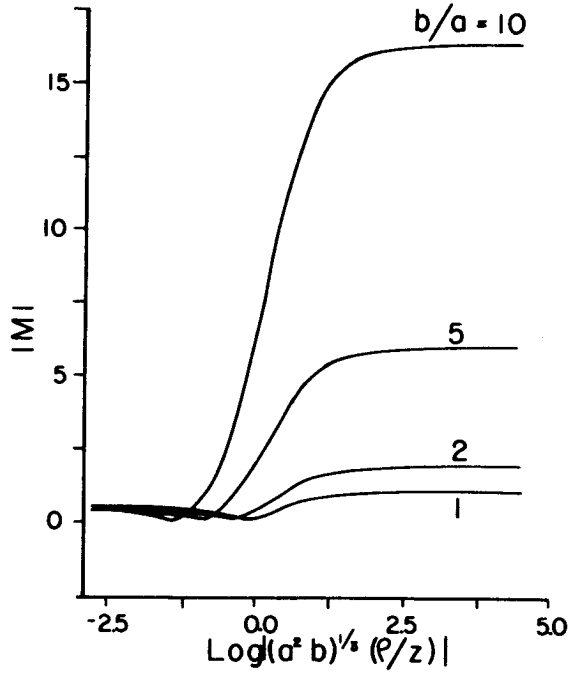

Figure 1.5.5a The magnitude of the normalized axial dipole moment for various spheroidicities.

[1891] and express the potential Φ as the total contribution of all the induced dipoles. Thus,

$$\Phi \simeq -E_0 R\cos\theta + N\frac{M(a^2 b)}{R^2}E_0 R\cos\theta \tag{44}$$

An equivalent expression is

$$\Phi \simeq -E_0 R\cos\theta + \frac{\rho-\rho_e}{\rho+2\rho_e}R_0{}^3 E_0 R^{-2}\cos\theta \tag{45}$$

in terms of the effective resistivity ρ_e of the spherical volume and the resistivity ρ of the background. Equating these two expressions, we have

$$\frac{\rho-\rho_e}{\rho+2\rho_e} = vM \tag{46}$$

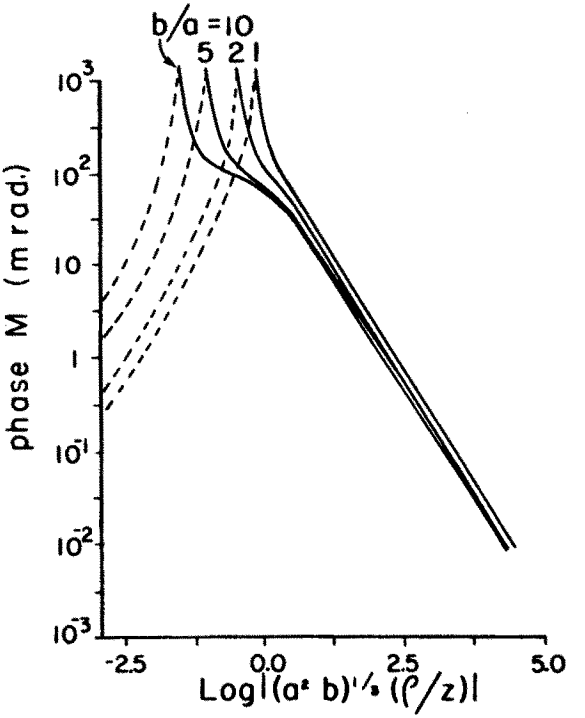

Figure 1.5.5b The phase of the normalized axial dipole moment for various spheroidicities.

where $v = Na^2b/R_0^3$ is the fractional volume loading of the particles within the spherical volume. From (46), we see that

$$\frac{\rho_e}{\rho} = \frac{1 - vM}{1 + 2vM} \simeq 1 - 3vM \tag{47}$$

Following the Maxwell prescription, we have assumed $v \ll 1$ which justifies the superposition of the individual induced dipoles.

Equation (47) can be employed to deduce the effective complex resistivity for axial excitation of a dissemination of aligned prolate spheroidal particles in terms of their normalized dipole moment M. The same reasoning applies to the case where the electric field is applied in the direction transverse to the axes of the particles. Then, in (47), we

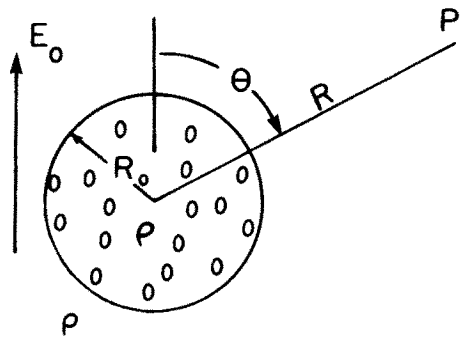

Figure 1.5.6 Ensemble of spheroidal particles.

merely replace M by $\overline{M}$ which is the appropriate normalized dipole moment for the transverse excitation.

A more sophisticated discussion of the effective medium approach is given elsewhere [Flanagan 1983, Wait 1983, Flanagan and Wait 1985]. In the present context, alternative formulas for the effective resistivity of the disseminated particles would not differ from (47) provided v were less than about 5%.

h. Results for the Apparent Complex Resistivity

To present meaningful results for the effective or apparent complex resistivity of the loaded medium, it is necessary to specify the interface impedance as a function of frequency. There are many choices; here, we will adopt a form recommended by Olhoeft [1982]. It has the form

$$Z(j\omega) = A + B/(j\omega)^{\nu} \tag{48}$$

where ν, A and B are constants to be fitted to observed data. For a pyrite/electrolyte interface, Olhoeft found that $\nu \cong 1/2$, $A = 0.9536\ \Omega\text{m}^2$ and $B = 1.7931\ \Omega\text{m}^2(\text{sec})^{-1/2}$ were consistent with experimental data. Leaving aside the physical or electrochemical implications, we will adopt this "Warburg" model. A plot of the amplitude and phase of $Z(j\omega)$ is shown in Fig. 1.5.7.

We now show the corresponding results for the effective or apparent complex resistivity $\rho_e(j\omega)$ of the disseminated model for various

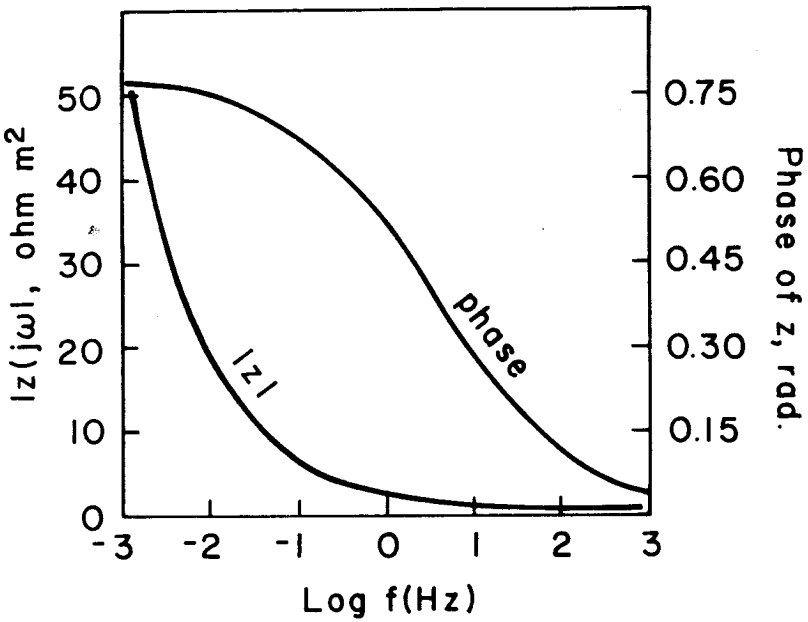

Figure 1.5.7 Interface impedance as a function of frequency for a pyrite/electrolyte boundary according to Olhoeft [1982].

assigned parameters. We use the approximate form given by (47) for the case of axial excitation. For transverse excitation we replace M by $\overline{M}$. The particle resistivity ρ_1 is assigned the value zero and the ambient medium resistivity ρ is set equal to 200 Ωm. The interface impedance is the plotted in Fig. 1.5.7 as described above.

The amplitude $|\rho_e/\rho|$ and the negative of the phase of ρ_e are plotted as a function of frequency in Figs. 1.5.8a and 1.5.8b for the case where $v = 0.05$ and $b/a = 5$ and for four particles (i.e. $a =$ 0.33, 1, 3.3 and 10 mm). Both axial and transverse excitations are shown. The results illustrate that the small particles have a maximum in the phase at higher frequencies as indicated in an early study using a coated sphere model [Wait 1958]. This behaviour is also present in the results computed by Wong and Strangway [1981] with their electrochemical model. In Fig. 1.5.8a, we can also note that $|\rho_e/\rho|$ changes most rapidly at frequencies near where the phase shift is maximum.

In Figs. 1.5.9a and 1.5.9b, we show the influence of the spheroidic-

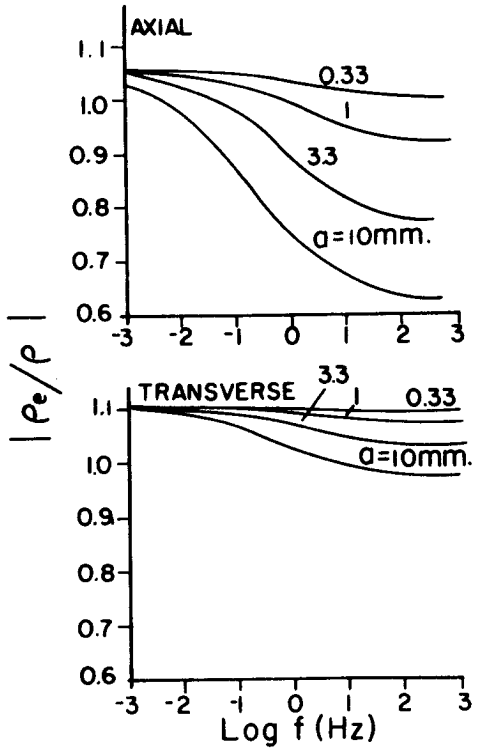

Figure 1.5.8a The magnitudes of the effective axial and transverse resistivities for various particle sizes.

ity ratio b/a on the frequency response curves using the same format as the curves in Figs. 1.5.8a and 1.5.8b. The axial and transverse excitations are designated by A and T, respectively. For the curves in Figs. 1.5.8a and 1.5.8b, $a = 1.0$ mm and $v = 0.05$. Clearly, the elongated particles have an enhanced IP response for axial excitation but the response for purely transverse excitation is only slightly dependent on b/a. In fact, it can be shown that for b/a greater than about 5, the response would be the same as a grating of infinitely long cylinders with the same diameter as the minor axis of the elongated spheroidal particles and with the same volume loading. We might add that the

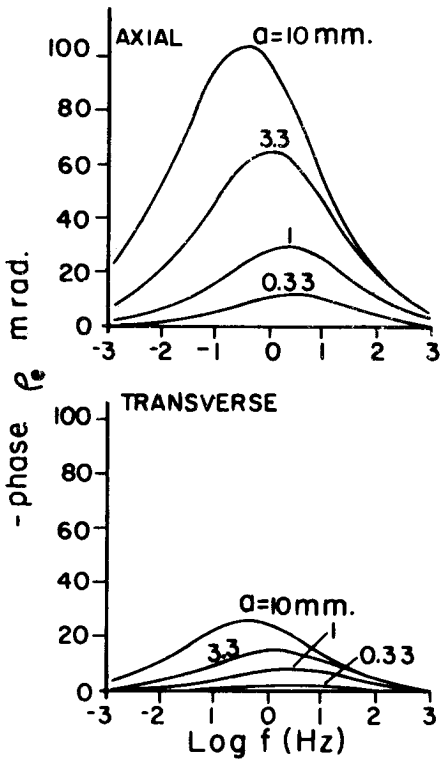

Figure 1.5.8b The phase-shifts of the effective axial and transverse resistivities for various particle sizes.

case designated $b/a = 1.1$ is essentially the same as a spherical particle insofar as the plots are concerned.

Finally, in Figs. 1.5.10a and 1.5.10b, we illustrate the dependence on volume loading v again using the same format as in Figs. 1.5.8a and 1.5.8b. In this case, v varies from 0.01 to 0.2 (i.e. 1 to 20%). The fixed parameters are $a = 1$ mm and $b/a = 5$. As indicated in the phase response, there is almost a linear increase with the volume loading v over this range. According to our simple adaptation of the Maxwell loading law, such a behavior is not surprising. For v greater than 0.05, the simple form given by (47) is in error. As discussed by Flanagan and Wait [1985], a modified mixture formula such as the Brueggman-Hanai form should be preferred but the differences in the

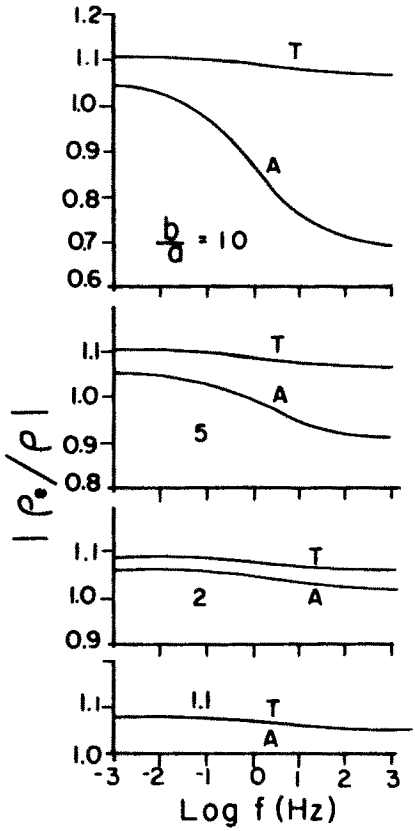

Figure 1.5.9a The magnitudes of the effective axial and transverse resistivities for particles of various spheroidicities.

plots in Figs. 1.5.10a and 1.5.10b, even for $v = 0.20$, would not be significant.

Final Remarks

There are many similarities between our results and those of Wong and Strangway [1981]. In their electrochemical model, an interface impedance descriptor was not used. They dealt explicitly with the active cations which reacted at the metal interface to yield a net charge

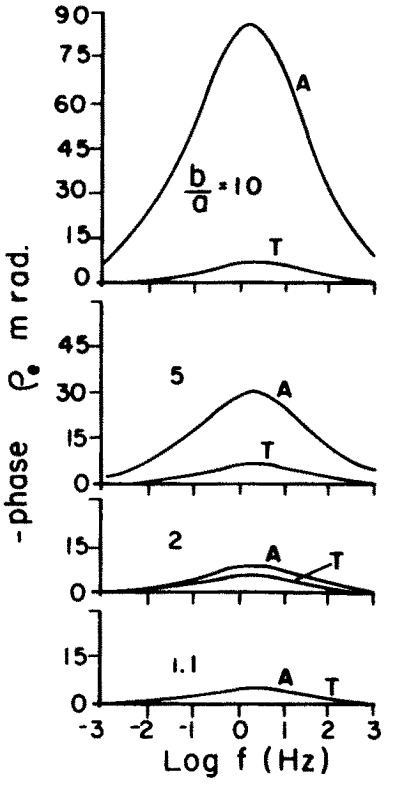

Figure 1.5.9b The phase-shifts of the effective axial and transverse resistivities for particles of various spheroidicities.

transfer. They also needed to solve the coupled time-dependent wave equation to describe the concentration perturbations of both the active and the inactive ions. They neglected the coupling of higher modes for the perturbation solutions. It is difficult to see how this step is justified although the qualitative behavior of the results should not be changed appreciably for the slightly elongated particles. Of course the coupling disappears in the spherical limit [Wong 1979]. But any serious attempt to model elongated particles should address the question of mode coupling which becomes most significant when the particle becomes highly elongated such as a needle. In our interface impedance model, we have attempted to show how to cope with this problem by dealing with the coupled equation set for the modal coefficients.

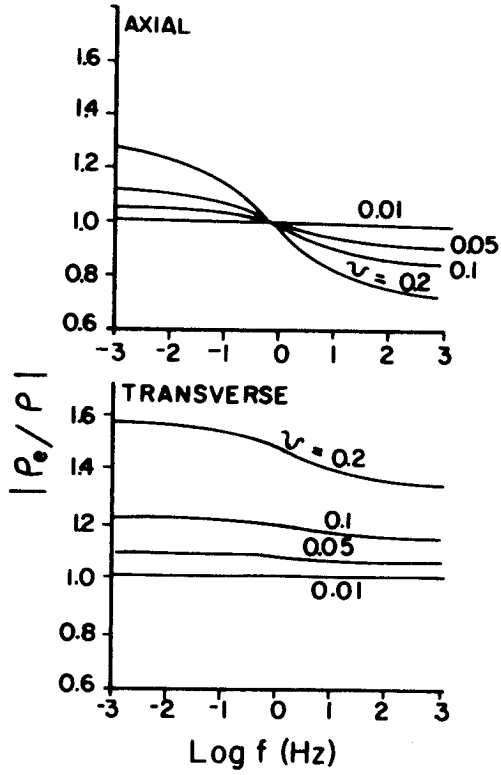

Figure 1.5.10a The magnitudes of the effective axial and transverse resistivities for various volume loadings.

Our results are limited by the assumption that the electrochemical processes can be modelled by an interface impedance. When the radius of curvature of the particle becomes small, such a descriptor will clearly be in doubt. In this case, the local current density at the tips of the particle may be high enough to cause non-linearities in the response. Of course, this limitation also appears in the so called electrochemical formulations.

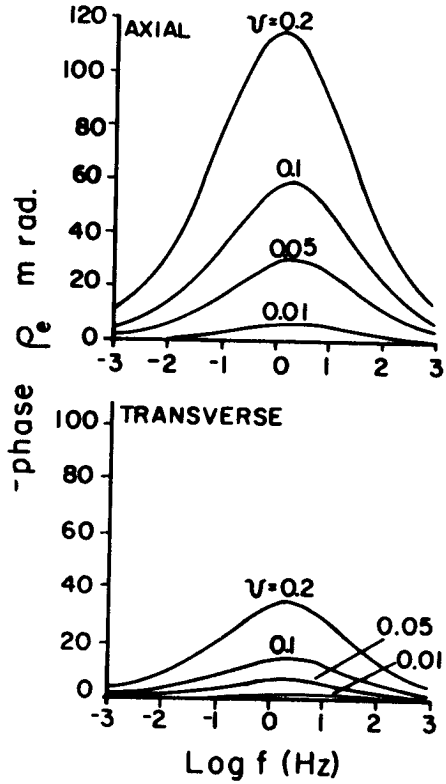

Figure 1.5.10b The phase-shifts of the effective axial and transverse resistivities for various volume loadings.

References

[1] Flanagan, P. W., *M.S. Thesis*, Dept. of Geosciences, University of Arizona, 1983.

[2] Flanagan, P. W. and J. R. Wait, "Induced polarization response of disseminated mineralization for spheroidal geometries," *Radio Science*, **30**, 147–148, 1985.

[3] Maxwell, J. C., *A Treatise on Electricity and Magnetism*, **3rd. ed. part 1**, 314–315, Clarendon Press, Oxford, 1891.

[4] Olhoeft, G. R., "Warburg impedances at single water/mineral interfaces," *Extended Abstracts, Society of Exploration Geophysicists Meeting, Dallas*, 17–21, Oct. 1982.

[5] Wait, J. R., "A phenomenological theory of induced electrical polarization," *Can. Jour. Phys.*, **36**, 1634–1644, 1958.

[6] Wait, J. R., "EM response of a medium loaded with conductive particles," *IEEE Trans. on Geoscience and Remote Sensing*, **GE-20**, 500–503, 1983.

[7] Wait, J. R., "Complex conductivity of disseminated spheroidal ore grains," *Gerlands Beitr. Geophysik (Leipzig)*, **92**, 49–69, 1983.

[8] Wong, J., "An electrochemical model of the induced polarization phenomena in disseminated sulphide ores," *Geophysics*, **44**, 1245–1265, 1979.

[9] Wong, J. and D. W. Strangway, "Induced polarization in disseminated sulphide ores containing elongated mineralization," *Geophysics*, **46**, 1258–1268, 1981.

1.6 Response of Disperse Systems for Simple Particles

a. Introduction

A common feature of geologic media is the lumpy nature of the structure. Thus, at least in an idealized sense, we can represent such a region as a homogeneous host with various kinds of suspended particles. Central to this viewpoint is the characterization of the electromagnetic response of a single particle when it is placed in a uniform field. Also it is appropriate to allow for any boundary layer effects at the interface between the host and the particle. To treat this problem fully, we should really build in the requisite electrochemistry to properly describe the ionic reactions and the transfer of charges across the interface. This aspect of the problem is described in a separate chapter. Here, we argue that the interface can be characterized, at least in a phenomenological sense, by a surface admittance and/or an interface impedance. The meaning of this statement should become clear as we proceed.

b. Formulation

We begin with a very simple model of a solid conducting spherical particle of radius a and of resistivity ρ_1 immersed in a homogeneous host medium of resistivity ρ. To allow for a possible discontinuity of potential across the surface of the particle, we endow it with an interface impedance $Z(j\omega)$ that may be frequency dependent. The applied or primary field E_0 is uniform and directed along the polar axis of a spherical coordinate system (r, θ) centered at the particle. The time factor is $\exp(j\omega t)$ and the frequency is sufficiently low that Laplace's equation governs the fields both inside and outside the particle.

The imposed condition at the boundary $r = a$ amounts to saying that voltage drop $v = ZJ_r$ where J_r is the radial current density. It is understood that Z is both complex and frequency dependent. However, we will avoid non-linear effects and say that Z does not depend on J_r.

c. Potential Theory Solutions (Spherical Model)

Suitable forms for the potentials are

$$\Psi_1 = A_0 r \cos\theta \qquad \text{for} \qquad 0 < r < a \qquad (1)$$

and

$$\Psi = -E_0 r \cos\theta + A r^{-2} \cos\theta \qquad \text{for} \qquad r > a \tag{2}$$

Here A_0 and A are constants to be determined from the boundary conditions. It is evident that $\Psi = -E_0 r \cos\theta$ if $\rho = \rho_1$.

Continuity of radial current density requires that

$$\frac{1}{\rho_1}\frac{\partial \Psi_1}{\partial r} = \frac{1}{\rho}\frac{\partial \Psi}{\partial r} \qquad \text{for} \qquad r = a \tag{3}$$

Also the required potential discontinuity means that

$$\Psi_1 = \Psi - \frac{Z}{\rho}\frac{\partial \Psi}{\partial r} \qquad \text{for} \qquad r = a \tag{4}$$

Applying (3) and (4) to (1) and (2) leads immediately to the solution

$$A_0 = \frac{-3E_0\rho_1}{2\rho_1 + \rho + (2Z/a)} \tag{5}$$

and

$$A = E_0 a^3 \frac{\rho - \rho_1 - (Z/a)}{2\rho_1 + \rho + (2Z/a)} \tag{6}$$

Thus, for the case $r > a$, we can write

$$\Psi = -E_0 r \cos\theta + a^3 E_0 \chi_0 r^{-2} \cos\theta \tag{7}$$

where

$$\chi_0 = \frac{\rho - \rho_0 - (Z/a)}{2\rho_1 + \rho + (2Z/a)} \tag{8}$$

In the case where the double layer is absent, we have $Z = 0$ and the solution reduces to the case where the potential is continuous across the boundary.

The solution given above for the sphere with the interface impedance property is really a special case of that given in the preceding chapter for the spheroid model. In the spherical limit the higher order multipoles are zero.

A slightly more complicated case is to allow the normal current to be discontinuous at the boundary. As a consequence, the tangential electric field just inside the boundary will drive a surface current that

is proportional to the surface admittance $Y(j\omega)$. Now the boundary condition given in (3) is to be replaced by

$$\frac{1}{\rho_1}\frac{\partial \Psi}{\partial r} + \frac{Y}{a}\frac{\partial}{\partial r}\left(r^2\frac{\partial \Psi_1}{\partial r}\right)\Bigg]_{r=a-0} = \frac{1}{\rho_1}\frac{\partial \Psi}{\partial r}\Bigg]_{r=a+0} \tag{9}$$

and (4) is written in a slightly amended form

$$\Psi_1\Big]_{r=a-0} = \Psi - \frac{Z}{\rho}\frac{\partial \Psi}{\partial r}\Bigg]_{r=a+0} \tag{10}$$

For this double shell model, we can write the exterior potential in the form

$$\Psi = -E_0 r\cos\theta + \frac{a^3 E_0 \chi}{r^2}\cos\theta \tag{11}$$

where

$$\chi = \frac{1-\delta}{1+2\delta} \tag{12}$$

with

$$\delta = \frac{(1/\rho)}{(1/\rho_1)+(2Y/a)} + \frac{Z}{\rho a} \tag{13}$$

Here χ can be identified as the normalized induced dipole of the particle. If $Y \to 0$, we recover the solution given by (7) and (8).

The mathematics of the double shell model has been discussed in more detail elsewhere [Wait 1985]. Physically, at zero frequency, the situation corresponds to a solid core of radius a encased by a thin conductive shell which, in turn, is covered by a thin resistive coating. For non-zero frequency, the displacement currents or similar phase shifted currents cause both Y and Z to be complex. Thus χ is complex in general. The electrochemical theorists [e.g. Wong 1979, Chew and Sen 1982] obtain representations for χ involving interactions within the double layer. As we have already indicated, χ, at least in a phenomenological sense, is a characteristic of the particle and its surface layers. Similar suggestions were put forth by Schwan et al. [1962] and Schwartz [1962] who may not have been aware of earlier work by the author and his colleagues [Wait et al. 1956, Wait 1958].

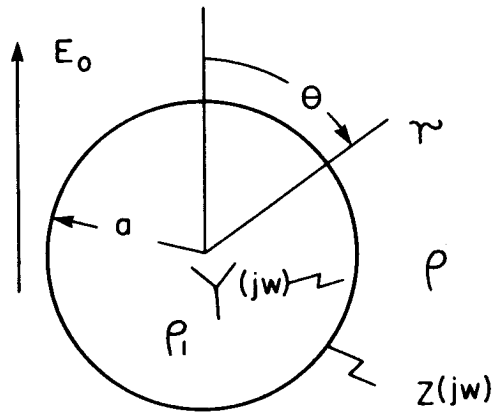

Figure 1.6.1 Basic spherical model as characterized by an interface impedance and/or admittance.

d. Cylindrical Rod Model

While it may seem artificial, another useful model is an infinitely long circular cylinder of radius b which has a resistivity ρ_1. The host medium is homogeneous with resistivity ρ. The cylinder is oriented with its axis at right angle to the applied primary field E_0. We can still refer to Fig. 1.6.1 if this is viewed as a cross section. Again the surface of the *particle* is characterized by an interface impedance $Z(j\omega)$ and a surface admittance $Y(j\omega)$ which, in general, are both complex and frequency dependent.

We now employ cylindrical coordinates (r, θ) not to be confused with the spherical coordinates used above. The appropriate forms for the potentials are now

$$\Psi_1 = B_0 r \cos\theta \qquad \text{for} \qquad 0 < r < a \tag{14}$$

and

$$\Psi = -E_0 r \cos\theta + B r^{-1} \cos\theta \qquad \text{for} \qquad r > a \tag{15}$$

Here B_0 and B are constants to be determined. The boundary conditions, in analogy to the spherical counterpart, are now written

$$\frac{1}{\rho_1}\frac{\partial \Psi_1}{\partial r} + \frac{Y}{a} r \frac{\partial}{\partial r}\left(r \frac{\partial \Psi_1}{\partial r}\right)\Bigg]_{r=a-0} = \frac{1}{\rho_1}\frac{\partial \Psi}{\partial r}\Bigg]_{r=a+0} \tag{16}$$

and

$$\Psi_1\Big]_{r=a-0} = \Psi - \frac{z}{\rho}\frac{\partial \Psi}{\partial r}\Big]_{r=a+0} \tag{17}$$

which, apart from the term involving Y, have the same form as (9) and (10). Using the obtained value for B, we can write (for $r > a$)

$$\Psi = -E_0 r\cos\theta + E_0 a^2 r^{-1}\chi\cos\theta \tag{18}$$

where

$$\chi = \frac{1-\delta}{1+\delta} \tag{19}$$

with

$$\delta = \frac{(1/\rho)}{(1/\rho_1)+(Y/a)} + \frac{Z}{\rho a} \tag{20}$$

This solution for the cylindrical model is almost the same for the spherical model (i.e. compare (18), (19), and (20) with (11), (12), and (13) respectively). An independent justification for the boundary conditions (16) and (17), for the cylindrical model, is given in the Appendix.

e. Ensemble of Spherical Particles

To deal with an ensemble of basic particles, it is desirable to ignore the interaction between the particles. At least, such an idealization is a first step as we have indicated in the preceding section. Thus, we consider the configuration shown in Fig. 1.6.2 where N spherical particles of the same radius a are contained within a spherical volume of radius r_0. The resistivity of the host region both inside and outside the spherical volume is ρ. A uniform field E_0 is applied in the axial direction.

We now follow the original concept put forth by Maxwell that we have alluded to in the preceding section. We begin by writing down an expression for the total potential P at (r,θ) as a superposition of the potentials of each of the particles. Neglecting the interaction between the particles, we have

$$\Psi = -E_0 r\cos\theta + \sum_i^N \frac{E_0 a^3 \chi}{r_i^2}\cos\theta_i \tag{21}$$

where the spherical coordinate system (r_i,θ_i) is chosen for the ith particle with its polar axis (i.e. $\theta_i = 0$) aligned with the applied field.

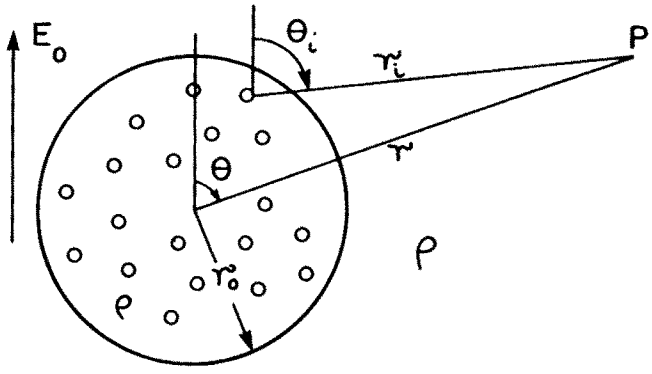

Figure 1.6.2 Ensemble of identical spherical particles enclosed in a spherical volume.

At a sufficiently large distance such that $r \gg r_0$, we can argue that r_i and θ_i in (21) can be replaced by r and θ, respectively. Within this approximation

$$\Psi \simeq -E_0 r \cos\theta + \frac{Na^3\chi}{r^2} E_0 \cos\theta \tag{22}$$

Then, if we regard the spherical region of radius r_0 as a continuum with an effective resistivity ρ_e, we write

$$\Psi = -E_0 r \cos\theta + \frac{r_0^3}{r^2} \frac{\rho - \rho_e}{\rho + 2\rho_e} E_0 \cos\theta \tag{23}$$

We now equate the right hand sides of (22) and (23) to give

$$v\chi = \frac{\rho - \rho_e}{\rho + 2\rho_e} \tag{24}$$

where $v = Na^3/r_0^3$ is the volume of particles per cubic meter; v is called the fractional volume loading. From (24), we deduce the important result

$$\frac{\rho_e}{\rho} = \frac{1 - v\chi}{1 + 2v\chi} \tag{25}$$

which is a generalization of Maxwell's formula. The limitation is that the volume loading v is small compared with 1 but there is no restriction on the particle's properties. In the following section, we review

various attempts to extend the theory to allow for higher volume loading.

It is useful to outline the corresponding solution for a cylindrical volume of radius r_0 loaded with N cylindrical rods of radius a. The sketch shown in Fig. 1.6.2 is still applicable if we view this as the cross section of the cylindrical model. The applied electric field E_0 is taken here to be transverse or perpendicular to the axes of the cylindrical rods. We employ the same procedure as used for the spherical model with essentially the same assumptions. Then, we deduce that the apparent resistivity normalized by the homogeneous host resistivity is given by

$$\frac{\rho_e}{\rho} = \frac{1 - v\chi}{1 + v\chi} \tag{26}$$

where now $v = Na^2/r_0^2$ which again can be identified as the fractional volume loading. In this case, χ is defined by (20) as appropriate for the cylindrical geometry.

f. Extension to Cole-Cole Form

It is interesting to note that the derived formulas, for both the spherical and cylindrical models, yield expressions for the complex resistivity which are reducible to the Cole-Cole form. To explain what we mean by this statement, we will write (25) for the spherical model in the simplified form

$$\frac{\rho_e}{\rho} = \frac{1 - v\chi}{1 + 2v\chi} \simeq 1 - 3v\chi \tag{27}$$

which is justified because $v \ll 1$. We also note that

$$\chi = \frac{1 - \delta}{1 + 2\delta} = 1 - \frac{3}{2}\frac{1}{1 + (2\delta)^{-1}} \tag{28}$$

After a little algebra, we see that

$$\frac{\rho_e}{\rho} \simeq 1 + \frac{3}{2}v - \frac{9}{2}v\left[1 - \frac{1}{1 + (2\delta)^{-1}}\right] \tag{29}$$

The Cole-Cole form for the complex resistivity, as discussed in section 1.2, is written

$$\rho_e(j\omega) = \rho_0\left\{1 - m_0\left[1 - \frac{1}{1 + (j\omega\tau)^k}\right]\right\} \tag{30}$$

where $\rho_0 = \rho_e(0)$ is the DC or zero-frequency apparent resistivity.

By inspection, it is clear that (29) and (30) can be made equivalent if we set

$$\rho_0 = 1 + \frac{3}{2}v \tag{31}$$

$$m_0 = \frac{9}{2}\frac{\rho}{\rho_0}v = \frac{9}{2}v\frac{1}{1+(3v/2)} \simeq \frac{9}{2}v \tag{32}$$

and

$$(j\omega\tau)^k = (2\delta)^{-1} \tag{33}$$

The chargeability m_0 as obtained here is consistent with the simple relation

$$m_0 = \frac{\rho_e(0) - \rho_e(\infty)}{\rho_e(0)} \tag{34}$$

To discuss the fractional frequency term, we first specialize the particle to a perfectly conducting core (i.e. $\rho_1 = 0$ or $y = \infty$). Then, in accordance with (13), $\delta = Z(j\omega)/\rho a$ and thus

$$Z(j\omega) \simeq \frac{\rho a/2}{(j\omega\tau)^k} \tag{35}$$

In other words, the interface impedance is proportional to $(j\omega)^{-k}$. As we discuss elsewhere, this is a realistic approximation to the behavior at an interface between a metal and an electrolyte where k could vary from say 0.2 to 0.4. If the interface impedance as measured fits the law

$$Z(j\omega) = \frac{\alpha_0}{(j\omega)^k} \tag{36}$$

where α_0 and k are adjusted constants, we deduce from (35) that the corresponding time constant τ is given by

$$\tau = \left(\frac{\rho a}{2\alpha_0}\right)^{1/k} \tag{37}$$

This tells us that τ is proportional to (particle radius)$^{1/k}$ where the power $1/k$ is typically in the range from 2 to 5.

Jumping now to the cylindrical model we would write, in place of (29), that

$$\frac{\rho_e}{\rho} \simeq 1 + 2v - 4v\left[1 - \frac{1}{1+\delta^{-1}}\right] \tag{38}$$

This representation is the same as the Cole-Cole form if in (30) we set

$$\rho_0 = 1 + 2v \tag{39}$$

$$m_0 = 4v(1 + 2v)^{-1} \simeq 4v \tag{40}$$

and

$$(j\omega\tau)^k = \delta^{-1} \tag{41}$$

Here a^2/r_0^2 is the fractional volume loading of the cylindrical rods and δ is defined by (20). The remarks made above for the spherical model are unchanged for the cylindrical model but we need replace 2 in (35) and (37) by 1.

It is tempting to argue that, for the more general case, the replacement of δ by a fractional frequency dependence [i.e. proportional to $(j\omega)^{-k}$] is a reasonable supposition. In fact, if we are dealing with an insulating particle, then $\rho_1 \to \infty$ and the corresponding assumption is that surface admittance Y is now proportional to $(j\omega)^k$. Some support for this contention is found in a study by Olhoeft [1985] who found that the empirical law, time constant = $(\text{radius})^2/3.4 \times 10^{-6}$ sec., fitted the experimental data for diffusion-limited processes for particle radii varying from 10^{-9} to 10^{-1} m. In this case, the effective value of the dispersion index k is $1/2$.

In the next section, we consider further generalizations of this particle model and take up again the question of non-spherical particles.

References

[1] Chew, W. C., and P. N. Sen, "Dielectric enhancement due to electrochemical double layer; thin double layer approximation," *J. Chem. Phys.*, **77**, 4683–4692, 1982.

[2] Schwan, H. P., G. Schwarz, J. Maczuk, and H. Pauly, "On the low frequency dielectric dispersion of colloidal particles in electrolyte solution," *J. Phys. Chem. Phys.*, **66**, 2626–2635, 1962.

[3] Schwarz, G., "A theory of the low frequency dielectric dispersion of colloidal particles in electrolyte solution," *J. Phys. Chem.*, **66**, 2636–2642, 1962.

[4] Wait, J. R., "A phenomenological theory of induced electric polarization," *Can. J. Phys.*, **36**, 1634–1644, 1958.

[5] Wait, J. R., H. O. Seigel, L. S. Collett, W. E. Bell, and A. A. Brant, *Method and Apparatus for Geophysical Exploration*, US Patent 2,766,421, 1956. (Application No. 273,422, 1952.) [includes brief derivation of coated particle model].

[6] Wait, J. R., *Electromagnetic Wave Theory*, Harper and Row/ Wiley, 1986. (see chap. 2).

[7] Wong, J., "An electrochemical model of the IP phenomenon in disseminated sulphide ores," *Geophysics*, **44**, 1245–1265, 1979.

[8] Olhoeft, G. R., "Low-frequency electrical properties," *Geophysics*, **50**, 2492–2503, 1985.

1.7 Generalizations of the Spheroidal Model

a. Problem Statement

In discussing the response of an ensemble of coated particles, we have assumed spherical geometry. It is useful to indicate how the formulation can be extended to spheroidal shaped particles. Here, we restrict attention to small volume loadings. Our approach is based on the Maxwell/Wagner technique of enclosing the particles in a closed volume and then deducing the macroscopic or complex resistivity of the ensemble. An important question is how we choose the geometry of the reference volume. This point does not seem to have been addressed by previous workers, e.g. van Beek's [1967] extensive review. We present a relevant analysis here without making any claim about whether the last word on the subject has been said.

The situation is illustrated in Fig. 1.7.1. An ensemble of N identical spheroidal particles of resistivity ρ_1 are enclosed in a spheroidally shaped volume whose macroscopic or effective resistivity ρ_e is to be determined. As indicated in the inset, the basic particle has semi-minor axis a and semi-major axis b. The surface of the particle has an interface impedance Z_0. The reference volume has a semi-minor axis a_e and a semi-major axis b_e. The major axes of both the particle spheroid and the reference spheroid are taken to be parallel to each other and to the applied electric field E_0. To facilitate the analysis, we choose the confocal model for the interface impedance [Wait, 1983a].

The total potential at an external point P for the sparse distribution of particles is given approximately by

$$\Psi \cong -E_0 R\cos\theta + E_0 a^2 b M \sum_{i=1}^{N} \frac{1}{R_i^2}\cos\theta_i \tag{1}$$

where M is a normalized dipole moment of the basic ith particle. Here R_i and θ_i are the appropriate spherical coordinates for the individual ith particle. In writing (1), we have assumed that $R_i \gg a$ and b. The next step now is to write down the corresponding expression for the potential at the point P where we regard the spheroidal reference volume, with its enclosed particles, to be an equivalent uniform medium with complex resistivity ρ_e. Thus

$$\Psi \cong -E_0 R\cos\theta + E_0 a_e^2 b_e M_e \frac{1}{R^2}\cos\theta \tag{2}$$

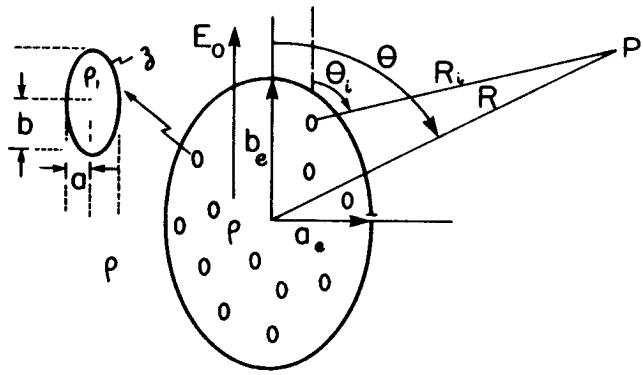

Figure 1.7.1 Ensemble of prolate spheroidal particles within a prolate spheroidal reference volume.

where R is assumed to be large compared with a_e and b_e and where M_e is the effective dipole moment of the volume. In accord with this restriction on R, we can replace R_i and θ_i by R and θ, respectively. Then, we follow the Maxwell/Wagner prescription and equate the righthand sides of (1) and (2) to yield the deceptively simple expression to determine M_e

$$M_e = v\,M \tag{3}$$

where $v = Na^2b/(a_e^2 b)$ is the fractional volume loading of the particles contained within the reference spheroid.

b. Modified Effective Medium Approach

We now call upon the potential theory solution [Wait 1983] for the dipole moment M for an isolated particle of prolate spheroidal form with an interface impedance under the influence of a uniform applied electric field E_0. The appropriate form is

$$M = M_\infty \left[\frac{1-(\Omega+\rho_1/\rho)}{1-(\Omega+\rho_1/\rho)(M_\infty/M_0)}\right] \tag{4}$$

Here M_∞ is the normalized dipole moment for a perfectly conducting spheroidal particle (with axes a and b) *without* any coating (i.e. $Z_0 = 0$). On the other hand, M_0 is the normalized dipole moment of the corresponding spheroidal particle which is perfectly insulating (i.e.

$Z_0 = \infty$). The dimensionless interface parameter Ω is defined by

$$\Omega = \frac{Z_0 a}{\rho b^2}$$

where Z_0 is the actual interface impedance at the waist of the spheroid. In analogy, we have the following expression for the dipole moment parameter for the volume

$$M_e = M_{e\infty} \frac{1 - (\rho_e/\rho)}{1 - (\rho_e/\rho)(M_{e\infty}/M_{e0})} \tag{5}$$

We now combine (3), (4), and (5) to write

$$\frac{\rho - \rho_e}{\rho + \alpha_e \rho_e} M_{e\infty} = v M_\infty \frac{1 - (\Omega + \rho_1/\rho)}{1 + (\Omega + \rho_1/\rho)\alpha} \tag{6}$$

where $\alpha = -M_\infty/M_0$ and $\alpha_e = -M_{e\infty}/M_{e0}$. It is also useful to note that $M_\infty = (1+\alpha)/3$ and $M_{e\infty} = (1+\alpha_e)/3$. In principle, (6) can be employed to deduce the apparent complex resistivity $\rho_e(j\omega)$ in terms of the geometrical parameters and the specified interface impedance function $Z_0(j\omega)$.

While we have been talking about prolate spheroidal particles (i.e. $a < b$), the theory is directly applicable to oblate spheroidal particles (i.e. $a > b$). The results are also applicable to transverse field excitation where the M's are then replaced by the appropriate $\overline{M}$ functions [Wait 1982, 1983a].

To help understand the problem, we show plots of the normalized dipole moment functions in Fig. 1.7.2. Complete expressions for these functions are given elsewhere [Wait 1982, 1983a]. Here, we just indicate the limiting behavior as follows :

For $b \gg a$ (i.e. needle like particles),

$$\left.\begin{aligned} M_\infty &\simeq \frac{(b/a)^2}{3[\ln(2x) - 1]} \\ M_0 &\simeq -1/3 \end{aligned}\right\} \text{ longitudinal excitation}$$

$$\left.\begin{aligned} \overline{M}_\infty &\simeq 2/3 \\ \overline{M}_0 &\simeq -2/3 \end{aligned}\right\} \text{ transverse excitation}$$

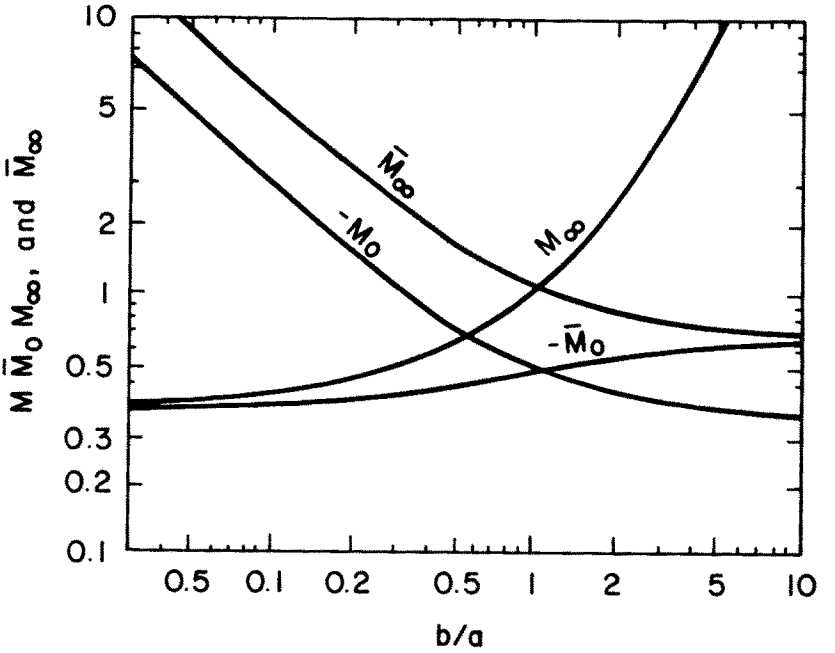

Figure 1.7.2 Normalized dipole moments for perfectly conducting and insulated spheroidal particles for axial and transverse excitations as a function of the ratio of the semi-major axis b to the semi-minor axis a. Prolate spheroidal particles corresponds to $b/a > 1$ while oblate spheroidal particles corresponds to $b/a < 1$.

For $b/a = 1$ (i.e. spherical particles),

$$M_\infty = 1 \qquad \text{and} \qquad M_0 = -1/2$$

For $a \gg b$ (i.e. disc particles),

$$\left.\begin{aligned} M_\infty &\simeq 1/3 \\ M_0 &\simeq -2a/(3\pi b) \end{aligned}\right\} \text{ longitudinal excitation}$$

$$\left.\begin{aligned} \overline{M}_\infty &\simeq 4a/(3\pi b) \\ \overline{M}_0 &\simeq -1/3 \end{aligned}\right\} \text{ transverse excitation}$$

In the case of the spherical limit for both the particle shape and the reference volume, it is clear that $M = M_e = 1$ and $\alpha = \alpha_e = 2$.

Then (6) reduces to

$$\frac{\rho - \rho_e}{\rho + 2\rho_e} = v\frac{1 - (\Omega_s + \rho_1/\rho)}{1 + 2(\Omega_s + \rho_1/\rho)} \tag{7}$$

where

$$\Omega_s = \frac{Z_0}{\rho a}$$

in terms of the particle radius a and the interface impedance $Z_0(j\omega)$ which is constant over the spherical surface. Equation (7) is the form given by Wait [1958]. If $Z_0 \to 0$, we have

$$\frac{\rho - \rho_e}{\rho + 2\rho_e} = v\frac{\rho - \rho_1}{\rho + 2\rho_1} \tag{8}$$

which is the famous Maxwell [1891] result.

c. *Choice of Reference Volume*

In dealing with non-spherical particles, it is necessary to return to (6). One obvious simplification is to allow both the particle and reference spheroids to have the same spheroidicity. That is $b/a = b_e/a_e$. Then (6) reduces to

$$\frac{\rho - \rho_e}{\rho + \alpha\rho_e} = v\frac{1 - (\Omega + \rho_1/\rho)}{1 + \alpha(\Omega + \rho_1/\rho)} \tag{9}$$

where $\alpha = -M_\infty/M_0 = -M_{e\infty}/M_{e0}$. When $Z_0 = 0$ or $\Omega = 0$, (9) reduces to

$$\frac{\rho - \rho_e}{\rho + \alpha\rho_e} = v\frac{\rho - \rho_1}{\rho + \alpha\rho_1} \tag{10}$$

which is often found in the literature [e.g. van Beek 1967, Sen 1981, Fricke 1924, 1953, Sillars 1937]. Here we might note that $\alpha = -1 + L^{-1}$ where L is the depolarization factor commonly employed.

Another possibility is to choose the reference volume to be spherical even when dealing with elongated particles. This assumption was adopted by Wong and Strangway [1981] and Wait [1982]. Further discussion on the choice of the reference spheroid and other generalizations are to be found in Flanagan [1983], Wait [1983a] and Flanagan and Wait [1985]. An obvious consideration is whether the mean separation of the aligned particles are the same or different in the longitudinal and the transverse directions. The general question is still unresolved.

d. Deduced Frequency Dependence

It is useful to examine the general form given by (6) to see if we can draw some general conclusions about the frequency dependence of the observed conductivity in terms of the specified interface impedance $Z_0(j\omega)$. In particular, we would like to see how the empirical Cole-Cole form [e.g. see Pelton 1977] might be related to this effective medium formulation.

We can easily solve (9) directly for $\rho_e(j\omega)$. If we just retain terms in first order of v, it follows quite readily that

$$\begin{aligned}\rho_e(j\omega) &\simeq \rho\left[1 - v(1+\alpha_e)\frac{M_\infty}{M_{e\infty}}\left(\frac{1-\Omega_e}{1+\alpha\Omega_e}\right)\right] \\ &\simeq \rho\left[1 - v(1+\alpha)\frac{(1-\Omega_e)}{(1+\alpha\Omega_e)}\right] \end{aligned} \tag{11}$$

where

$$\Omega_e = \Omega + \frac{\rho_1}{\rho}$$

We note that by simple algebra

$$\frac{1-\Omega_e}{1+\alpha\Omega_e} = 1 - \left(1+\frac{1}{\alpha}\right)\frac{1}{1+(\alpha\Omega_e)^{-1}} \tag{12}$$

Thus (10) can be cast in the form

$$\rho_e(j\omega) = \rho_0\left\{1 - m_0\left[1 - \frac{1}{1+(\alpha\Omega_e)^{-1}}\right]\right\} \tag{13}$$

where

$$\begin{aligned}\rho_0 &= \rho\left[1 + \frac{1+\alpha_e}{\alpha}\frac{M_\infty}{M_{e\infty}}v\right] = \rho\left[1 + \frac{3M_\infty}{\alpha}v\right] \\ &= \rho\left[1 + \frac{1+\alpha}{\alpha}v\right] \end{aligned} \tag{14}$$

and

$$m_0 = \frac{\rho}{\rho_0}\frac{(1+\alpha_e)(1+\alpha)}{\alpha}\frac{M_\infty}{M_{e\infty}}v = \frac{\rho}{\rho_0}\frac{(1+\alpha)^2}{\alpha}v \tag{15}$$

We now follow previous workers and direct our attention to metallic particles located in an electrolytic host medium. Then $\rho_1/\rho \ll 1$ and

furthermore we assume that the frequency dependence of the interface impedance is characterized by

$$Z_0(j\omega) = \frac{\delta_0}{(j\omega)^k} \tag{16}$$

where δ_0 is a constant and where k is an exponent typically in the range from $1/4$ to 1. We can set

$$\frac{1}{\alpha\Omega_e} \simeq \frac{1}{\alpha\Omega} = (j\omega\tau)^k \tag{17}$$

where τ is time constant (in seconds). In fact we see that

$$\tau = \left[\left(\frac{\rho b^2}{a}\right)\frac{1}{\alpha\delta_0}\right]^{1/k} \tag{18}$$

which follows from (5). By using (17), it is evident that (13) becomes

$$\rho_e(j\omega) = \rho_0\left[1 - m_o\left(1 - \frac{1}{1+(j\omega\tau)^k}\right)\right] \tag{19}$$

which has precisely the Cole-Cole form as promulgated by Pelton [1977]. We may identify ρ_0 as the zero frequency or DC response and m_0 is called the "chargeability factor". In fact we may confirm that

$$m_0 = \frac{\rho_e(0) - \rho_e(\infty)}{\rho_e(0)} \tag{20}$$

which is consistent with conventional definitions, at least for small values of m_0 (i.e. m_0 or $v \ll 1$).

It is interesting to note that much of the experimental data on induced polarization in rock/mineral environments shows that $k \simeq 1/2$ as evidenced by the fact that τ varies as the mean particle size [Olhoeft 1981]. This factual statement lends some support for the Warburg diffusion process at metal/electrolyte interfaces.

e. Extension to Asymmetrical Excitation

In our previous discussion we have selected identical spheroidal particles with their axes of symmetry parallel to the applied field. It

is a simple matter to extend the formulation to the case when the applied field is transverse or perpendicular to the axes of symmetry of the particles. As we indicated above, we merely replace the functions M_e and α_e by $\overline{M}_e$ and $\overline{\alpha}_e$ in (6). The formula now gives the apparent resistivity $\overline{\rho}_e$ in the transverse direction. Another interesting extension is when we are dealing with a random orientation of the particles. Then, the medium is isotropic at least in a macroscopic sense. In this case, we have

$$\frac{(\rho-\rho_e)(1+\alpha_e)}{\rho+\alpha_e\rho_e} = \frac{v}{3}(1+\alpha)\left[\frac{1-(\Omega+\rho_1/\rho)}{1+(\Omega+\rho_1/\rho)\alpha}\right] + \frac{2v}{3}(1+\overline{\alpha})\left[\frac{1-(\Omega+\rho_1/\rho)}{1+(\Omega+\rho_1/\rho)\overline{\alpha}}\right] \tag{21}$$

where α_e is the polarizability coefficient for the reference spheroid while α and $\overline{\alpha}$ are the polarizability coefficients for the longitudinal and transverse excitations of the particles respectively. In this situation, we should probably select the reference spheroid to be a sphere in which case $\alpha_e = 2$. When the coating parameter Ω is set equal to zero, (21) agrees with Fricke [1953].

The extension of the mixture formulas, to the case where the loading parameter v is not small, is not simple. A sizeable literature on this topic exists at least for particles of spherical shape [e.g. Bruggeman 1931 and Hanai 1968]. Also uncoated spheroidal particles have been given some attention even for fractional volume loadings approaching unity [e.g. Sen 1981 and Wait 1983b]. Here we indicate how this so called Bruggeman-Hanai approach can be applied to the coated spheroid model.

We begin with (6) which is written in equivalent form as

$$\frac{\Lambda_e-\Lambda}{L_e\Lambda_e-(L_0-1)\Lambda} = v\frac{\Lambda_1-\Lambda}{L\Lambda_1-(L-1)\Lambda} \tag{22}$$

where the newly defined admittance functions are defined as follows

$$\frac{1}{\Lambda}=\rho, \quad \frac{1}{\Lambda_e}=\rho_e \quad \text{and} \quad \frac{1}{\Lambda_1}=\rho_1+\frac{Z_0}{b^2/a}$$

and where the often used depolarization factors are defined by

$$L_e = 1/(1+\alpha_e) \quad \text{and} \quad L = 1/(1+\alpha)$$

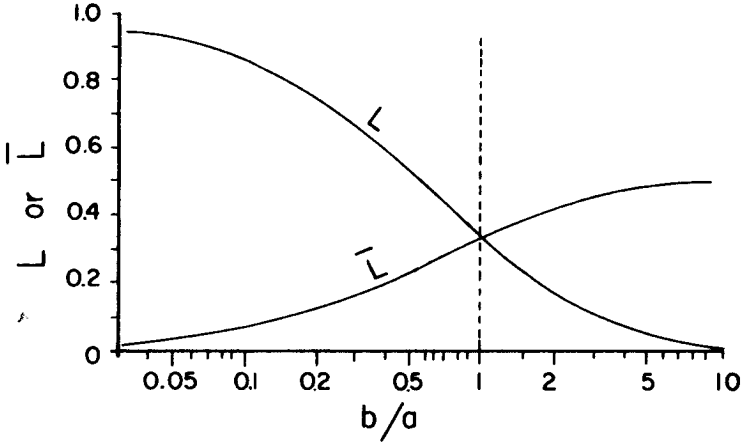

Figure 1.7.3 The axial (L) and the transverse ($\overline{L}$) depolarization factors.

Plots of L and $\overline{L}$ (for transverse excitation) are shown in Fig. 1.7.3.

In (22), we can set $v = 1-\phi$ in terms of the porosity ϕ which is 1 if the particles are absent. We now point out that (11) can be applied in a sequence of small steps to handle any value of v or ϕ. At least that is the claim following the original proposal of Bruggeman [1931]. We return to (22) and we argue that, as a result of filling the composite with grains to the intermediate concentration $1-\phi$, a medium with effective admittivity is obtained. We now augment every unit volume of this intermediate medium with a small volume du of spheroids (with the same common eccentricity and alignment) having an admittivity Λ_1. Then, according to (22), we can assert that the corresponding increment of effective admittivity is

$$\frac{d\Lambda_e}{\Lambda_e} = \frac{\Lambda_1 - \Lambda_e}{L\Lambda_1 - (L-1)\Lambda_e} du \tag{23}$$

which is independent of the parameter L_e for the reference spheroid.

Now some of the augmented grains of volume $v\,du$ have actually replaced grains already present. Thus, the resultant increment dv is related to du by the equation

$$dv = (1-v)du$$

or

$$\frac{d\phi}{\phi} = -du \tag{24}$$

Using (24), we can write (22) in the form

$$\left[\frac{L\Lambda_1 - (L-1)\Lambda_e}{\Lambda_1 - \Lambda_e}\right]\frac{d\Lambda_e}{\Lambda_e} = -\frac{d\phi}{\phi} \tag{25}$$

This can be arranged to

$$\frac{L}{\Lambda_e}d\Lambda_e + \frac{1}{\Lambda_1 - \Lambda_e}d\Lambda_e + \frac{1}{\phi}d\phi = 0 \tag{26}$$

which is equivalent to

$$\frac{d}{d\phi}\left[\Lambda_e^L \frac{1}{\Lambda_e - \Lambda_1}\right] = 0 \tag{27}$$

The solution of this differential equation is trivial if we use the initial condition that $\Lambda_e = \Lambda$ when $\phi = 1$ (or $v = 0$). Then, we obtain the interesting result

$$\left(\frac{\Lambda_e}{\Lambda}\right)^L \left(\frac{\Lambda - \Lambda_1}{\Lambda_e - \Lambda_1}\right)\phi = 1 \tag{28}$$

This formula reduces to the classic formula first derived by Bruggeman [1931] for spherical particles with no interface impedance (i.e. $L = 1/3$ and $Z_0 = 0$). There is now convincing experimental data [e.g. Hanai 1968 and Sen 1981] that the Bruggeman formula, at least for spherical particles or occlusions, is more accurate than the Maxwell-Wagner forms at larger values of v or $1 - \phi$. But the jury is still out on this question and doubts concerning the iterations of the first order formulation to higher volume loadings are without any rigorous foundation.

As we have indicated, (28) satisfies the initial condition $\Lambda_e = \Lambda$ for $\phi = 1$ corresponding to the absence of grains or particles. It is interesting to note that, in the limit $\phi \to 0$, we have $\Lambda_e \to \Lambda$ or $\rho_e \to \rho_1$ in the case of uncoated particles. This limit is highly artificial because the particles would fill all the space and the dipole induced moment concept, for individual particles, would obviously break down. Nevertheless, the trend of this limit does instill some confidence in the usefulness of the Bruggeman/Hanai type formulas for dense packing of the particles (i.e. low porosity).

f. Sen's Geometrical Model

We have tried to be fairly general in our discussion of the mixture or effective medium concept. Both particle shape and interface impedance properties can be included via our definitions of the admittivity concept. However, it is useful to digress here and consider just the influence of particle shape following up some of the cogent comments of Sen [1981]. Thus we dispense with electrochemical characteristics and just focus on the geometrical effects. To this end, we will consider the particles or occlusions as being pure dielectrics characterized by a permittivity ϵ_1. In (28), $\Lambda_1 = j\epsilon_1\omega$ where we have already noted that $Z_0 = 0$. We also assume that the suspending medium is effectively brine with a real conductivity $\Lambda = \sigma$ (i.e. $\sigma \ll \epsilon\omega$). For $L = 1/(1+\alpha)$, (28) can be written

$$\left(\frac{\Lambda_e}{\sigma}\right)\left[\frac{1-(j\epsilon_1\omega/\sigma)}{1-(j\epsilon_1\omega/\Lambda_e)}\right]^{-\frac{1+\alpha}{\alpha}} = \phi^{\frac{1+\alpha}{\alpha}} \tag{29}$$

We further argue that $\epsilon_1\omega/\sigma$ and $\epsilon_1\omega/\Lambda_e$ will be small. To first order, $\Lambda_e \simeq \sigma_e + j\epsilon_e\omega$ where the effective (real) conductivity is given by

$$\sigma_e \simeq \sigma(\phi)^{\frac{1+\alpha}{\alpha}} \tag{30}$$

and the effective (real) permittivity is

$$\epsilon_e \simeq \frac{1+\alpha}{\alpha}\epsilon_1\left(1-\phi^{\frac{1+\alpha}{\alpha}}\right) \tag{31}$$

We note here that (28) has the same form as Archie's law written as $\sigma_e = \sigma\phi^m$ where $m = (1+\alpha)/\alpha$ in our notation. For spheres, we have $m = 3/2$ which indicates that $\sigma_e = \sigma\phi^{3/2}$, a form that has been verified experimentally by Sen, Scala, and Cohen [1981] for polystyrene glass beads in a salt solution. In actual porous media in a geological setting, the observed value of m, called the cementation index, may vary from 1.5 for loosely compacted rocks to 2.5 or higher for tight material [Sumner 1976]. We can also write $m = (1-L)^{-1}$ where L is the depolarization coefficient. For disc shaped occlusions, $L \simeq 1$ and m becomes very large. For example, if $b/a \ll 1$, $m \simeq 2a/\pi b$

which leads to a strong dependence on porosity when the current flow is perpendicular to the axis of such pancake-shaped dielectric particles even when their volume is relatively small.

The effective permittivity ϵ_e, as given by (31) for disc particles with their axes parallel to the field, is given by

$$\epsilon_e \simeq \frac{2a}{\pi b}\epsilon_1 \left(1 - \phi\frac{2a}{\pi b}\right) \tag{32}$$

The relative dielectric constant ϵ_e/ϵ_1, can be very large if $a/b \gg 1$ (i.e. very thin discs) even for moderately large values the porosity ϕ. In this case, the discs are acting as small condensors with very high capacitance. This phenomena is related, of course, to the classical Maxwell-Wagner effect in the context of planar layered media [van Beek 1967].

When we deal with transverse excitation of the aligned spheroids, we replace L by $\overline{L}$ or α by $\overline{\alpha}$. For needle like particles (i.e. $b/a \gg 1$), we see that $\overline{\alpha} = 1$ so that the cementation index $m \simeq 2$. In the case of discs, $\overline{\alpha} \simeq 4a/\pi b \gg 1$ for $m \simeq 1$.

Another possibility is that we work with (21) corresponding to randomly oriented particles. The resulting differential equation for the effective isotropic conductivity is then found to be

$$d\Lambda_e \simeq -\frac{d\phi}{3\phi}(\Lambda_1 - \Lambda_e)\left[\frac{1}{1 + L(\Lambda_1 - \Lambda_e)/\Lambda_e} + \frac{2}{1 + \overline{L}(\Lambda_1 - \Lambda_e)/\Lambda_e}\right] \tag{33}$$

An analogous equation was derived by Veinberg [1967] for magnetic systems such as a ferromagnetic powder cemented with non-magnetic material. Following Veinberg, we may integrate (33) with the initial condition that $\Lambda_e \to \Lambda$ as $\phi \to 1$ but the result is complicated. A simple limiting case is when the occlusions are pure insulators such that $\Lambda_1 \simeq 0$ (which is only strictly possible at DC). In this case, (33) reduces to

$$d\Lambda_e \simeq \frac{d\phi}{3\phi}\Lambda_e\left(\frac{1}{1 - L} + \frac{2}{1 - \overline{L}}\right) \tag{34}$$

The solution now reads

$$\Lambda_e = \Lambda\phi^M \tag{35}$$

where

$$M = \frac{2}{3}\left(\frac{1+\alpha}{2\alpha} + \frac{1+\overline{\alpha}}{\overline{\alpha}}\right) = \frac{1}{3}\left(\frac{1}{1-L} + \frac{2}{1-\overline{L}}\right) \tag{36}$$

In terms of resistivities,

$$\rho_e = \rho\phi^{-M} \tag{37}$$

which again has the same form as Archie's empirically derived law mentioned above.

As expected, M reduces to $3/2$ for spherical cavities or occlusions. For needle-shaped cavities $\alpha \to \infty$ and $\overline{\alpha} \to 1$ whence $M \simeq 5/3 = 1.66\ldots$. For disc-shaped cavities, $\alpha \simeq \pi b/2a$ and $\overline{\alpha} \simeq 4a/\pi b$ in which case $M \simeq (1/3)(2a/\pi b)$ can be very large in spite of the weighting factor $1/3$.

References

[1] Archie, G. E., "The electrical resistivity log as an aid in determining some reservoir characteristics," *Trans. AIME*, **146**, 54–62, 1942.

[2] Bruggeman, D. A. G., "Berechnung verschiedner physikalischer Komstanten von heterogeren Substanzen," *Ann. der Physik* (Leipzig), **24**, 636–664, 1931.

[3] Flanagan, P. W., *M.S. Thesis,* Dept. of Geosciences, University of Arizona,1983.

[4] Flanagan, P. W., and J. R. Wait, "Induced polarization response of disseminated mineralization for spheroidal geometries," *Radio Science*, **30**, 147–148, 1985.

[5] Fricke, H., "A mathematical treatment of the electric conductivity and capacity of disperse systems," *Phys. Rev.*, **24**, 575–587, 1924.

[6] Fricke, H., "The Maxwell-Wagner dispersion in a suspension of ellipsoids," *J. Phys. Chem.*, **57**, 934–937, 1953.

[7] Hanai, T., "Electrical properties of emulsions," *Emulsion Science*, (P. Sherman, ed.), Academic Press, 354–478, 1968.

[8] Maxwell, J. C., *A Treatise on Electricity and Magnetism, 3rd. ed. PtII*, Clarendon Press, 1891 (reprinted Dover Publications, New York, 1954).

[9] Olhoeft, G. R., "Electrical properties of rocks," *Physical Proper-*

ties of Rocks and Minerals, (Y. S. Touloukian, ed.), McGraw-Hill, New York, 257–330, 1981.

[10] Pelton, W. H., *Interpretation of Induced Polarization and Resistivity data*, Ph.D. Thesis, Univ. of Utah, 256 pages, 1977.

[11] Sen, P. N., C. Scala, and M. Cohen, "A self similar model for sedimentary rocks with application to the dielectric constant of fused glass beads," *Geophysics*, **46**, 781–795, 1981.

[12] Sen, P. N., "Relation of certain geometrical features to the dielectric anomaly of rocks," *Geophysics*, **46**, 1714–1720, 1981.

[13] Sillars, R. W., "The properties of a dielectric containing semiconducting particles of various shapes," *J. Inst. of Elect. Engs.*, (London) **80**, 378–394, 1937.

[14] Sumner, J. S., *Principles of Induced Polarization for Geophysical Exploration*, Elsevier, Amsterdam, New York, 1976.

[15] van Beek, L. K. H., "Dielectric behavior of heterogeneous systems," *Progress in Dielectrics*, **7**, 69–114, 1967 (Heywood Books, London).

[16] Veinberg, A. K., "Permeability, electrical conductivity, dielectric constant, and thermal conductivity of a medium with spherical and ellipsoidal inclusions, " *Sov. Phys. Dokl.*, **11**, 593–595, 1967.

[17] Wait, J. R., "A phenomenological theory of induced electrical polarization," *Can. J. Phys.*, **36**, 1634–1644, 1958.

[18] Wait, J. R., "Electromagnetic response of a medium loaded with coated (spheroidal) conductive particles," *IEEE Trans.*, **GE-20**, 500–504, 1982.

[19] Wait, J. R., "Effective electrical properties of heterogeneous earth models," *Radio Science*, **18**, 19–24, 1983b (errata 18, 796, 1983).

[20] Wong, J. and D. W. Strangway, "Induced polarization in disseminated sulphide ores containing elongated mineralization," *Geophysics*, **46**, 1258–1268, 1981.

[21] Wait, J. R., "Complex conductivity of disseminated spheroidal ore grains," *Gerlands Beitr. Geophysik*, **92**, 49–69, 1983a.

[22] Wait, J. R., "Physical model for the complex conductivity of the earth," *Electronics Letters*, **23**, 979–980, 1987.

1.8 The Electrochemical Perspective

a. Introduction

The actual processes of electrical polarization are found to occur at the microscopic level in the electrolyte filled pores at the grain and pore interfaces. On a macroscopic level, the complex resistivity effect is a consequence of these polarization effects. The frequency dispersive charge separation effects at the grain interfaces can be included explicitly in the model by undertaking a rigorous analysis of the electrochemistry of the metal grain interface such as propounded by Wong [1979] who employed a spherical model of the ore particle. The analysis was extended to spheroidal shaped particles by Wong and Strangway [1981] which allows rock texture into the model. Sometime earlier [Wait 1958, 1959] *, the electrochemistry at the metal-electrolyte interface was described phenomenologically by an interface impedance with any desired frequency dependence. Such an approach was also employed by Komarov [1972]. More recently, the electrochemical charge separation effects around small resistive spheres was treated by Chew and Sen [1982]. They assumed that the diffuse double layer is given by the Boltzmann distribution in terms of the potential following the Guoy-Chapman theory. Chew and Sen obtain analytical results in the limit that the double layer thickness is small compared with the radius of the particle. Their results are highly relevant to the important question of the huge dielectric enhancements observed in clay bearing geological materials.

Common to all of the microscopic theories, the induced electric dipoles in the elemental particles are superimposed to deduce an effective complex conductivity or permittivity of the assemblage. Attempts to generalize such theories to dense packing of the basic particles lead to fundamental difficulties. But some interesting and ingenious suggestions have been made to extend the validity of the mixture formulas beyond the sparse loading idealization. (e.g. see discussions in sections 1.4, 1.5 and 1.6)

Here, we review some of the basic electrochemical concepts which hopefully provide needed insight into the underlying mechanisms. Also, we wish to provide a justification for the phenomenological model which represents the boundary region adjacent to the particle as an in-

* see Section 1.4 references.

terface impedance or surface admittance or some combination thereof.

b. Classical Diffusion Concept

Basically, an electrolytic solution is a mixture of positively charged cations and negatively charged anions. Normally, the solution is regarded as being in equilibrium where the net charge density q is zero. Thus,

$$q = ep - en = 0 \tag{1}$$

where p and n are the densities of the anions and cations, respectively, while e is the unit electrical charge. Now a net movement of charged ions (i.e. current flow) will occur when an electrical field $\overline{E}$ is applied or when the ionic concentrations p and n are perturbed. Thus, the respective cationic and anionic flux densities are

$$\overline{J}_p = -D\nabla p + \mu p\overline{E} \tag{2}$$

and

$$\overline{J}_n = -D\nabla n - \mu n\overline{E} \tag{3}$$

where D is the diffusivity coefficient and μ is the electrical mobility. Clearly, the second terms on the R.H.S. of (2) and (3) describe the migration of the ions under the effect of the electric field. On the other hand, the first terms on the R.H.S. of (2) and (3) describe the diffusion of the ions under a concentration perturbation. For a uniform external field applied to an electrolyte initially at equilibrium, the charge flow is described exclusively by the migration term since there is no initial concentration gradient.

Now, according to the divergence theorem

$$\nabla \cdot \overline{J}_p = \frac{\partial p}{\partial t} \tag{4}$$

and

$$\nabla \cdot \overline{J}_n = \frac{\partial n}{\partial t} \tag{5}$$

Thus, the accumulation of charge with time are described by

$$\frac{\partial p}{\partial t} = D\nabla^2 p - \mu\nabla \cdot (p\overline{E}) \tag{6}$$

and

$$\frac{\partial n}{\partial t} = D\nabla^2 n + \mu\nabla \cdot (n\overline{E}) \tag{7}$$

where $\nabla^2 = \nabla \cdot \nabla$ is the Laplacian operator. In what follows, we also assume that $E = -\nabla V$ when V is a potential. Actually, (2) and (3) are Fick's first law while (6) and (7) are Fick's second law [Bockris and Reddy, 1973]. Here, we have assumed single valence ionic species. Of course, if the divergence terms on the R.H.S. at (6) and (7) are ignored, we have the simple diffusion equation for p and n. This is a good approximation when the ion concentration gradients are sufficiently small.

In actual rock-electrolyte systems, the gradient of the charge densities may be large near interfaces when an electric field is applied. In fact, charge separation may occur spontaneously in the electrolytic pore fluid. When the external field is removed, the charge accumulation may discharge in a manner roughly akin to a charged capacitor. This particular process is known as the Maxwell-Wagner effect [Hasted 1973]. The relaxation is very rapid except in special cases of thin pancake shaped occlusions which exhibit high effective internal capacitances [Sen 1981].

c. Chew and Sen's Model *

In the frequency range of interest (0.01 – 1000 Hz), it has been observed that small resistive particles such as clays occurring in sizes of the order of 10^{-8} m in diameter do indeed give a large dielectric enhancement. As indicated by Chew and Sen [1982], the surface conduction around the periphery of the resistive or insulating particle can lead to a major dielectric enhancement. In their electrochemical model, the frequency dependence of the conduction or admittance layer is a consequence of their theory rather than an "ad hoc" supposition.

In the case where the basic particles are metallic ore grains, there are species of ions present in the electrolyte which produce a redox reaction across the given interface during the charging and discharging process. This redox reaction constitutes a leakage current that in effect shunts the equivalent capacitance of the interfacial charge separation. Thus, the rate or time constant of the discharge of the induced

* W. C. Chew and P. N. Sen, "Dielectric enhancement due to electrochemical double layer ; thin double layer approximation," *Jour. Chem. Phys.*, 77, 4683–4692, 1982.

dipole is no longer controlled by this capacitance of the interface as it would be in the Maxwell-Wagner model. Instead, it becomes a complicated function of the diffusion rate of the reactive ionic species in the neighborhood of the grain and of the rate of the associated redox reaction.

d. Butler-Volmer Equation

Here, we will look at the charge transfer mechanism at a metal/electrolyte boundary. The ore mineral grain will be modeled as a metallic conducting particle while the rock matrix is described as an electrolyte by virtue of the conduction in the fluid field pores. As indicated by Angoran and Madden [1977], only Cu^{++} and S^{--} ions have measurable activity in copper/iron sulfide ore systems. Thus, it seems reasonable to use a model of a single active species electrolyte for the rock pore fluid.

Actually, for a metal particle immersed in such a system, there will be a continuous charge transfer across the interface occurring even at equilibrium conditions. The redistribution of charge on the electrolyte side of the interface sets up a plane of charge a short distance away. A corresponding plane of image charges then appears in the conductor with equal and opposite polarity. The resultant structure is referred to as the "double layer" and it is depicted in Fig. 1.8.1a. The quantity $\Delta\phi_e$ is the equilibrium potential associated with the interface decays from a constant value at the particle surface to zero at a point within the electrolyte as sketched in Fig. 1.8.1b. The position of the closest approach of non-adsorped cations is termed the Outer Helmholtz Plane (OHP) as shown in Fig. 1.8.1c. The charge balancing the image charge in the metal does not all lie in the OHP but some of it is diffused into the bulk electrolyte. The region is the Gouy-Chapman diffuse layer. However, most of the potential drop occurs between the electrode and the Outer Helmholtz Plane. As a consequence, the structure behaves as a capacitor when the intervening dielectric is affected by the oriented water dipoles between the OHP and the metal surface. The water dipoles are shown as arrows in Fig. 1.8.1a. For time varying conditions, the capacitive property will allow passage of displacement current even if there were no charge transfer. This contribution to the total *effective* current flow is described as being "non-faradaic".

Under truly non-equilibrium conditions, there is a net charge flow across the interface and this portion is called "faradaic." It may occur

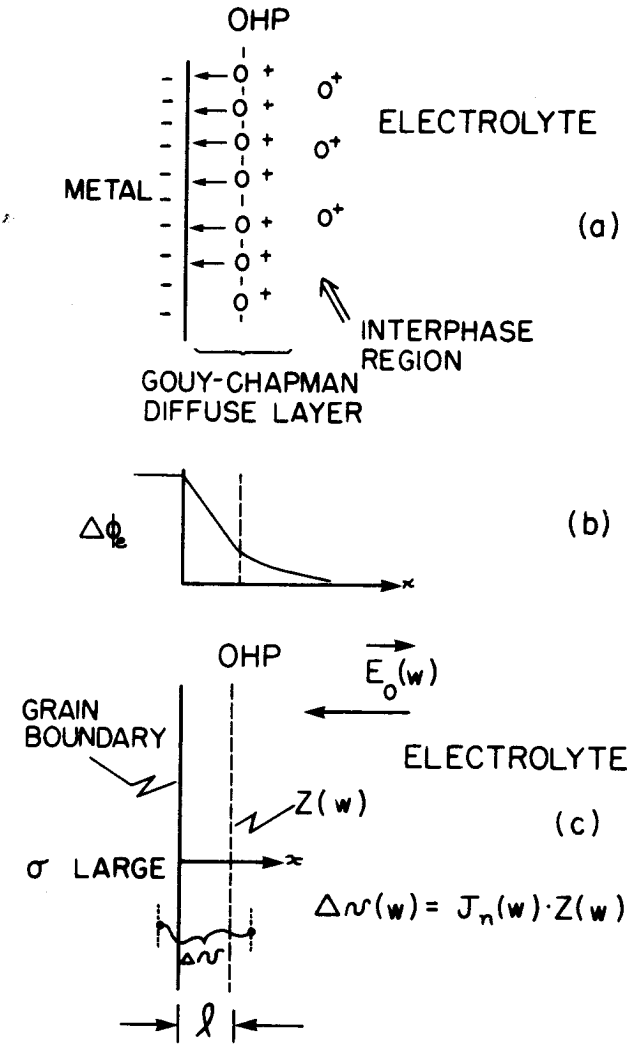

Figure 1.8.1 The electrochemical double layer. In Fig. (c), $J_n(j\omega)$ is the net normal current density at the interface and $\Delta v(j\omega)$ is the voltage drop.

if there is a perturbation in the concentration of the ionic species in the interphase region or alternatively there is an "overvoltage" v applied across the interface. This excess current i_e is described by the Butler-Volmer equation which, followed Bockris and Reddy [1973], is written

$$i_e = i_0^F \exp\left(\frac{ev}{2kT}\right) - i_0^B \exp\left(-\frac{ev}{2kT}\right) \tag{8}$$

where e is the electronic charge, k is Boltzman's constant, T is the absolute temperature and where i_0^F and i_0^B are the forward and backward equilibrium reaction currents. For sufficiently small overpotentials, (8) can be approximated by the linear form

$$i_e = i_0^F(1 + \frac{ev}{2kT}) - i_0^B(1 - \frac{ev}{2kT}) \tag{9}$$

which corresponds to the common assumption that the I.P. response is linear with respect to low current densities in the bulk volume. We can further write

$$i_0^F = eKp \quad \text{and} \quad i_0^B = eKn \tag{10}$$

where K is the forward or backward reaction rate (assumed equal). Then (9) is reduced to

$$i_e = eK\left[(p-n) + (p+n)\frac{ev}{2kT}\right] \tag{11}$$

e. More on the Interface Impedance

We proceed further by noting that the thickness of the double layer (e.g. 10^{-9} m) is certainly small compared with the radius of the typical mineral grain (e.g. 10^{-3} m). Thus, it is safe to assume that the surface of the grain and the interaction region can be described locally in a planar geometry where $x > 0$ represents the electrolyte and where $x < 0$ is the metal. We abstract here from Flanagan and Wait [1985] and Flanagan [1983]*.

With the one dimensional geometry indicated, we may reduce (6) and (7) to

$$\frac{\partial^2 V}{\partial x^2} = -\frac{e}{\epsilon}(p-n) \tag{12}$$

* see references in Section 1.4

$$j\omega p = D\frac{\partial p^2}{\partial x^2} - \mu\frac{\partial p}{\partial x}\frac{\partial V}{\partial x} - \mu p\frac{\partial^2 V}{\partial x^2} \tag{13}$$

$$j\omega n = D\frac{\partial^2 n}{\partial x^2} + \frac{\partial n}{\partial x}\frac{\partial V}{\partial x} + \mu n\frac{\partial^2 V}{\partial x^2} \tag{14}$$

where we have adopted a time factor $\exp(j\omega t)$. Solutions of (12), (13), and (14), which are the basic electrokinetic equations for the problem can be obtained under appropriate boundary conditions. An obvious condition is that the potential V at $x = 0$ on the metal surface is a constant. Then the voltage $v(j\omega)$ across the interface region of thickness ℓ, is related to the net current flow $i_e(j\omega)$ by the linear relation

$$v(j\omega) = Z(j\omega)\, i_e(j\omega) \tag{15}$$

where $Z(j\omega)$ can be aptly defined as the *interface impedance.* On the basis of (11) and (15), we have

$$Z(j\omega) = \frac{1}{ek}\frac{V(\ell)}{(p-n) + (p+n)eV(\ell)/2kT} \tag{16}$$

where $V(\ell)$ is the voltage drop and where p and n are the effective values at $x = \ell$. The point being made here is that the electrochemistry of the double layer can be represented by a frequency dependent impedance which is merely the voltage drop across the layer divided by the normal current density. Linearity of the response is a vital ingredient of this conclusion. But linearity is always something that can be checked in the laboratory or field setting (e.g. by confirming lack of harmonic distortion)

f. Perturbation Approach

An alternative approach is to deal only with first order perturbation of the time varying ion densities. Following Wong [1979], we set

$$p = p_0 + p(x,t) \tag{17}$$

and

$$n = n_0 + n(x,t) \tag{18}$$

where p_0 and n_0 are background concentrations and $p(x,t)$ and $n(x,t)$ are perturbations. When the time variation is according to

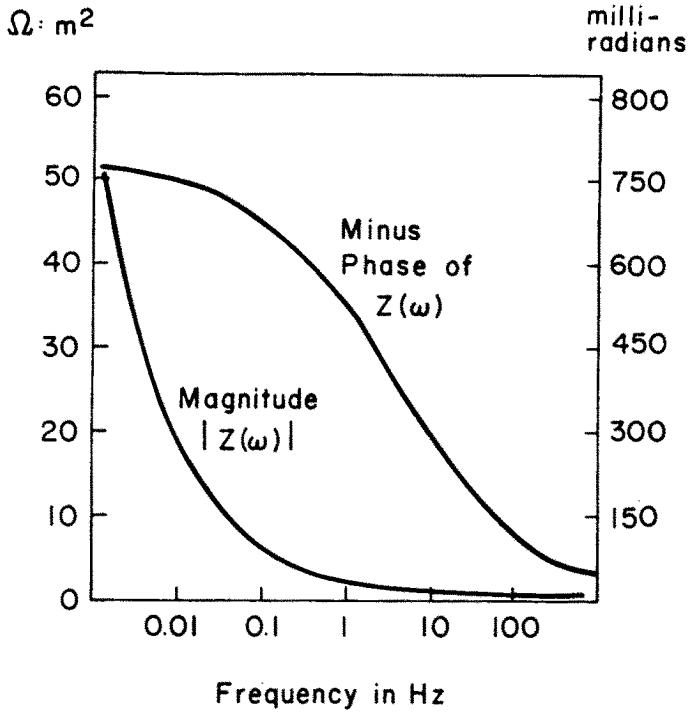

Figure 1.8.2 Fit of Olhoeft's [1982] data for pyrite/electrolyte interface to modified Warburg model.

$\exp(j\omega t)$, we can linearize the resulting equations provided second order quantities are neglected. The interface impedance concept then refers to the proportionality of the net perturbation current flow (at a frequency $\omega/2\pi$) and the corresponding perturbation voltage across the double layer. It is also possible to include the non-faradaic portion of the alternating current flow in the interface impedance current flow because it is basically in parallel with the faradaic portion.

We make no attempt here to calculate the actual interface impedance $Z(j\omega)$ for a given situation. But certainly, such an approach is possible following the lead of Angoran and Madden [1977], Wong [1979], and Wong and Strangway [1982]. Instead, we will argue that $Z(j\omega)$ is an intrinsic parameter of the interface which can be specified at the outset. Fortunately there are good data (e.g. Olhoeft, [1982]) on actual measurements of the frequency dependence of the interface impedance for a pyrite/electrolyte solution. An example of

many such data is shown in Fig. 1.8.2 where both the amplitude and phase of $Z(j\omega)$ are shown for a wide frequency range. Olhoeft [1982] found an empirical fit, for the frequency dependence, to be of the form

$$Z(j\omega) = Z_\infty + Z_1/(j\omega)^{\frac{1}{2}} \tag{19}$$

While the particular form of the frequency dependence given by (19) is not universal, it is a convenient reference to employ in further theoretical studies. Also, while it is referred to as a Warburg impedance because of the $1/(j\omega)^{1/2}$ term, we are certainly aware of other electrochemical factors that may contribute to the frequency dependence. For example, Fink [1980] and more recently Klein et al. [1984] have indicated that there are two physical processes responsible for the electrode polarization at mineral/electrode interfaces. For minerals such as chacocite, the response is related to a reversible oxidation-reduction couple with copric ions in solution. But for other minerals such as pyrite and chalcopyrite, diffusion of active species in the electrolyte as propounded by Wong [1979] is not the controlling process. Alternative mechanisms are surface controlled processes such as surface diffusion or adsorption phenomena. In any case, the interface impedance is a valid description from the standpoint of formulating a boundary value problem for a given particle or mineral grain located within the electrolyte.

References

[1] Angoran, Y. and T. R. Madden, "I.P. : A preliminary study of its chemical basis," *Geophysics*, **42**. 788–803, 1977.

[2] Antropov, L., *Theoretical Electrochemistry*, Mir Publishers, Moscow, 1972.

[3] Bockris, J. O'M and A. K. N. Reddy, *Modern Electrochemistry*, Plenum Press, 1970.

[4] Chew, W. C., "Dielectric enhancement and electrophoresis due to electrochemical double layer — a uniform approximation," *J. Chem. Phys.*, **80**, No. 9, 1984.

[5] Fink, J., "Warburg impedance — what it is and what it isn't," *50th. Annual SEG Meeting, Houston,* Nov. 1980.

[6] Hasted, J. B., *Aqueous Dielectrics*, Chapman and Hall, London, 1973.

[7] Johnson, D. L., and P. N. Sen (Editors), *Physics and Chemistry of Porous Media*, American Institute of Physics, New York, 1984.

[8] Kan, R. and P. N. Sen, "Electrolytic conduction in periodic arrays of insulators with charges," *Jour. of Chemical Physics*, **86**, 5748–5756, 1987.

[9] Klein, J. D., T. Biegler, and M. D. Horne, "Mineral interfacial processes in the method of induced polarization," *Geophysics*, **49**, 1105–1114, 1984.

[10] Komarov, V. A., "The importance of the IP method for the exploration of ore deposits," *Econ. Geol. Report, (Geol. Survey of Canada)*, **26**, 1967.

[11] Olhoeft, G. R., "Warburg impedances at single water/mineral interfaces," *52nd. Annual SEG Meeting, Dallas*, Oct. 1982.

[12] Sen, P. N., "Dielectric anomaly in inhomogeneous materials with application to sedimentary rocks," *Appl. Phys. Letters*, **39**, 667–668, 1981.

[13] Shaw, D. J., *Introduction to colloid and surface Chemistry*, Butterworth's, London, 2nd. Ed., 1970.

[14] Tomkiewicz, M. and P. N. Sen (Editors), *Chemistry and Physics of Composite Media*, Electrochemical Society, New Jersey, 1985.

[15] Wait, J. R., "Physical model for the complex resistivity of the earth", *Electronics Letters*, **23**, 979–980, 1987.

[16] Wong, J., "An electrochemical model of the IP phenomena in disseminated sulphide ores," *Geophysics*, **44**, 1245–1265, 1979.

[17] Wong, J. and D. W. Strangway, "IP in disseminated sulphide ores containing elongated mineralization," *Geophysics*, **46**, 1258–1268, 1981.

Appendix — Thin Sheet Boundary Conditions

The transition region between two homogeneous media can often be handled by effective boundary conditions in order to simplify subsequent applications. To illustrate the concept, we present here an analysis of a sector of a cylindrical shell whose thickness is small compared with the radius of curvature a.

The situation is illustrated in Fig. 1.A.1 with reference to cylindrical coordinates (ρ, ϕ, z). We assume here the problem is entirely two dimensional so that $\partial/\partial z = 0$. The shell is composed of two regions such that the conductivity is σ_1 for $a + \ell > \rho > a$, and the conductivity is σ_2 for $a > \rho > a - s$.

We do not need to specify explicitly the regions outside the shell (i.e. $\rho > a+\ell$ and $\rho < a-s$) except to say their properties do not vary with ϕ. Also we will assume that the fields are everywhere solutions of Laplace's equation. This means that the frequency is sufficiently low that all significant distances of the problem are small compared with the effective wavelength in any of the regions [Wait 1985]. Displacement currents can be included in the problem by regarding σ_1 and σ_2 as being complex (e.g. let $\sigma_1 \to \sigma_1 + j\epsilon_1\omega$, $\sigma_2 \to \sigma_2 + j\epsilon_2\omega$; ϵ_1, ϵ_2 are the respective permittivities). Another possibility is to replace σ_1 by $(\rho_1)^{-1}$ and σ_2 by $(\rho_2)^{-1}$ in terms of the complex resistivities of the two shell regions.

For later convenience we specify that the conductivity in the external region (i.e. for $\rho > a + \ell$) is σ and the conductivity for the internal region (i.e. for $\rho < a - s$) is σ_i. We later let ℓ and s become vanishingly small.

Solutions for the potentials Ψ_1 and Ψ_2 in the two regions are

$$\Psi_1 = \left[A\left(\frac{\rho}{a}\right)^m + B\left(\frac{a}{\rho}\right)^m\right] e^{-jm\phi} \tag{1}$$

and

$$\Psi_2 = \left[C\left(\frac{\rho}{a}\right)^m + D\left(\frac{a}{\rho}\right)^m\right] e^{-jm\phi} \tag{2}$$

where m is the order of the harmonic. Here A, B, C and D are constants. The corresponding radial current densities (using J_p =

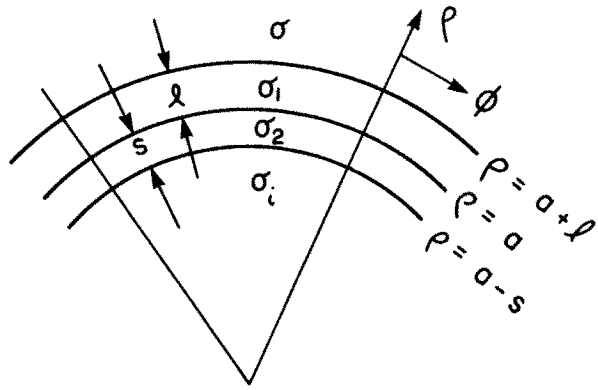

Figure 1.A.1 Segment of the cross section of the cylindrical shell model used to justify the effective boundary conditions for a curved interface.

$-\sigma\partial\Psi/\partial\rho$) are then

$$J_{\rho_1} = -\sigma_1 m \left[A\left(\frac{\rho^{m-1}}{a^m}\right) - B\left(\frac{a^m}{\rho^{m+1}}\right)\right] e^{-jm\phi} \tag{3}$$

and

$$J_{\rho_2} = -\sigma_2 m \left[C\left(\frac{\rho^{m-1}}{a^m}\right) - D\left(\frac{a^m}{\rho^{m+1}}\right)\right] e^{-jm\phi} \tag{4}$$

Continuity of Ψ and J_ρ at $\rho = a$ leads nicely to

$$A\left(1 + \frac{\sigma_1}{\sigma_2}\right) + B\left(1 - \frac{\sigma_1}{\sigma_2}\right) = 2C \tag{5}$$

and

$$A\left(1 - \frac{\sigma_1}{\sigma_2}\right) + B\left(1 + \frac{\sigma_1}{\sigma_2}\right) = 2D \tag{6}$$

which, of course, indicate that C and D are linearly related to A and B.

The "voltage" v across the shell is given by

$$\begin{aligned} v &= \Psi_2(a-s) - \Psi_1(a+\ell) \\ &= \left\{-A\left(\frac{a+\ell}{a}\right)^m - B\left(\frac{a}{a+\ell}\right)^m \right. \\ &\quad \left. + C\left(\frac{a-s}{a}\right)^m + D\left(\frac{a}{a-s}\right)^m\right\} e^{-jm\phi} \end{aligned} \tag{7}$$

Using (5) and (6), we see that

$$v = A\left\{\left[-\left(1+\frac{\ell}{a}\right)^{m}+\frac{1}{2}\left(1+\frac{\sigma_1}{\sigma_2}\right)\left(1-\frac{s}{a}\right)^{m}+\frac{1}{2}\left(1-\frac{\sigma_1}{\sigma_2}\right)\left(1-\frac{s}{a}\right)^{-m}\right]\right\}$$
$$+B\left\{\left[-\left(1+\frac{\ell}{a}\right)^{-m}+\frac{1}{2}\left(1-\frac{\sigma_1}{\sigma_2}\right)\left(1-\frac{s}{a}\right)^{m}+\frac{1}{2}\left(1+\frac{\sigma_1}{\sigma_2}\right)\left(1-\frac{s}{a}\right)^{-m}\right]\right\}e^{-jm\phi} \quad (8)$$

which so far is exact! We now let ℓ and s become small compared with, say, a. Also we assume $\sigma_2 \gg \sigma_1$ (i.e. inner shell region is a good conductor, relatively speaking). Now (8) reduces to

$$v = -(\ell m/a)(A-B)e^{-jm\phi} \quad (9)$$

The other quantity of interest is the radial current density at the outer surface of the double shell. Clearly, it is given by (3) at $\rho = a+\ell$. That is

$$J_{\rho_1}(a+\ell) = -\sigma_1 m\left[A\frac{(a+\ell)^{m-1}}{a^m}-B\frac{a^m}{(a+\ell)^{m+1}}\right]e^{-jm\phi}$$
$$= -\frac{\sigma_1 m}{a}\left[A\left(1+\frac{\ell}{a}\right)^{m-1}-B\left(1+\frac{\ell}{a}\right)^{-m+1}\right]e^{-jm\phi} \quad (10)$$

Then, if $\ell \ll a$ (i.e. thin shell),

$$J_{\rho_1}(a+\ell) \simeq -\frac{\sigma_1 m}{a}(A-B)e^{-jm\phi} \quad (11)$$

which is proportional to (9). The latter fact suggests that we define an interface impedance Z_0 according to

$$Z_0 = \frac{v}{J_{\rho_1}(a+\ell)} \quad (12)$$

In terms of the thin shell approximation, we simply have

$$Z_0 = \frac{\ell}{\sigma_1} \quad (13)$$

but, in general, we need to use (8) and (10) in the definition of (12). In that case Z_0, the "interface impedance" depends on the ratio B/A which is a function of the fields internal and/or the external to the shell. As defined, (12) is also a function of m since a general representation of the potentials involve summation over all integer values of m. However, in the thin sheet approximation, Z_0 is independent of m as given by (13).

Another property of the double shell is the difference of the radial current densities at the inner and outer surfaces. Clearly, this quantity is given by

$$\begin{aligned}\Delta J_\rho &= J_{\rho_2}(a-s) - J_{\rho_1}(a+\ell) \\ &= \sigma_1 m \left[A\frac{(a+\ell)^{m-1}}{a^m} - B\frac{a^m}{(a+\ell)^{m+1}}\right] e^{-jm\phi} \\ &\quad - \sigma_2 m \left[C\frac{(a-s)^{m-1}}{a^m} - D\frac{a^m}{(a-s)^{m+1}}\right] e^{-jm\phi} \end{aligned} \tag{14}$$

Using (5) and (6) again, we have

$$\begin{aligned}\Delta J_\rho = \Bigg\{ & A\left[\frac{\sigma_1 m}{a}\left(1+\frac{\ell}{a}\right)^{m-1} - \frac{\sigma_2 m}{2a}\left(1+\frac{\sigma_1}{\sigma_2}\right)\left(1-\frac{s}{a}\right)^{m-1}\right. \\ & \left. + \frac{\sigma_2 m}{2a}\left(1-\frac{\sigma_1}{\sigma_2}\right)\left(1-\frac{s}{a}\right)^{-(m+1)}\right] \\ & + B\left[-\frac{\sigma_1 m}{a}\left(1+\frac{\ell}{a}\right)^{-(m+1)} - \frac{\sigma_2 m}{2a}\left(1-\frac{\sigma_1}{\sigma_2}\right)\left(1-\frac{s}{a}\right)^{m-1}\right. \\ & \left. + \frac{\sigma_2 m}{2a}\left(1+\frac{\sigma_1}{\sigma_2}\right)\left(1-\frac{s}{a}\right)^{-(m+1)}\right]\Bigg\} e^{-jm\phi} \end{aligned} \tag{15}$$

In passing to the thin shell limit, we need be a bit more subtle here. First of all, we consider only that $\sigma_2 \gg \sigma_1$ (i.e. inner shell is a relatively good conductor as before) but there is no restriction on geometry. Then (15) reads

$$\begin{aligned}\Delta J_\rho \simeq A e^{-jm\phi} \Bigg\{ & -\frac{\sigma_2 m}{2a}\left[\left(1-\frac{s}{a}\right)^{m-1} - \left(1-\frac{s}{a}\right)^{-(m+1)}\right] \\ & + \frac{\sigma_1 m}{a}\left[\left(1+\frac{\ell}{a}\right)^{m-1} - \frac{1}{2}\left(1-\frac{s}{a}\right)^{m-1} - \frac{1}{2}\left(1-\frac{s}{a}\right)^{-(m+1)}\right]\Bigg\} \end{aligned}$$

$$+ Be^{-jm\phi}\left\{ -\frac{\sigma_2 m}{2a}\left[\left(1-\frac{s}{a}\right)^{m-1} - \left(1-\frac{s}{a}\right)^{-(m+1)}\right]\right.$$
$$\left. -\frac{\sigma_1 m}{a}\left[\left(1+\frac{\ell}{a}\right)^{-(m+1)} - \frac{1}{2}\left(1-\frac{s}{a}\right)^{m-1} - \frac{1}{2}\left(1-\frac{s}{a}\right)^{-(m+1)}\right]\right\} \tag{16}$$

Now, we regard s/a and ℓ/a as small such that terms containing $(s/a)^2$ and $(\ell/a)^2$ and higher powers can be neglected. Then (16) looks like

$$\Delta J_\rho \simeq Ae^{-jm\phi}\left\{-\frac{\sigma_2 m}{2a}\left[1-\frac{s}{a}(m-1)-1-\frac{s}{a}(m+1)\right]\right.$$
$$\left.+\frac{\sigma_1 m}{a}\left[1+\frac{\ell}{a}(m-1)-\frac{1}{2}\left(1-\frac{s}{a}(m-1)+1+\frac{s}{a}(m+1)\right)\right]\right\}$$
$$+ Be^{-jm\phi}\left\{-\frac{\sigma_2 m}{2a}\left[1-\frac{s}{a}(m-1)-1-\frac{s}{a}(m+1)\right]\right.$$
$$\left.-\frac{\sigma_1 m}{a}\left[1-\frac{\ell}{a}(m+1)-\frac{1}{2}\left(1-\frac{s}{a}(m-1)+1+\frac{s}{a}(m+1)\right)\right]\right\} \tag{17}$$

which, after cancellation of terms, gives

$$\Delta J_\rho \simeq (A+B)\frac{s}{a^2}m^2\sigma_2 e^{-jm\phi} \tag{18}$$

noting that $\partial/\partial\phi = -jm$, we see that the effective boundary condition for the discontinuity of the normal current density is

$$J_{\rho_2}(a-s) - J_{\rho_1}(a+\ell) \simeq -\frac{s\sigma_2}{a^2}\frac{\partial^2\Psi_1(a)}{\partial\Phi^2} \tag{19}$$

where

$$\Psi_1(a) = (A+B)e^{-jm\phi} \tag{20}$$

is the potential at $\rho = a$. For operational convenience, we note that

$$\Psi_2(a-s) = \left[C\left(1-\frac{s}{a}\right)^m + D\left(1-\frac{s}{a}\right)^{-m}\right]e^{-jm\phi} \simeq \Psi_1(a) \tag{21}$$

which is simply a statement that the potential drop across the inner shell is negligible. Thus, the boundary condition (19) is replaced by

$$J_\rho(a-s) - J_\rho(a+\ell) \simeq -\frac{s\sigma_2}{a^2}\frac{\partial^2\Psi}{\partial\phi^2}(a-s) \tag{22}$$

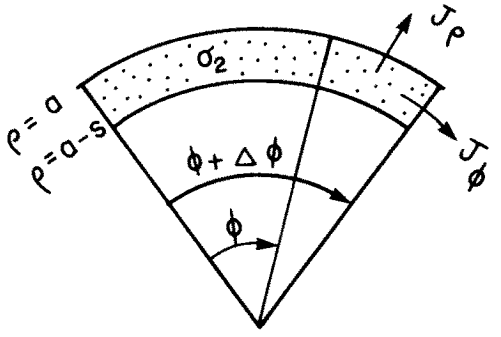

Figure 1.A.2 Portion of inner shell and elemental volume.

which, with the use of Laplace's equation, is equivalent to

$$J_\rho(a-s) - J_\rho(a+\ell) \simeq \frac{Y_0}{a^2}\left[\rho\frac{\partial}{\partial\rho}\rho\frac{\partial\Psi}{\partial\rho}\right]_{\rho=a-s} \tag{23}$$

where $Y_0 = s\sigma_2$ is the conductance of the inner shell.

It is useful to consider the physical aspects of the boundary condition given by (23). Here, we just focus on the inner highly conducting shell of thickness s which is shown in Fig. 1.A.2 (not drawn to scale). We now apply the divergence theorem $\Delta\cdot\bar{J} = 0$ to the volume bounded by $a < \rho < a-s$ and by ϕ and $\phi+\Delta\phi$. We can write approximately

$$\Delta\phi(a-s)J_\rho(a-s) - \Delta\phi a J_\rho(a) + \int_{a-s}^{a}\Big[J_\phi(\phi) - J_\phi(\phi+\Delta\phi)\Big]d\rho = 0 \tag{24}$$

or, using differentials,

$$a\Big[J_\rho(a-s) - J_\rho(a)\Big]d\phi + s\left(-\frac{\partial J_\phi}{\partial\phi}\right)d\phi = 0 \tag{25}$$

Noting $J_\phi = -(\sigma_2/a)(\partial\Psi/\partial\phi)$ within the shell, we obtain

$$J_\rho(a-s) - J_\rho(a) = -\frac{s\sigma_2}{a^2}\frac{\partial^2\Psi(a)}{\partial\phi^2} \tag{26}$$

or

$$J_\rho(a-s) - J_\rho(a) = \frac{s\sigma_2}{a^2}\left[\rho\frac{\partial}{\partial\rho}\rho\frac{\partial\Psi}{\partial\rho}\right]_{\rho=a} \tag{27}$$

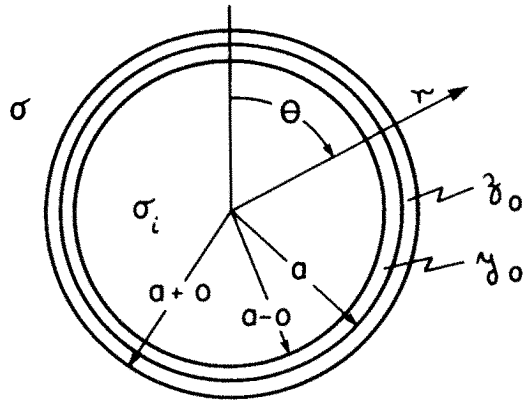

Figure 1.A.3 The double shell spherical model for the solid particle of conductivity σ_i immersed in a medium of conductivity σ.

which, not surprisingly, are consistent with (21) and (23). Again, we note that $Y_0 = s\sigma_2$.

It is now clear that in the limit where ℓ and $s \to 0$, the boundary conditions for the double shell model can be succinctly written

$$\left(\sigma \frac{\partial \Psi}{\partial \rho}\right)_{\rho=a+0} = \left[\sigma_i \frac{\partial \Psi}{\partial \rho} + \frac{Y_0}{a^2}\left(\rho \frac{\partial}{\partial \rho} \rho \frac{\partial \Psi}{\partial \rho}\right)\right]_{\rho=a-0} \tag{28}$$

and

$$\left(\Psi - Z_0 \sigma \frac{\partial \Psi}{\partial \rho}\right)_{\rho=a+0} = (\Psi)_{\rho=a-0} \tag{29}$$

where σ_i and σ are the conductivities inside and outside the shell respectively.

The thin sheet boundary conditions are useful to solve problems involving particles where the source of the field is outside the particle. We have attempted to show the development and justification for a cylindrical model. The corresponding case in spherical geometry is illustrated in Fig. 1.A.3. The spherical particle has a radius a. To account for bound ions or other related surface conduction mechanisms, we imbue the particle with a surface admittance Y_0. Then, the outer more resistive region (i.e. diffuse ionized layer) just adjacent to the particle is represented by an interface impedance Z_0. The effective boundary conditions, which connect the interior potential for $r < a$ and the exterior potential for $r > a$, are then written as follows

$$\left(\sigma \frac{\partial \Psi}{\partial r}\right)_{r=a+0} = \left[\sigma_i \frac{\partial \Psi}{\partial r} + \frac{Y_0}{a^2} \frac{\partial}{\partial r}\left(r^2 \frac{\partial \Psi}{\partial r}\right)\right]_{r=a-0} \tag{30}$$

and

$$\left(\Psi - Z_0\sigma\frac{\partial\Psi}{\partial r}\right)_{r=a+0} = (\Psi)_{r=a-0} \tag{31}$$

These two equations are completely analogous to (28) and (29). Their application was already indicated (e.g. Chap. 2 in [Wait 1985]).

References

[1] Wait, J. R., *Electromagnetic Wave Theory*, Harper & Row/ Wiley, 1985.

Additional I.P. References

[1] Aguirre, G. and J. R. Wait, "Resistivity and I. P. response of a thin sheet," *Pure and Appl. Geophysics*, **123**, 882–892, 1985.

[2] Appario, A. and V. S. Sarma, "A modified pseudo-depth section as a tool in resistivity and I. P. prospecting," *Geophysical Research Bulletin (India)*, **19**, 187–208, 1981.

[3] Balasanyar, S. Yu., "The mechanism of I. P. of geological medium Izvestia," *Earth Physics*, **16**, 543–545, 1980, (an editorial on the "fallacy" of the common approach to the mechanism of I. P. by transplantation of the theories of physical chemistry into geophysics).

[4] Barnett, C. T., "Theoretical modelling of I. P. effects due to arbitrarily shaped bodies," *Ph.D. thesis,* Colorado School of Mines, Golden, Colorado, 1972.

[5] Belluigi, A., "The need of revising the apparatus employed in the measurement of the electrochemical effect of the ground," *Beitr. z. angew. Geophys.*, **5**, 169–177, 1936.

[6] Bertin, J. and J. Loeb, *Experimental and theoretical aspects of I. P.*, Gebrŏder Borntraeger, Berlin, 1976.

[7] Bleil, D. F., "I. P.: A method of geophysical surveying," *Geophysics,* **18**, 636–661, 1953.

[8] Buchheim, W., "Prinzipielles zur I. P.-Method mit Frequenz Variation," *Geophysik u. Geologie*, **No. 5**, 14–16, 1963.

[9] Buchheim, W. and G. Irmer, "Theory of induced galvanic polarization in solids with electrolyte-filled pores," *Gerlands Beitr. Geophys.,* **88**, 53–72, 1979.

[10] Chew, W. C. and P. N. Sen, "Dielectric enhancement due to electrochemical double layer: Thin double layer approximation," *Journal Chemical Physics,* **77**, 4683–4692, 1982.

[11] Collett, L. S., "Laboratory investigations at overvoltage," (i.e. I. P.) in *Overvoltage Research and Geophysical Applications*, (ed. by J. R. Wait), Pergamon, 1959.

[12] Daknov, V. N., M. G. Latishova, and V. A. Ryapolov, "Investigations of wells by the I. P. method," *The Log Analyst*, 46–82, Nov./Dec. 1967.

[13] Daniels, J. J., "3-D resistivity and I. P. modelling using buried electrodes," *Geophysics*, **42**, 1006–1019, 1977.

[14] DeWitt, G. W., "Parametric studies of I. P. spectra," *unpublished M.S. thesis*, University of Utah, 1978.

[15] Dias, C. A., "A non-grounded method for measuring induced electric polarization and conductivity," *Ph.D. thesis*, University of California, Berkeley, 1968.

[16] Dieter, K., N. R. Patterson, and F. S. Grant, "I. P. and resistivity type curves for 3-D bodies," *Geophysics,* **34**, 615–632, 1969.

[17] Edwards, L. S., "A modified pseudosection for resistivity and I. P.," *Geophysics,* **42**, 1020–1035, 1977.

[18] Eskola, L., E. Floranta, and R. Puranen, "A method for calculating I. P. anomalies with surface polarization," *Geophysical Prospecting,* **32**, 79–87, 1984.

[19] Fink, J., "Warburg Impedance — what it is and what it isn't" *S. E. G. 50th Annual Meeting,* Houston, November, 1980.

[20] Freedman, R. and J. P. Vogiatzis, "Theory of I. P. logging in a borehole," *Geophysics,* **57**, 1830–1849, 1986.

[21] Fricke, H. and S. Morse, "An experimental study of the electrical conductivity of disperse systems, I.," *Phys. Rev.*, **26**, 361–367, 1925.

[22] Fricke, H., "A mathematical treatment of the electrical conductivity and capacity of disperse systems, II," *Phys. Rev.* , **26**, 678–681, 1925.

[23] Fricke, H., "The electric conductivity and capacity of disperse systems," *Physics*, **1**, 106–115, 1931. (Deals with suspensions of biological cells whose interior is a well conducting salt solution but, at its surface, there is an insulating membrane. He discusses a postulated equivalent circuit and shows measured effective capacitance of the suspension at audio frequencies.)

[24] Fricke, H., "The Maxwell-Wagner dispersion in a suspension of ellipsoids," *J. Physical Chemistry*, **57**, 934–937, 1953.

[25] Grisseman, C., "Examination of the frequency-dependent conductivity of ore-containing rock or artificial models," *Sci. Report*, **No. 2**, Electronics Lab, University of Innsbruck, July 15, 1971. [U. S. Government Contract F-44620-71-C-007, NTIA Doc. AD 73131225.] (Employed "Wait model" to predict I. P. response of coated mineral grains with a Warburg interface impedance and showed reasonable agreement with laboratory data.)

[26] Grow, L. M., "I. P. for geophysical exploration," *Leading Edge*, (SEG publication), **1**, 55–56, 69–70, 1982.

[27] Gruszka, T. P. and J. R. Wait, "EM coupling "removal" from I. P.," *URSI Open Symposium on Wave Propagation*, Durham, New Hampshire, July 1986.

[28] Guptasarma, P., "Effect of surface polarization or resistivity modelling," *Geophysics*, **48**, 98–106, 1983. [Eqn. (1) seems invalid because it refers to a pure dielectric.]

[29] Hallof, P. G. and W. H. Pelton, "The removal of inductive coupling effects from spectral I. P. data," *WEG 50th Int'l. Meeting*, November 1980.

[30] Hohmann, G. H., P. P. Kintzinger, G. D. van Voorhis, and S. H. Ward, "Evaluation of the measurement of induced electric polarization with an inductive system," *Geophysics*, **35**, 901–915, 1970.

[31] Hohmann, G. W., "3-D I. P. and EM modelling," *Geophysics*, **40**,

309–324, 1975.

[32] Iliceto, V., A. Santarato, and S. Veronese, "An approach to the identification of fine sediments by I. P. laboratory measurements," *Geophysical Prospecting,* **30**, 331–347, 1982.

[33] Kan, R. and P. N. Sen, "Electrolytic conduction in periodic arrays of insulators with charges," *J. Chemical Physics*, **86**, 5748–5756, 1987.

[34] Karous, M., "I. P. anomaly above a sphere," *GeoExploration*, **21**, 49–63, 1983.

[35] Klein, J. K., T. Biegler, and M. D. Horne, "Mineral interfacial processes in the method of I. P.," *Geophysics*, **49**, 1105–1114, 1984. (Using the rotation electrode method, shows that Warburg impedance model is not valid for pyrite/electrolyte interface.)

[36] Lee, T., "The Cole-Cole model in time domain I. P.," *Geophysics,* **46**, 860–868, 1981.

[37] Levislaaya, T. S. M., "Dielectric relaxation in rock," *Izvestiya Earth Physics,* **20**, 777–780, 1984. (bridge measurements of ϵ and tan δ from 50 to 29,000 Hz. for NaCl saturated samples.)

[38] Lewis, R. G. and T. B. Lee, "The detection of I. P. with a transient EM system," *IEEE Trans.,* **GE-22**, 69–80, 1984.

[39] Major, J. and J. Silic, "Restrictions on the use of Cole-Cole dispersion models in complex resistivity interpretation," *Geophysics*, **46**, 916–931, 1981.

[40] Maxwell Garnett, J. C., "Colours in metal glasses and in metallic films," *Phil. Trans. Roy. Soc. A*, **203**, 385–420, 1904. (extends J. Clerk Maxwell's mixture formulae to optical scattering from particulates)

[41] McChadran, R. C. and D. R. McKenzie, "The conductivity of spheres I, the simple cubic lattice," *Proc. Roy. Soc. London,* **A-359**, 45–63, 1978. (gives corrections to Rayleigh's 1892's formulations)

[42] Losito, G. and G. Finizi-Cortini, "Laboratory instrumentation to study changes of electrical conductivity of rocks with changes of frequency, temperature and pressure," *Geophysical Prospecting,* **29**, 923–931, 1981.

[43] Madden, T. R. and D. J. Marshall, "I. P., a study of its causes," *Geophysics,* **24**, 790–816, 1959.

[44] Mahon, M. K., J. D. Redman, and D. W. Strangway, "Complex resistivity of synthetic sulphide bearing rock," *Geophysical Prospecting,* **34**, 743–761, 1986.

[45] Mandel, M., "The dielectric constant and Maxwell-Wagner dispersion of a suspension of oriented prolate spheroids," *Physics*, **27**, 827–840, 1961.

[46] Muller, M., "Ergebnisse geoelactrischer Polarisationsmessungen," *Zeits. f. Geophysik,* **16**, 274–284, 1940.

[47] Nabighian, M. S. and C. L. Elliot, "Negative I. P. effects from layered media," *Geophysics*, **41**, 1236–1255, 1976.

[48] Ogilivy, A. and E. N. Kuzmina, "Hydrogeologic and engineering — geologic possibilities of employing method of I. P.," *Geophysics,* **37**, 839–861, 1972.

[49] Olhoeft, G. R., "Electrical properties of natural clay permafrost," *Can. J. Earth Science,* **Vol. 14**, 16–24, 1977.

[50] Olhoeft, G. R., "Electrical properties of rocks, Chapter 9," in *Physical Properties of Rocks,* (ed. by Y. S. Youlovkiana and C. Y. Ho), McGraw-Hill, 1981.

[51] Parra, G. O., "Effects of pipelines on spectral I. P. surveys," *Geophysics*, **49**, 1979–1992, 1984.

[52] Patella, D. and D. Schiavone, "On the determination of the apparent frequency-effect in the frequency domain I. P. method," *GeoExploration*, **14**, 81–91, 1976.

[53] Patella, D., "Tutorial interpretation of MT measurements over an electrically dispersive 1-D earth," *Geophysical Prospecting*, **35**, 1–11, 1987.

[54] Pelton, W. H., L. Rijo, and C. H. Swift, Jr., "Inversion of 2-D resistivity and I. P. data," *Geophysics,* **43**, 788–803, 1978.

[55] Ramachandyan, M. and N. Sanyal, "EM coupling in IP measurements using some common electrode arrays over a uniform halfspace," *GeoExploration,* **18**, 97–109, 1980.

[56] Rayleigh, Lord, (J. W. Strutt), "On the influence of obstacles arranged in rectangular order for the properties of a medium," *Phil.*

Magazine, **34**, 481–502, 1892.

[57] Schwan, H. P., G. Schwarz, J. Maczuk, and H. Pauly, "On the low frequency dielectric dispersion of colloidal particles in electrolyte solution," *J. Physical Chemistry,* **66**, 2626–2635, 1962.

[58] Schwarz, G., "A theory of the low frequency of dielectric dispersion," *Journal of Physical Chemistry,* **66**, 2636–2642, 1962.

[59] Scott, W. J. and G. F. West, "I. P. of synthetic, high-resistivity rocks containing disseminated sulphides," *Geophysics,* **34**, 87–100, 1969.

[60] Seigel, H. O. and A. W. Howland-Rose, "The magnetic I. P. method," Chapter 3, in *Developments in Geophysical Exploration Methods,* (ed. by A. A. Fitch), Appl. Sci. Publishers, Essex, 1982.

[61] Seigel, H. O., "The magnetic I. P. method," *Geophysics,* **39**, 321–339, 1974.

[62] Sidorov, V. A. and A. M. Yakin, "IP in rocks with inductive excitation," *Izvestia Earth Physics,* **15**, 810–814, 1979.

[63] Sihvola, A. and J. A. Kong, "Effective permittivity of dielectric mixtures," *Proc., URSI Commission F Symposium,* University of New Hampshire, Durham, July 1986.

[64] Snyder, Y. Y., K. H. Merkel, and J. F. Williams, "Complex formation resistivity — the forgotten half of the resistivity log: Soc. Prof. Well Log." *Analysts Meeting (18th Annual Symposium),* Houston, 1977.

[65] Stoyer, C. H., "Consequences of I. P. in MT interpretation," *Pure and Appl. Geophys.,* **114**, 435–449, 1976.

[66] Sumner, J. S., "The I. P. exploration method," in *Geophysics and Geochemistry in the search for Metallic Dyes,* (ed. by P. J. Hood). *Geological Survey of Canada Report,* 123–133, 1979.

[67] van Voorhsi, G. D., P. H. Nelson, and T. L. Drake, "Complex resistivity spectra of porphyry copper mineralization," *Geophysics,* **38**, 49–60, 1973.

[68] Vinegar, H. J. and M. H. Waxman, "I. P. of shaly sands," *Geophysics,* **49**, 1267–1287, 1984.

[69] Wait, J. R., H. O. Seigel, L. S. Collett, W. E. Bell, and A. A. Brant, "Method and apparatus for geophysical exploration," U.

S. Patent 2,766,421, 1956. (Application, No. 272,422, February, 1952.)

[70] Wait, J. R., "Relaxation phenomena and I. P.," *GeoExploration,* **Vol. 22**, 107–127, 1984.

[71] Wait, J. R. and P. Debroux, "I. P. in EM inductive schemes," *Geophysical Prospecting*, **32**, 1147–1154, 1984.

[72] Wait, J. R., "Extension to the phenomenological theory of I. P.," *IEEE Trans.*, **GE-24**, 409–414, 1986.

[73] Wait, J. R., "Physical model for the complex resistivity of the earth," *Electronic Letters,* **23**, 979–980, 1987.

[74] Wong, P. Z., "Fractal surfaces in porous media," in *Physics and Chemistry of Porous Media*, 300–318, (ed. by J. Benavar) A.I.P., New York, 1987.

[75] Wong, J., "An electrochemical model of the I. P. phenomenon in disseminated sulphide ores," *Geophysics,* **44**, 1245–1265, 1979.

[76] Wynn, J. C. and K. L. Zonge, "EM coupling, its intrinsic value, its removal and the cultural coupling problem," *Geophysics*, **40**, 831–850, 1975. [Unfortunate errors in equations (8), (9) and (12) which invalidate anisotropic model calculations.]

[77] Xiong, Z., Y. Luo, S. Wang, and G. Wu, "I. P. and EM modelling of a 3-D body buried in a 2-layered anisotrophic earth," *Geophysics*, **51**, 2235–2246, 1986.

[78] Zonge, K. L. and J. C. Wynn, "Recent advances and applications in complex resistivity measurements," *Geophysics*, **40**, 851–864, 1975.

Epilogue

This (survey) deals with the electromagnetic theory and the phenomenology of the complex resistivity of geophysical media. The phenomena are important in understanding the bases of subsurface probing for mineral and petroleum resources using electrical methods. An attempt is made to lead the reader from the basic potential theory to quasi-static concepts and culminating in comprehensive discussions of the prevailing macroscopic theories from the current literature.

The material presented has been used as lecture notes in first year graduate courses in geoelectromagnetism at the University of Arizona. The author has benefitted from many useful suggestions from students and interested colleagues in the geophysical community in the U.S., Canada and abroad.

While the topic selection may seem rather specialized, the results are relevant to other fields such as sub-surface telecommunications, earth conduction and corrosion, non-destructive testing, and hyperthermia. However most of the illustrative examples are shown in a geophysical context to permit an orderly flow of information.

I am grateful to the eminent Professor Jin Au Kong of M.I.T. for the invitation to publish this survey in his series on PIER. I must also thank Dr. Tom Gruszka and Peter Flanagan, former graduate students, for their input which is fully acknowledged in the text.

Most of the writing of this survey was done while I was a visiting professor at the University of British Columbia in Vancouver during the latter half of 1987. I am particularly appreciative here for the hospitality extended by Professors Ed Jull in Electrical Engineering and Doug Oldenburg in Geophysics.

Finally, I wish to thank the diligent Son Nghiem for numerous and useful suggestions.

James R. Wait
Regents Professor
University of Arizona

Mail address:
2210 East Waverly
Tucson, AZ 85719